

**B. SUPPLEMENTARY MATERIAL — PART B**

**$\text{Li}^+ - \text{H}_2$  COMPLEX**

## VIBRATIONAL ENERGY LEVELS

TABLE BI:  $\text{Li}^+\text{-H}_2(I=0)$ . Positions ( $E$ ) and widths ( $\Gamma$ ) of ‘vibrational’ levels  $b k v_R$   $J=k$   $p$  associated with the  $v=0-1$   $j=0-4$  thresholds ( $b\sim j$ ). The positions are relative to the respective  $v j=0$  threshold. The positions of the  $j>0$  thresholds<sup>a</sup> are shown in lines marked with  $\varepsilon$ . All data are in  $\text{cm}^{-1}$ .

$b$	$k$	$v_R$	$v=0$ ( $\varepsilon=0^b$ )				$v=1$ ( $\varepsilon=4158.571$ )			
			$p=1$		$p=-1$		$p=1$		$p=-1$	
			$E$	$\Gamma^c$	$E-$ $E(p=1)$	$\Gamma^c$	$E$	$\Gamma^d$	$E-$ $E(p=1)$	$\Gamma^e$
0	0	0	-1674.606	0			-1780.080	2.37 (-2)		
		1	-1269.455	0			-1369.531	6.84 (-2)		
		2	-924.249	0			-1016.090	1.12 (-1)		
		3	-638.892	0			-719.617	1.46 (-1)		
		4	-412.415	0			-479.275	1.54 (-1)		
		5	-242.898	0			-293.678	1.42 (-1)		
		6	-126.201	0			-160.125	1.11 (-1)		
		7	-53.841	0			-72.835	7.46 (-2)		
		8	-16.453	0			-24.154	*3.86 (-2)		
		9	-1.463	0			* - 3.384	*1.23 (-2)		
2	2	0	-1410.848	0	0.000	0	-1531.768	2.88 (-2)	0.000	2.88 (-2)
		1	-1000.198	0	0.001	0	-1116.200	7.95 (-2)	-0.001	7.94 (-2)
		2	-649.119	0	0.001	0	-757.453	1.32 (-1)	0.003	1.32 (-1)
		3	-357.328	0	0.000	0	-455.339	1.70 (-1)	0.005	1.72 (-1)
		4	* - 123.714	0	0.001	0	-209.105	1.82 (-1)	0.000	1.82 (-1)
		5	54.279	1.72 (-4)	0.000	0	-16.570	1.73 (-1)	0.000	1.73 (-1)
		6	181.463	1.22 (-4)	0.000	0	125.573	1.42 (-1)	0.000	1.42 (-1)
		7	265.674	7.72 (-5)	0.000	0	223.459	1.03 (-1)	0.000	1.02 (-1)
		8	316.923	2.43 (-5)	0.001	0	285.233	6.48 (-2)	0.000	6.48 (-2)
		9	344.468	3.45 (-4)	0.186	0	319.911	3.40 (-2)	0.004	3.39 (-2)
		10					334.810	9.68 (-3)	0.019	9.77 (-3)
2	1	0	-982.522	0	0.266	0	-1086.260	2.21 (-2)	0.262	2.31 (-2)
		1	-621.269	0	0.333	0	-720.657	7.08 (-2)	0.340	8.78 (-2)
		2	-318.794	0	0.368	0	-409.786	1.16 (-1)	0.297	1.16 (-1)
		3	-76.129	0	0.351	0	-155.060	1.42 (-1)	0.283	1.48 (-1)
		4	106.755	4.98 (-3)	0.317	0	43.104	1.53 (-1)	0.269	1.49 (-1)
		5	232.093	3.35 (-3)	0.275	0	185.276	1.27 (-1)	0.241	1.24 (-1)
		6	306.427	1.96 (-3)	0.235	0	275.139	8.13 (-2)	0.210	7.92 (-2)
		7	342.400	1.26 (-3)	0.212	0	320.789	3.69 (-2)	0.190	3.56 (-2)
		8	354.251	1.37 (-3)	0.110	7.92 (-3)	336.101	1.42 (-2)	-0.042	5.85 (-3)
2	0	0	-606.428	0			-685.307	1.59 (-2)		
		1	-303.126	0			-380.288	3.34 (-2)		
		2	-57.127	0			-125.325	5.48 (-2)		
		3	130.541	1.64 (-1)			75.205	3.51 (-1) <sup>f</sup>		
		4	259.938	1.07 (-1)			218.930	2.92 (-1)		
		5	327.186	5.79 (-2)			303.584	1.60 (-1)		
		6	352.005	*1.41 (-2)			*334.790	*3.05 (-2)		
$\varepsilon$			354.300				336.285			

TABLE BI: continued

4	4	0	-658.879	0	0.000	0	-821.633	4.87 (-2)	0.001	4.87 (-2)
		1	-242.132	0	0.000	0	-400.014	1.28 (-1)	0.000	1.28 (-1)
		2	115.046	5.51 (-8)	0.000	0	-35.385	2.09 (-1)	0.000	2.09 (-1)
		3	413.152	6.70 (-4)	0.000	6.67 (-4)	272.661	2.60 (-1)	0.000	2.60 (-1)
		4	653.564	1.23 (-3)	0.000	1.20 (-3)	525.362	2.75 (-1)	0.000	2.75 (-1)
		5	837.255	2.88 (-3)	0.001	1.89 (-3)	723.049	2.60 (-1)	0.001	2.59 (-1)
		6	972.314	9.61 (-4)	0.002	1.07 (-4)	872.203	2.15 (-1)	0.003	2.17 (-1)
		7	1063.672	2.38 (-2)	0.000	1.16 (-5)	976.913	1.59 (-1)	0.000	1.59 (-1)
		8	1121.099	2.94 (-5)	0.000	1.03 (-5)	1045.170	1.05 (-1)	0.000	1.05 (-1)
		9	1167.498	2.11 (-5)	-0.013	3.05 (-3)	1085.525	5.91 (-2)	0.000	5.91 (-2)
		10					1105.121	2.28 (-2)	0.000	2.28 (-2)
4	3	0	-337.791	0	0.000	0	-484.916	4.22 (-2)	0.002	4.25 (-2)
		1	43.791	6.29 (-7)	0.000	0	-98.985	1.19 (-1)	-0.002	1.20 (-1)
		2	365.522	4.97 (-3)	0.000	4.50 (-3)	230.351	1.96 (-1)	-0.001	1.96 (-1)
		3	627.361	4.85 (-3)	0.000	4.65 (-3)	502.815	2.51 (-1)	0.000	2.51 (-1)
		4	830.325	4.29 (-3)	-0.010	6.97 (-2)	719.045	2.59 (-1)	0.000	2.59 (-1)
		5	977.745	1.39 (-2)	0.013	6.75 (-3)	881.759	2.19 (-1)	0.020	2.09 (-1)
		6	1073.003	1.44 (-2)	0.048	4.56 (-3)	990.978	1.81 (-1)	0.045	1.75 (-1)
		7	1130.221	1.57 (-2)	0.059	2.47 (-3)	1059.478	1.08 (-1)	0.009	1.07 (-1)
		8	1168.600	1.53 (-1)	0.202	2.21 (-1)	1108.666	7.36 (-3)	0.052	3.58 (-3)
4	2	0	-69.497	0	-0.581	0	-199.742	1.80 (-2)	-0.014	3.97 (-2)
		1	279.752	5.22 (-5)	0.009	0	153.177	6.30 (-2)	0.009	6.34 (-2)
		2	568.621	4.48 (-2)	0.015	3.67 (-2)	449.386	1.91 (-1)	0.010	1.85 (-1)
		3	796.505	4.52 (-2)	0.017	3.57 (-2)	688.204	2.27 (-1)	-0.012	2.15 (-1)
		4	964.206	4.07 (-2)	0.024	2.84 (-2)	869.610	2.10 (-1)	0.018	2.01 (-1)
		5	1075.070	3.76 (-2)	0.057	1.76 (-2)	995.318	1.63 (-1)	0.048	1.49 (-1)
		6	1137.590	6.60 (-2)	0.387	5.30 (-3)	1064.278	2.43 (-1)	1.500	1.29 (-1)
		7	1163.090	7.54 (-2)	0.286	4.35 (-3)	1102.416	3.87 (-2)	0.006	3.85 (-2)
4	1	0	129.644	3.94 (-2)	3.591	0	18.620	2.18 (-2)	1.861	2.17 (-2)
		1	455.260	2.83 (-1)	1.883	7.25 (-3)	345.520	3.65 (-1) <sup>f</sup>	1.455	2.00 (-1) <sup>e</sup>
		2	716.334	2.85 (-1)	1.598	8.13 (-3)	613.188	4.09 (-1)	1.217	2.56 (-1)
		3	914.312	2.54 (-1)	1.376	6.92 (-3)	821.537	3.82 (-1)	1.037	2.55 (-1)
		4	1050.477	2.06 (-1)	1.169	4.67 (-3)	970.774	2.99 (-1)	0.861	1.98 (-1)
		5	1129.508	1.48 (-1)	0.923	2.39 (-3)	1062.739	1.78 (-1)	0.683	1.21 (-1)
		6	1163.559	9.20 (-2)	0.559	7.68 (-4)	1104.043	5.98 (-2)	0.361	3.88 (-2)
4	0	0	243.658	1.08 (-2)			151.015	1.98 (-2)		
		1	559.743	*2.29 (-2)			466.586	*4.51 (-1) <sup>f</sup>		
		2	803.985	1.95			* 715.923	*2.98 (-1)		
		3	981.014	1.41			* 901.463	*1.95 (-1)		
		4	1094.319	8.33 (-1)			*1025.395	*1.21 (-1)		
		5	1151.769	3.48 (-1)			*1091.675	*5.33 (-2)		
$\varepsilon$			1168.550				1108.829			

<sup>a</sup>The thresholds obtained from the PES of the LiHH<sup>+</sup> system are used. In comparison with the accurate data for H<sub>2</sub><sup>1</sup>, the values of  $\varepsilon_{v,j}-\varepsilon_{0,0}$  are too low by 0.073, 0.247, 2.595, 2.982, and 3.979 cm<sup>-1</sup> for (v, j)=(0, 2), (0, 4), (1, 0), (1, 2), and (1, 4), respectively. These deviations become larger (~4–2 times) when the Born-Oppenheimer energies of H<sub>2</sub> are taken as reference, which is probably more appropriate. See Fig. B1.

<sup>b</sup>Lies 4339.9 cm<sup>-1</sup> above the minimum of the PES.

<sup>c</sup>All widths  $\Gamma > 0$  in the column are due to rotational predissociation.

<sup>d</sup>The widths in the column that pertain to states of negative energies (relative to  $\varepsilon_{10}$ ) are due to vibrational predissociation.

<sup>e</sup>The widths in this column are due to pure vibrational predissociation for states with  $E$  up to  $\varepsilon_{12}$ ;  $f$ -parity states cannot predissociate to  $v=1$   $j=0$  channel.

<sup>f</sup>The substantial increase of the width, as compared to the preceding value in the column, is due to contribution of rotational predissociation to  $v=1$   $j=b-2$  channel.

TABLE BII:  $\text{Li}^+-\text{H}_2(I=1)$ . Positions ( $E$ ) and widths ( $\Gamma$ ) of ‘vibrational’ levels  $b k v_R$   $J=k$   $p$  associated with the  $v=0-1$   $j=1-5$  thresholds ( $b\sim j$ ). The positions are relative to the respective  $v j=0$  threshold. The positions of the  $j>0$  thresholds are shown in lines marked with  $\varepsilon$ . All data are in  $\text{cm}^{-1}$ .

			$v=0$ ( $\varepsilon=0$ )				$v=1$ ( $\varepsilon=4158.571$ ) $-2.595^a$			
$b$	$k$	$v_R$	$p=1$		$p=-1$		$p=1$		$p=-1$	
			$E$	$\Gamma^b$	$E-$ $E(p=1)$	$\Gamma^b$	$E$	$\Gamma^c$	$E-$ $E(p=1)$	$\Gamma^c$
1	1	0	-1606.666	0	0.150	0	-1716.209	2.49 (-2)	0.152	2.49 (-2)
		1	-1199.367	0	0.138	0	-1303.813	6.97 (-2)	0.140	6.95 (-2)
		2	-851.638	0	0.125	0	-948.181	1.17 (-1)	0.127	1.17 (-1)
		3	-563.320	0	0.109	0	-649.210	1.51 (-1)	0.112	1.51 (-1)
		4	-333.412	0	0.092	0	-406.117	1.62 (-1)	0.096	1.62 (-1)
		5	* -159.590	0	0.076	0	-217.337	1.50 (-1)	0.081	1.50 (-1)
		6	* -36.978	0	0.058	0	-79.032	1.22 (-1)	0.062	1.22 (-1)
		7	42.312	0	0.047	0	14.268	8.58 (-2)	0.049	8.58 (-2)
		8	88.791	0	0.038	0	71.188	5.16 (-2)	0.037	5.16 (-2)
		9	112.056	0	0.036	0	101.337	2.52 (-2)	0.036	2.52 (-2)
		10				112.137	3.94 (-3)	0.055	4.02 (-3)	
1	0	0	-1080.273	0			-1174.657	1.67 (-2)		
		1	-734.044	0			-822.709	6.37 (-2)		
		2	-445.659	0			-524.636	1.01 (-1)		
		3	-218.247	0			-287.689	7.32 (-2)		
		4	-50.548	0			-97.985	1.19 (-1)		
		5	55.281	*0			30.615	6.92 (-2)		
		6	106.443	*0		96.446	3.99 (-2)			
$\varepsilon$			118.462			112.448				
			$-0.025^a$			$-0.126^a$				
3	3	0	-1092.972	0	0.000	0	-1231.797	3.62 (-2)	0.000	3.62 (-2)
		1	-679.058	0	0.000	0	-812.993	9.86 (-2)	0.000	9.86 (-2)
		2	-324.724	0	0.000	0	-451.021	1.59 (-1)	0.000	1.59 (-1)
		3	-28.565	0	0.000	0	-146.515	2.05 (-1)	0.004	2.02 (-1)
		4	207.129	7.38 (-4)	0.011	9.72 (-4)	103.162	2.20 (-1)	0.004	2.20 (-1)
		5	388.822	4.80 (-5)	0.000	4.67 (-5)	298.959	2.06 (-1)	0.001	2.07 (-1)
		6	519.863	6.36 (-5)	0.000	6.26 (-5)	444.635	1.71 (-1)	0.000	1.71 (-1)
		7	607.866	4.52 (-5)	0.000	4.62 (-5)	546.103	1.25 (-1)	0.000	1.25 (-1)
		8	662.484	2.40 (-5)	0.000	2.53 (-5)	611.397	8.12 (-2)	0.000	8.13 (-2)
		9	692.736	1.99 (-5)	0.000	3.17 (-7)	649.272	4.46 (-2)	0.000	4.46 (-2)
		10				666.892	1.58 (-2)	0.004	1.58 (-2)	
3	2	0	-727.971	0	0.007	0	-850.106	2.97 (-2)	0.002	2.97 (-2)
		1	-354.991	0	0.002	0	-472.902	8.43 (-2)	0.002	8.43 (-2)
		2	-41.538	0	-0.023	0	-151.641	1.39 (-1)	0.016	1.41 (-1)
		3	211.980	2.93 (-3)	0.014	7.21 (-4)	113.152	1.78 (-1)	0.030	1.78 (-1)
		4	406.939	1.21 (-2)	0.252	1.02 (-2)	319.591	2.40 (-1)	0.185	2.33 (-1)
		5	543.214	8.11 (-3)	0.015	7.51 (-3)	473.890	1.79 (-1)	-0.004	1.70 (-1)
		6	631.116	8.57 (-2)	-0.255	3.01 (-3)	576.210	1.28 (-1)	0.058	1.18 (-1)
		7	679.345	1.99 (-3)	0.036	1.48 (-3)	635.519	6.64 (-2)	0.017	6.56 (-2)
		8	701.382	1.21 (-3)	0.051	8.00 (-4)	663.158	2.95 (-2)	0.024	2.63 (-2)
3	1	0	-421.973	0	0.692	0	-523.992	2.07 (-2)	0.650	1.98 (-2)
		1	* -88.692	0	0.590	0	-187.718	5.27 (-2)	0.463	5.30 (-2)
		2	184.644	9.17 (-2)	0.483	8.20 (-2)	92.970	8.36 (-2)	0.359	8.42 (-2)
		3	397.160	8.48 (-2)	0.378	7.93 (-2)	317.117	2.94 (-1) <sup>d</sup>	0.262	2.95 (-1) <sup>d</sup>
		4	549.184	6.26 (-2)	0.244	6.18 (-2)	483.772	2.60 (-1)	0.126	2.44 (-1)
		5	643.938	3.62 (-2)	0.028	3.74 (-2)	593.481	1.65 (-1)	0.252	1.74 (-1)
		6	691.025	2.13 (-2)	-0.393	1.59 (-2)	652.320	1.04 (-1)	-0.580	7.95 (-2)

TABLE BII: continued

3	0	0	-203.844	0			-276.520	5.54 (-2)		
		1	96.882	*0			18.241	3.90 (-2)		
		2	335.225	6.60 (-1)			263.967	1.77 (+0) <sup>d</sup>		
		3	510.348	5.31 (-1)			448.554	1.51 (+0)		
		4	624.462	3.27 (-1)			574.713	1.01 (+0)		
		5	684.050	1.41 (-1)			644.425	4.07 (-1)		
		6	*704.774	*2.91 (-2)			668.328	3.60 (-2)		
$\epsilon$			705.372			669.425				
			-0.147 <sup>a</sup>			-0.800 <sup>a</sup>				
5	5	0	* -114.529	0	0.000	0	-306.902	6.92 (-2)	0.000	6.92 (-2)
		1	304.730	3.82 (-9)	0.000	1.23 (-9)	117.223	1.74 (-1)	0.001	1.74 (-1)
		2	664.545	1.15 (-7)	0.000	0.71 (-9)	484.428	2.77 (-1)	0.000	2.77 (-1)
		3	965.451	6.74 (-4)	0.000	6.73 (-4)	795.096	3.40 (-1)	-0.021	3.35 (-1)
5	4	0	174.714	3.27 (-7)	0.000	1.69 (-7)	-3.112	6.65 (-2)	0.000	6.64 (-2)
		1	562.972	2.06 (-5)	0.000	1.84 (-5)	389.469	3.49 (-1)	0.148	1.81 (-1)
		2	891.314	4.65 (-3)	0.000	4.64 (-3)	725.420	2.97 (-1)	0.002	2.98 (-1)
		3	1159.911	5.24 (-3)	0.000	5.22 (-3)	1004.302	3.73 (-1)	0.000	3.73 (-1)
5	3	0	417.711	1.85 (-3)	0.084	2.56 (-3)	254.897	3.75 (-2)	-0.008	3.62 (-2)
		1	778.160	1.89 (-2)	0.002	1.83 (-2)	619.276	9.82 (-2)	0.013	1.03 (-1)
		2	1077.956	2.40 (-2)	-0.001	2.54 (-2)	926.338	2.14 (-1)	0.002	2.11 (-1)
5	2	0	608.285	1.63 (-4)	0.160	1.09 (-5)	459.550	3.74 (-2)	0.066	1.20 (-2)
		1	946.235	1.14 (-1)	0.136	7.84 (-2)	800.780	1.44 (-1)	0.084	1.15 (-1)
5	1	0	735.651	1.32	6.612	3.05 (-1)	602.791	4.52 (-2)	4.649	4.85 (-3)
		1	1059.582	2.02	5.378	5.22 (-1)	928.766	1.50	4.170	2.18 (-1)
5	0	0	* 799.754	* 7.58			* 679.742	* 1.26		
		1	*1120.386	*12.0			*1000.814	*12.0		
$\epsilon$			1739.815				1650.598			
			-0.375 <sup>a</sup>				-2.158 <sup>a</sup>			

<sup>a</sup>Deviation of the threshold position from the accurate value for H<sub>2</sub><sup>1</sup>.

<sup>b</sup>All  $\Gamma > 0$  widths in the column are due to rotational predissociation.

<sup>c</sup>Widths of levels below  $v=1 j=1$  are due to vibrational predissociation.

<sup>d</sup>Increased due to fast rotational predissociation to  $v=1 j=1$  channel.

## COMMENTS

As indicated with the shaded strips in the captions of the above tables, the term ‘vibrational’ is used here (and also in Part C of this material) to name the  $J=k$  levels. Purely vibrational energy is represented, of course, only by the  $J=0$  ones.

A number of ro-vibrational states with low  $J$ -values ( $\leq 5$ ) were determined from the same PES in Ref. 2. New results in Tables BI and BII are the energies and widths of all quasi-bound states assigned with  $k > 0$  and the energies and widths of bound and quasi-bound  $k=0$  states marked with an asterisk. The symbol \*0 in the width column means that the bound state was presented in Ref. 2 as a resonance, in some cases having even quite a large width. Generally, the widths of the  $J=0$  resonances determined there agree very well with the present values. However, in some ( $v_r b v_R$ ) cases, like (108), (026), (041), (141), they are substantially (at least 3 times) larger. Evidently, the stabilization method used in Ref. 2 has a difficulty with accounting for the impact of the higher  $v j$  thresholds on stability of the states.

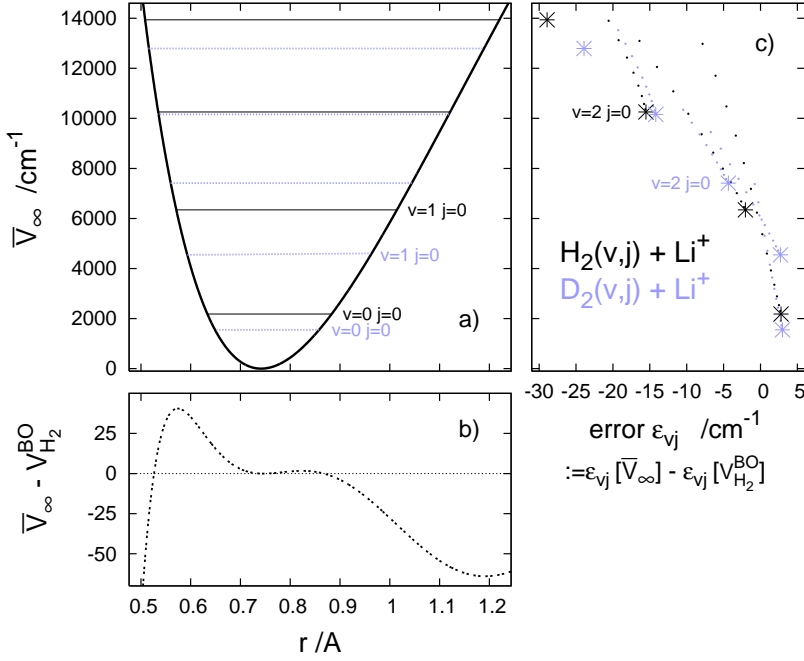


**Fig. B1.** Accuracy of the PES of the ground electronic state of the  $\text{LiHH}^+$  system<sup>2</sup> in the  $\text{H}_2 + \text{Li}^+$  fragmentation region.

(a) 1D cut of the surface  $\bar{V}(r, R, \theta)$  at  $R=R_\infty=50$  Å. Several lowest vibrational energy levels of  $\text{H}_2$  and  $\text{D}_2$  (blue) in the potential  $\bar{V}(r, R_\infty, \theta) := \bar{V}_\infty(r)$ .

(b) Comparison of  $\bar{V}_\infty$  with the Born-Oppenheimer potential of  $\text{H}_2$  (taken from Ref. 3).

(c) Deviations of vibration-rotation energies of  $\text{H}_2(\text{D}_2)$  resulting from the two potentials.  $y$ -coordinates of the error points are the energies in the potential  $\bar{V}_\infty$ .

## COMMENT

The errors of the threshold positions for fragmentation of the  $\text{Li}^+ - \text{H}_2(\text{D}_2)$  complexes displayed in panel c) are believed to adequately reflect the accuracy of the asymptotic region of the used PES of  $\text{LiHH}^+$ . The lowest threshold, the zero-point energy of  $\text{H}_2$  ( $\text{D}_2$ ) taking the values of 2183.27 (1549.85)  $\text{cm}^{-1}$ , appear too high by 2.87 (2.97)  $\text{cm}^{-1}$  [by 4.0 (3.3)  $\text{cm}^{-1}$  if compared to the “experimental ZPEs” given in Ref. 4]. The positions of higher thresholds,  $\epsilon_{vj} - \epsilon_{00}$ , are too low by 0.093 (0.042), 0.278 (0.127), 0.921 (0.413), 4.832 (0.278), 5.402 (0.573), and 18.30 (4.45)  $\text{cm}^{-1}$  for  $(v, j) = (0, 1)$ ,  $(0, 2)$ ,  $(0, 4)$ ,  $(1, 0)$ ,  $(1, 2)$ , and  $(2, 0)$ , respectively. The errors of  $\epsilon_{00}$  and of  $\epsilon_{10} - \epsilon_{00}$  for  $\text{H}_2$  are considerably larger than the deviations of the calculated  $v_r=0 \rightarrow 1$  transition energies from the experimental data [all within the  $-1$  to  $1$   $\text{cm}^{-1}$  range, as shown in Fig. 4 of the paper]. Evidently, the PES is much more accurate in the well region than it is in the fragmentation region.

TABLE BIII:  $\text{Li}^+-\text{H}_2$  versus  $\text{Li}^+-\text{D}_2$ . Positions of  $J=0$  levels above the PES minimum in vibrational states  $[v_r 0 0]$ ,  $[0 v_\theta 0]$ , and  $[0 0 v_R]$  with  $v_r=0-2$ ,  $v_\theta(:=b-k)=0-2$  and  $v_R=0-2$  represented by the diatomic-molecule formula:  $G^m(v_m) = \omega_e^m (v_m + \frac{1}{2}) - \omega_e^m x_e^m (v_m + \frac{1}{2})^2$  for  $m=r, \theta, R$ . Comparison with results from other PESs.

	$m$	$\omega_e^m$	$\omega_e^m x_e^m$	$(X(\text{Ref. } \ddagger)/X - 1) \times 100\%$	
				$X = \omega_e^m$	$X = \omega_e^m x_e^m$
$\text{Li}^+-\text{H}_2$	$r$	4286.8	116.9	[ 2.8] [ 0.5]	[-8.7] [ 9]
	$\theta$	714.8	60.2	[ 0.1] [14.7] {-11.8}	[ 5.6] [44] {-190}
	$R$	465.1	30.0	[-1.1] [11.9] { -1.1}	[ 1.9] [57] {-146}
$\text{Li}^+-\text{D}_2$	$r$	3036.1	60.3	[ 2.8]	[-8.9]
	$\theta$	507.1	29.2	[-0.2] {-11. }	[ 4.8] {-163}
	$R$	370.1	18.5	[-0.2] { -5.2}	[ 6.9] {-118}
$\frac{\text{Li}^+-\text{H}_2}{\text{Li}^+-\text{D}_2}$ ‡	$r$	1.41	1.94		
	$\theta$	1.41	2.06		
	$R$	1.26	1.62		

‡ Deviations within the symbols [ ] concerns the results from Ref. 5, in square brackets — from Ref. 6, in braces — from Refs. 7 and 8.

‡ The ratios of the constants for the two complexes. The ratios of  $\omega_e^m$  and  $\omega_e^m x_e^m$  for the  $m=r, \theta$  modes compare well with the mass factors  $\sqrt{\frac{m_{\text{DD}}}{m_{\text{HH}}}}$  and  $\frac{m_{\text{DD}}}{m_{\text{HH}}}=1.999$ , respectively, and in the case of the  $R$ -mode they are close to  $\sqrt{\frac{\mu_{\text{Li}^+-\text{DD}}}{\mu_{\text{Li}^+-\text{HH}}}}$  and  $\frac{\mu_{\text{Li}^+-\text{DD}}}{\mu_{\text{Li}^+-\text{HH}}}=1.635$ , respectively.

## COMMENTS

Table I of the paper is extended here with comparison of results from two more PESs, of Refs. 6 and 7, respectively. Not enough energies were generated from these PESs to make the comparison in terms of the same parameters as in Table I; hence the less adequate formula, neglecting mode's coupling, is exploited. Nevertheless, a context is provided to appreciate the consistency of the present PES and the PES of Ref. 5 in describing the two intermolecular modes; the deviations of the parameters  $\omega_e^\theta$ ,  $\omega_e^R$ ,  $\omega_e^\theta x_e^\theta$ , and  $\omega_e^R x_e^R$  resulting from these PESs are by far smaller ( $>10$  or even  $\gg 10$  times smaller) than the deviations with results from the other two PESs. This consistency is a positive sign, supporting our belief that results of the present calculations on the excited vibrational states of the complexes are reasonably accurate and may therefore be useful.

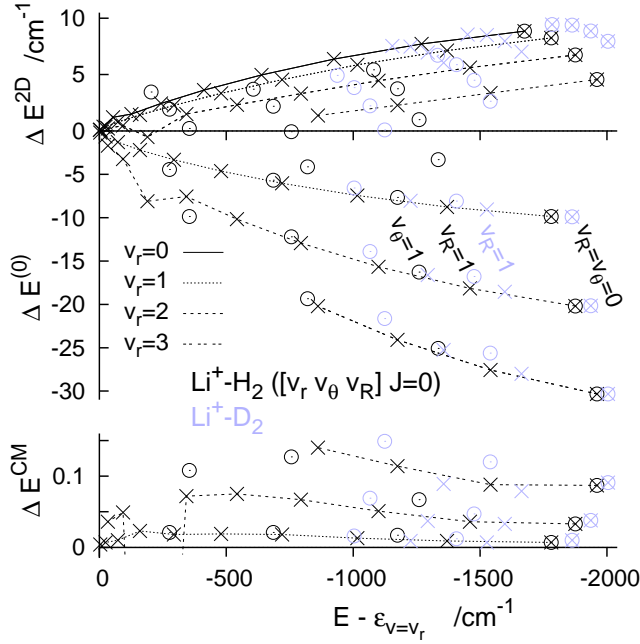
The sum  $\sum_m G^m(0)$  should be a good approximation to the ZPE value of a given complex on a given PES. Indeed, the values 2681.6 and 1929.6  $\text{cm}^{-1}$  obtained for  $\text{Li}^+-\text{H}_2$  and  $\text{Li}^+-\text{D}_2$ , respectively, from the parameters listed in columns ' $\omega_e^m$ ' and ' $\omega_e^m x_e^m$ ', are only by 0.6 and 0.36% larger than the 'exact' values, see the caption of Fig. 1.

No energies have been calculated from the PES of Ref. 6 for the  $\text{Li}^+-\text{D}_2$  complex. However, an estimation of the ZPE value for this complex on this PES can be obtained from the respective parameters  $\omega_e^m$  and  $\omega_e^m x_e^m$  for  $\text{Li}^+-\text{H}_2$  (not listed explicitly) by scaling them with the mass factors described in footnote ‡. The result, 1982.9  $\text{cm}^{-1}$ , is exploited in the description of the electronic structure input, in Sec. IIIB.



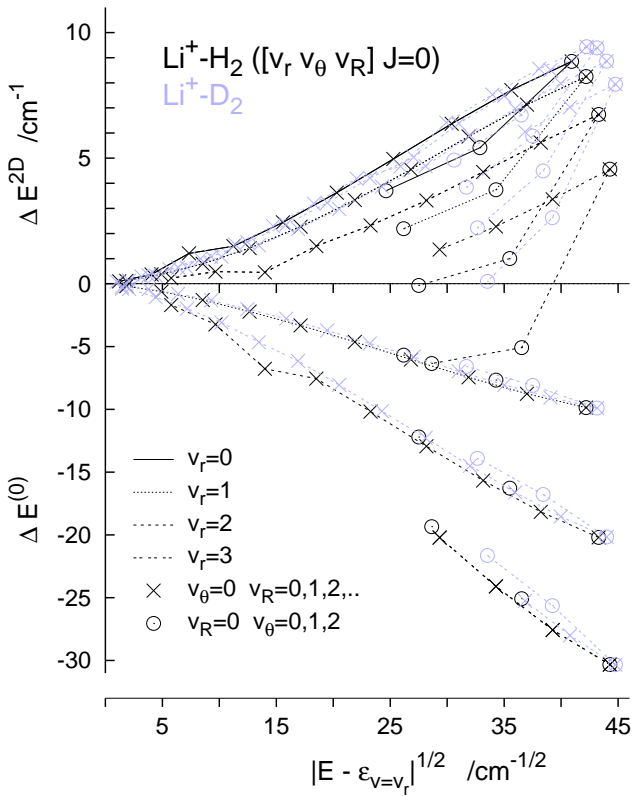
**Fig. B2.** Accuracy of 2D approximation  
in determination of vibrational energy levels

**B2a.** 2D versus 3D-CM approach



Shown are errors of energies obtained with the two approaches for  $J=0$  levels in various vibrational states  $[v_r v_\theta 0]$  and  $[v_r 0 v_R]$  of the  $\text{Li}^+-\text{H}_2$  ( $\text{D}_2$ ) complexes. The errors are defined as deviations from 3D ‘exact’ values ( $E$ ),  $\Delta E^a = E^a - E$  for  $a=2\text{D}, (0), \text{CM}$ . The superscript ‘(0)’ stands for 0-th order approximations to predissociating states ( $v_r > 0$ ) within the 3D-CM approach (bound states in appropriate  $Q$ -subspaces, chosen as described in Sec. III.A). In bound states cases (all  $v_r=0$  states shown here),  $E^{(0)}=E$  and the error  $\Delta E^{(0)}$  is strictly zero.

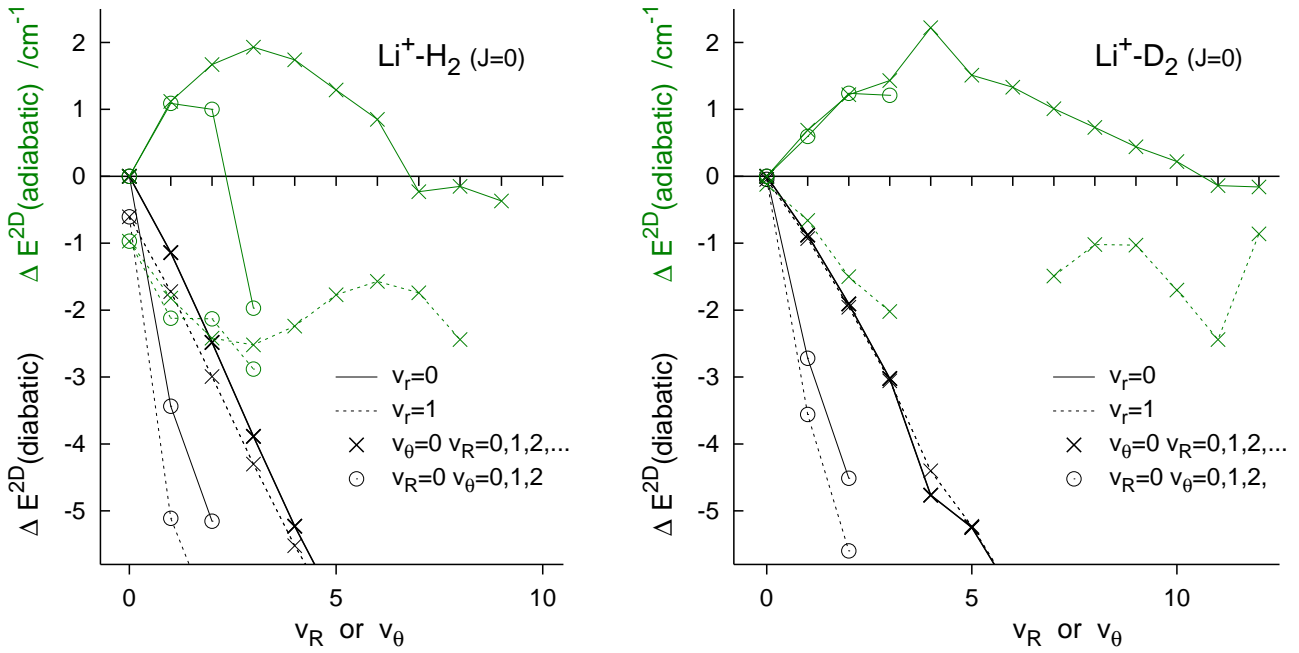
Obviously, the errors  $\Delta E^{2D}$  are, on average, much larger than  $\Delta E^{CM}$ . Really disadvantageous is, however, the fact that they vary so strongly with the numbers  $v_\theta$  and  $v_R$ . This variation translates into the substantial errors of the 2D transitions frequencies shown in Table II of the paper.



Errors  $\Delta E^{2D}$  and  $\Delta E^{(0)}$  as functions of square root of the binding energy in the  $Q$ -subspace.

The energies  $E^{(0)}$  of states with a given  $v_r > 0$  represent convergent results in the respective  $Q$ -subspace, i.e. they account for all important interactions within and between the  $v=v_r$  and  $v > v_r$  vibrational channels. Actually, the inter-channel interactions are strongly dominated by the  $v=v_r \leftrightarrow v=v_r+1$  ones. Some regularities are displayed by the errors  $\Delta E^{(0)}$  of states in the sequences  $[v_r 0 v_R=0, 1, \dots]$  and  $[v_r v_\theta=0, 1, 2 v_R=0]$ : the crosses and circles, black and blue, lie nearly on the same nearly straight lines with slopes nearly proportional to  $v_r$ . The energies  $E^{2D}$  disregard all, in particular the  $v=v_r \leftrightarrow v=v_r+1$ , vibrational couplings in the  $Q$ -subspace. In consequence, the errors  $\Delta E^{2D}$  show much less regularities in their dependencies on the quantum numbers, stronger variation with the number  $v_\theta$ , and larger sensitivity to the  $\text{H}_2 \rightarrow \text{D}_2$  substitution.

## B2b. 2D diabatic versus 2D adiabatic approach



The errors  $\Delta E^{2D}$  of part a) of the figure are shown here relative to the error of [000] state and as functions of the vibrational numbers  $v_R$  or  $v_\theta$ . The errors  $\Delta E^{2D}(\text{adiabatic})$  concern results obtained in Ref. 2 by exploiting an adiabatic separation scheme of intra- and intermolecular vibrations in atom-diatom complexes.

The adiabatic separation scheme of Ref. 2 is capable of providing reasonably accurate energies of all vibrational states of the present complexes provided the energies do not come too close together. /Such situation occurs in the case of states [104–6] of the  $\text{Li}^+-\text{D}_2$  complex. Their errors  $\Delta E^{2D}(\text{adiabatic})$  are not shown in the figure because of ‘wild’ behavior caused by crossing with states [120–2] and [140], cf. Table CI (in Part C, Ref. 9)./

The diabatic decoupling is much simpler to implement but reasonable accuracy,  $|\Delta E^{2D}|$  below  $2 \text{ cm}^{-1}$ , may be expected only in determining transition energies of low  $\Delta v$  transitions.

## ROTATIONAL ENERGY LEVELS

TABLE BIV:  $\text{Li}^+\text{-H}_2$ . Positions ( $E$ ) and widths ( $\Gamma$ ) of rotational levels ( $J$ ) in thirty groups ( $bk v_R$ ) below  $v=0 j=0$  and  $v=1 j=0$  thresholds.  $E=0$  is at the lowest threshold. All data are in  $\text{cm}^{-1}$ . ( $v_r \sim v$ ,  $e \sim p=1$ , and  $f \sim p = -1$ )<sup>a</sup>.

$b$	$k$	$v_R$	$J$	$v_r=0$				$v_r=1$			
				$E(e)$	$\Gamma(e)$	$E(f)-E(e)$	$\Gamma(f)$	$E(e)$	$\Gamma(e)^b$	$E(f)-E(e)$	$\Gamma(f)$
0	0	0	0	-1674.606				2378.491	2.37 (-2)		
			1	-1669.651				2383.418	2.33 (-2)		
			2	-1659.749				2393.270	2.98 (-2)		
			3	-1644.915				2408.018	2.26 (-2)		
			4	-1625.174				2427.653	2.31 (-2)		
			5	-1600.557				2452.139	2.42 (-2)		
			6	-1571.104				2481.439	2.33 (-2)		
			7	-1536.861				2515.506	2.24 (-2)		
			8	-1497.885				2554.287	2.13 (-2)		
			9	-1454.239				2597.720	2.02 (-2)		
			10	-1405.997				2645.735	1.91 (-2)		
			11	-1353.239				2698.256	1.78 (-2)		
			12	-1296.054				2755.196	1.65 (-2)		
			13	-1234.542				2816.461	1.52 (-2)		
			14	-1168.810				2881.947	1.39 (-2)		
			15	-1098.977				2951.542	1.27 (-2)		
			16	-1025.171				3025.126	1.13 (-2)		
			17	-947.531				3102.565	1.01 (-2)		
			18	-866.209				3183.718	8.96 (-3)		
			19	-781.367				3268.430	8.01 (-3)		
			20	-693.185				3356.540	6.61 (-3)		
			21	-601.856				3447.862	5.68 (-3)		
			22	-507.593				3542.204	4.81 (-3)		
			23	-410.629				3639.353	4.01 (-3)		
			24	-311.223				3739.078	3.27 (-3)		
			25	-209.665				3841.120	2.62 (-3)		
26	-106.285				3945.193	2.07 (-3)					
1	1	0	1	-1606.666		0.150		2442.362	2.49 (-2)	0.152	2.49 (-2)
			2	-1596.937		0.449		2452.038	2.46 (-2)	0.455	2.46 (-2)
			3	-1582.361		0.897		2466.531	2.44 (-2)	0.910	2.41 (-2)
			4	-1562.961		1.489		2485.847	3.36 (-2)	1.489	2.35 (-2)
			5	-1538.764		2.224		2509.903	2.38 (-2)	2.242	2.29 (-2)
			6	-1509.809		3.097		2538.705	2.25 (-2)	3.125	2.23 (-2)
			7	-1476.140		4.105		2572.202	2.14 (-2)	4.134	2.52 (-2)
			8	-1437.807		5.241		2610.343	2.03 (-2)	5.325	2.99 (-2)
			9	-1394.871		6.499		2653.072	1.92 (-2)	6.584	2.05 (-2)
			10	-1347.400		7.873		2700.310	1.87 (-2)	7.985	1.84 (-2)
			11	-1295.468		9.355		2752.016	1.67 (-2)	9.481	1.69 (-2)
			12	-1239.159		10.936		2808.084	1.55 (-2)	11.087	1.57 (-2)
			13	-1178.568		12.607		2868.438	1.50 (-2)	12.779	1.43 (-2)
			14	-1113.794		14.359		2932.971	1.31 (-2)	14.559	1.32 (-2)
			15	-1044.950		16.180		3001.580	1.24 (-2)	16.420	1.18 (-2)
			16	-972.157		18.059		3074.158	1.06 (-2)	18.324	1.54 (-2)
			17	-895.546		19.983		3150.572	9.41 (-3)	20.298	9.43 (-3)
			18	-815.262		21.939		3230.688	8.48 (-3)	22.300	8.27 (-3)
			19	-731.459		23.912		3314.365	8.35 (-3)	24.321	7.55 (-3)
			20	-644.309		25.886		3401.439	7.17 (-3)	26.352	7.16 (-3)
			21	-553.994		27.845		3491.740	6.19 (-3)	28.373	6.04 (-3)
			22	-460.719		29.769		3585.083	5.24 (-3)	30.367	5.55 (-3)
			23	-364.705		31.638		3681.263	4.42 (-3)	32.316	4.66 (-3)
			24	-266.199		33.428		3780.058	3.98 (-3)	34.197	3.87 (-3)
			25	-165.475		35.113		3881.222	3.33 (-3)	35.988	3.17 (-3)
			26	-62.844		36.661		3984.483	2.71 (-3)	37.660	2.56 (-3)
			27	41.336 <sup>c</sup>		38.031		4089.531	2.20 (-3)	39.181	2.03 (-3)

TABLE BIV: continued

2	2	0	2	-1410.848		0.000	2626.803	2.88 (-2)	0.000	2.88 (-2)
			3	-1396.149		0.000	2641.436	2.83 (-2)	0.000	2.83 (-2)
			4	-1376.585		0.000	2660.913	2.77 (-2)	-0.001	2.77 (-2)
			5	-1352.186		0.000	2685.205	2.69 (-2)	-0.002	2.69 (-2)
			6	-1322.991		0.000	2714.276	2.59 (-2)	-0.004	2.60 (-2)
			7	-1289.045		0.001	2748.083	2.49 (-2)	-0.007	2.49 (-2)
			8	-1250.400		0.003	2786.573	2.37 (-2)	-0.010	2.38 (-2)
			9	-1207.121		0.005	2829.687	2.25 (-2)	-0.015	2.25 (-2)
			10	-1159.275		0.010	2877.360	2.12 (-2)	-0.020	2.12 (-2)
			11	-1106.943		0.018	2929.514	1.98 (-2)	-0.025	1.98 (-2)
			12	-1050.211		0.031	2986.066	1.83 (-2)	-0.028	1.84 (-2)
			13	-989.178		0.050	3046.935	1.80 (-2)	-0.041	1.70 (-2)
			14	-923.949		0.079	3111.995	1.57 (-2)	-0.038	1.55 (-2)
			15	-854.644		0.120	3181.152	1.41 (-2)	-0.018	1.46 (-2)
			16	-781.390		0.180	3254.280	1.27 (-2)	-0.007	1.27 (-2)
			17	-704.329		0.263	3331.249	1.13 (-2)	0.022	1.14 (-2)
			18	-623.615		0.379	3411.908	1.05 (-2)	0.073	1.00 (-2)
			19	-539.422		0.540	3496.113	8.78 (-3)	0.147	8.88 (-3)
			20	-451.939		0.766	3583.677	7.58 (-3)	0.260	7.64 (-3)
			21	-361.387		1.086	3674.419	6.39 (-3)	0.422	6.53 (-3)
			22	-268.030		1.562	3768.121	5.49 (-3)	0.659	5.52 (-3)
			23	-172.226		2.327	3864.544	4.37 (-3)	1.005	4.59 (-3)
			24	-74.611		3.767	3963.398	3.86 (-3)	1.522	3.75 (-3)
			25	23.102	7.9 (-27)	7.322	4064.287	3.03 (-3)	2.359	3.11 (-3)
3	3	0	3	-1092.972		0.000	2926.774	3.62 (-2)	0.000	3.62 (-2)
			4	-1073.621		0.000	2946.060	3.93 (-2)	-0.003	3.50 (-2)
			5	-1049.488		0.000	2970.109	3.39 (-2)	-0.002	3.35 (-2)
			6	-1020.610		0.001	2998.893	3.38 (-2)	0.006	3.66 (-2)
			7	-987.033		0.002	3032.363	3.16 (-2)	0.003	3.19 (-2)
			8	-948.809		0.004	3070.471	3.11 (-2)	0.004	3.04 (-2)
			9	-906.001		0.007	3113.157	2.90 (-2)	0.006	2.88 (-2)
			10	-858.677		0.014	3160.353	2.60 (-2)	0.010	2.72 (-2)
			11	-806.917		0.025	3211.987	2.53 (-2)	0.014	2.54 (-2)
			12	-750.810		0.044	3267.973	2.44 (-2)	0.024	2.49 (-2)
			13	-690.454		0.076	3328.219	2.23 (-2)	0.038	2.27 (-2)
			14	-625.964		0.130	3392.624	2.08 (-2)	0.057	2.08 (-2)
			15	-557.470		0.224	3461.077	1.89 (-2)	0.085	1.89 (-2)
			16	-485.139		0.401	3533.456	1.71 (-2)	0.124	1.71 (-2)
			17	-409.227		0.785	3609.629	1.53 (-2)	0.179	1.53 (-2)
			18	-330.323		1.816	3689.449	1.35 (-2)	0.259	1.36 (-2)
			19	-242.940		-2.149	3772.756	1.19 (-2)	0.374	1.19 (-2)
			20	-157.113		-1.248	3859.368	1.03 (-2)	0.545	1.04 (-2)
			21	-67.685		-0.833	3949.070	8.80 (-3)	0.810	8.93 (-3)
			22	24.700		-0.483	4041.593	7.39 (-3)	1.248	7.58 (-3)
			23	117.382		2.093	4136.521	6.00 (-3)	2.064	6.35 (-3)
4	4	0	4	-658.879		0.000	3336.938	4.87 (-2)	0.001	4.87 (-2)
			5	-635.093		0.000	3360.669	4.71 (-2)	0.002	4.70 (-2)
			6	-606.631		0.000	3389.063	4.53 (-2)	0.008	4.46 (-2)
			7	-573.540		0.000	3422.022	1.16 (-1)	0.139	7.01 (-2)
			8	-535.875		0.000	3459.723	4.69 (-2)	-0.023	4.28 (-2)
			9	-493.709		0.002	3501.824	4.09 (-2)	-0.012	3.99 (-2)
			10	-447.010		-0.214	3548.381	3.76 (-2)	-0.007	3.71 (-2)
			11	-395.811		0.006	3599.310	3.28 (-2)	-0.056	4.25 (-2)
			12	-340.602		0.014	3654.537	3.28 (-2)	-0.003	3.20 (-2)
			13	-281.134		0.034	3713.950	2.99 (-2)	-0.002	3.01 (-2)
			14	-217.760		0.253	3777.432	2.72 (-2)	0.005	2.74 (-2)
			15	-149.794		-0.137	3844.541	2.89 (-2)	0.231	2.58 (-2)
			16	-78.385		-0.135	3917.750	3.15 (-2)	-0.070	2.99 (-2)
			17	-3.210		-0.535	3991.982	2.03 (-2)	0.079	2.04 (-2)
			18	75.563	1.22 (-5)	0.185	4070.606	1.74 (-2)	0.149	1.77 (-2)
			19	157.765	1.05 (-4)	0.114	4152.154	1.55 (-2)	0.841	1.71 (-2)
			20	243.213	1.49 (-3)	0.123	4238.690	2.20 (-2)	-0.130	1.90 (-2)

TABLE BIV: continued

0	0	1	0	-1269.455		2789.040	6.84 (-2)		
			1	-1264.932		2793.557	6.80 (-2)		
			2	-1255.894		2802.583	6.72 (-2)		
			3	-1242.358		2816.102	6.60 (-2)		
			4	-1224.349		2834.089	6.44 (-2)		
			5	-1201.903		2856.512	6.25 (-2)		
			6	-1175.060		2883.330	6.03 (-2)		
			7	-1143.873		2914.495	5.77 (-2)		
			8	-1108.402		2949.948	5.49 (-2)		
			9	-1068.717		2989.623	5.20 (-2)		
			10	-1024.898		3033.446	4.88 (-2)		
			11	-977.032		3081.332	4.55 (-2)		
			12	-925.220		3133.187	4.21 (-2)		
			13	-869.572		3188.908	3.86 (-2)		
			14	-810.209		3248.381	3.52 (-2)		
			15	-747.266		3311.480	3.17 (-2)		
			16	-680.887		3378.070	2.84 (-2)		
			17	-611.236		3448.000	2.52 (-2)		
			18	-538.489		3521.106	2.24 (-2)		
			19	-462.838		3597.217	1.89 (-2)		
			20	-384.496		3676.125	1.61 (-2)		
			21	-303.691		3757.624	1.36 (-2)		
			22	-220.657		3841.477	1.23 (-2)		
			23	-135.605		3927.433	9.18 (-3)		
			24	-48.554		4015.218	7.33 (-3)		
1	1	1	1	-1199.367	0.138	2854.758	6.97 (-2)	0.140	6.95 (-2)
			2	-1190.484	0.414	2863.631	7.20 (-2)	0.417	6.87 (-2)
			3	-1177.178	0.826	2876.910	6.77 (-2)	0.842	6.74 (-2)
			4	-1159.475	1.371	2894.592	6.60 (-2)	1.394	6.60 (-2)
			5	-1137.407	2.047	2916.634	6.37 (-2)	2.080	6.40 (-2)
			6	-1111.012	2.848	2942.999	6.12 (-2)	2.895	6.16 (-2)
			7	-1080.341	3.770	2973.636	7.18 (-2)	3.839	5.90 (-2)
			8	-1045.451	4.808	3008.511	5.62 (-2)	4.886	5.60 (-2)
			9	-1006.406	5.954	3047.538	5.28 (-2)	6.053	5.29 (-2)
			10	-963.283	7.201	3090.654	4.97 (-2)	7.286	9.70 (-2)
			11	-916.165	8.541	3137.785	4.60 (-2)	8.693	4.65 (-2)
			12	-865.147	9.965	3188.837	4.28 (-2)	10.145	4.35 (-2)
			13	-810.332	11.461	3243.712	4.07 (-2)	11.675	4.00 (-2)
			14	-751.838	13.020	3302.304	3.71 (-2)	13.271	3.70 (-2)
			15	-689.791	14.629	3364.493	3.36 (-2)	14.923	3.38 (-2)
			16	-624.332	16.274	3430.150	3.05 (-2)	16.616	3.04 (-2)
			17	-555.616	17.940	3499.130	2.70 (-2)	18.337	2.70 (-2)
			18	-483.815	19.613	3571.278	2.37 (-2)	20.072	2.33 (-2)
			19	-409.117	21.273	3646.422	2.06 (-2)	21.803	2.06 (-2)
			20	-331.735	22.900	3724.371	1.77 (-2)	23.512	1.77 (-2)
			21	-251.905	24.472	3804.916	1.50 (-2)	25.178	1.49 (-2)
			22	-169.894	25.962	3887.821	1.25 (-2)	26.778	1.25 (-2)
			23	-86.009	27.337	3972.824	1.03 (-2)	28.284	1.02 (-2)
			24	-0.612	28.556	4059.623	8.26 (-3)	29.664	8.21 (-3)
			25	85.867	29.565	4147.868	6.50 (-3)	30.875	6.46 (-3)

TABLE BIV: continued

2	2	1	2	-1000.198	0.001	3042.371	7.95 (-2)	-0.001	7.94 (-2)
			3	-986.790	0.003	3055.774	7.80 (-2)	0.001	7.80 (-2)
			4	-968.951	0.008	3073.610	7.80 (-2)	0.004	7.62 (-2)
			5	-946.715	0.019	3095.844	7.39 (-2)	0.010	7.40 (-2)
			6	-920.126	0.036	3122.438	7.13 (-2)	0.020	7.13 (-2)
			7	-889.232	0.064	3153.342	6.84 (-2)	0.036	6.84 (-2)
			8	-854.096	0.103	3188.499	6.51 (-2)	0.060	6.52 (-2)
			9	-814.787	0.158	3227.844	6.16 (-2)	0.093	6.17 (-2)
			10	-771.384	0.232	3271.301	5.79 (-2)	0.140	5.80 (-2)
			11	-723.978	0.329	3318.815	5.41 (-2)	0.173	5.41 (-2)
			12	-672.671	0.456	3370.209	5.02 (-2)	0.272	5.10 (-2)
			13	-617.579	0.622	3425.456	4.60 (-2)	0.391	4.64 (-2)
			14	-558.834	0.841	3484.415	4.19 (-2)	0.525	4.21 (-2)
			15	-496.592	1.139	3546.955	3.78 (-2)	0.701	3.80 (-2)
			16	-431.050	1.571	3612.929	3.42 (-2)	0.932	3.52 (-2)
			17	-362.497	2.268	3682.168	3.02 (-2)	1.234	3.04 (-2)
			18	-291.514	3.637	3754.477	2.64 (-2)	1.649	2.66 (-2)
			19	-219.661	7.046	3829.595	2.42 (-2)	2.262	2.31 (-2)
			20	-132.528	-2.125	3907.125	1.98 (-2)	3.276	1.98 (-2)
			21	-53.772	-0.457	3986.246	1.73 (-2)	5.298	1.68 (-2)
3	3	1	3	-679.058	0.000	3345.578	9.86 (-2)	0.000	9.86 (-2)
			4	-661.329	0.000	3363.350	9.60 (-2)	0.001	9.60 (-2)
			5	-639.226	0.000	3385.511	9.27 (-2)	0.002	9.27 (-2)
			6	-612.787	-0.001	3412.023	8.89 (-2)	0.009	8.89 (-2)
			7	-582.059	-0.002	3442.837	8.46 (-2)	0.026	8.46 (-2)
			8	-547.095	-0.003	3477.884	7.98 (-2)	0.075	7.97 (-2)
			9	-507.958	-0.006	3517.044	7.43 (-2)	0.221	7.45 (-2)
			10	-464.718	-0.008	3559.981	6.59 (-2)	0.738	6.88 (-2)
			11	-417.453	-0.008	3609.656	5.08 (-2)	-1.400	6.28 (-2)
			12	-366.253	-0.003	3660.830	5.01 (-2)	-1.024	5.65 (-2)
			13	-311.216	0.016	3716.218	4.57 (-2)	-0.924	5.00 (-2)
			14	-252.461	0.069	3775.524	4.02 (-2)	-0.879	4.34 (-2)
			15	-190.164	0.216	3838.582	3.47 (-2)	-0.803	3.68 (-2)
			16	-125.193	1.100	3905.240	2.92 (-2)	-0.628	3.05 (-2)
			17	-54.088	2.261	3975.322	2.39 (-2)	-0.281	2.45 (-2)
			18	18.102	1.546	4048.581	2.00 (-2)	0.357	2.17 (-2)
			19	93.462	2.548	4127.522	2.61 (-2)	-1.621	1.50 (-2)
0	0	2	0	-924.249		3142.481	1.12 (-1)		
			1	-920.179		3146.569	1.12 (-1)		
			2	-912.049		3154.737	1.10 (-1)		
			3	-899.876		3166.966	1.08 (-1)		
			4	-883.690		3183.232	1.05 (-1)		
			5	-863.527		3203.498	1.02 (-1)		
			6	-839.434		3227.720	9.82 (-2)		
			7	-811.469		3255.845	9.32 (-2)		
			8	-779.697		3287.808	8.92 (-2)		
			9	-744.195		3323.539	8.41 (-2)		
			10	-705.052		3362.953	7.87 (-2)		
			11	-662.363		3405.959	7.30 (-2)		
			12	-616.233		3452.453	6.68 (-2)		
			13	-566.768		3502.322	6.18 (-2)		
			14	-514.045		3555.441	5.59 (-2)		
			15	-457.868		3611.680	5.00 (-2)		
			16	-401.665		3670.927	4.43 (-2)		
			17	-339.605		3733.213	3.82 (-2)		
			18	-275.138		3795.315	2.31 (-2)		
			19	-219.661		3863.435	2.59 (-2)		
			20	-149.195		3933.004	2.47 (-2)		
			21	-79.554		4005.122	1.84 (-2)		
			22	-9.790		4081.287	1.44 (-2)		

TABLE BIV: continued

1	1	2	1	-851.638	0.125	3210.390	1.17 (-1)	0.127	1.17 (-1)
			2	-843.642	0.373	3218.420	1.16 (-1)	0.381	1.16 (-1)
			3	-831.671	0.743	3230.444	1.13 (-1)	0.759	1.14 (-1)
			4	-815.750	1.232	3246.437	1.11 (-1)	1.259	1.11 (-1)
			5	-795.917	1.837	3266.366	1.08 (-1)	1.877	1.08 (-1)
			6	-772.214	2.554	3290.188	1.04 (-1)	2.610	1.04 (-1)
			7	-744.698	3.376	3317.853	9.92 (-2)	3.452	9.93 (-2)
			8	-713.433	4.297	3349.300	9.42 (-2)	4.397	9.43 (-2)
			9	-678.492	5.311	3384.459	8.89 (-2)	5.437	8.90 (-2)
			10	-639.962	6.409	3423.252	8.32 (-2)	6.565	8.34 (-2)
			11	-597.940	7.582	3465.588	7.74 (-2)	7.773	7.75 (-2)
			12	-552.534	8.818	3511.366	7.13 (-2)	9.049	7.14 (-2)
			13	-503.868	10.108	3560.475	6.52 (-2)	10.383	6.53 (-2)
			14	-452.078	11.437	3612.790	5.91 (-2)	11.762	5.92 (-2)
			15	-397.319	12.791	3668.171	5.30 (-2)	13.173	5.31 (-2)
			16	-339.762	14.153	3726.463	4.71 (-2)	14.602	4.71 (-2)
			17	-279.601	15.505	3787.494	4.14 (-2)	16.030	4.13 (-2)
			18	-217.055	16.826	3851.072	3.59 (-2)	17.439	3.58 (-2)
			19	-152.374	18.088	3916.980	3.07 (-2)	18.806	3.05 (-2)
			20	-85.841	19.260	3984.972	2.59 (-2)	20.106	2.57 (-2)
			21	-17.784	20.291	4054.768	2.14 (-2)	21.307	2.12 (-2)
			22	51.470	21.065	4126.041	1.74 (-2)	22.367	1.71 (-2)
2	2	2	2	-649.119	0.001	3401.118	1.32 (-1)	0.003	1.32 (-1)
			3	-637.051	0.005	3413.249	1.30 (-1)	0.006	1.30 (-1)
			4	-621.007	0.017	3429.383	1.27 (-1)	0.011	1.27 (-1)
			5	-601.028	0.041	3449.483	1.23 (-1)	0.022	1.23 (-1)
			6	-577.169	0.090	3473.503	1.18 (-1)	0.043	1.18 (-1)
			7	-549.511	0.190	3501.389	1.13 (-1)	0.078	1.13 (-1)
			8	-518.204	0.432	3533.072	1.08 (-1)	0.133	1.08 (-1)
			9	-483.809	1.311	3568.481	1.02 (-1)	0.140	1.40 (-1)
			10	-442.669	-0.796	3607.509	9.53 (-2)	0.339	9.55 (-2)
			11	-401.044	-0.424	3650.047	8.86 (-2)	0.537	8.87 (-2)
			12	-355.359	-0.205	3695.926	8.17 (-2)	0.872	8.18 (-2)
			13	-306.407	-0.035	3744.842	7.53 (-2)	1.543	7.50 (-2)
			14	-254.311	0.132	3795.971	6.70 (-2)	3.267	6.77 (-2)
			15	-199.239	0.314	3857.450	5.93 (-2)	-2.116	6.00 (-2)
			16	-141.372	0.525	3913.640	4.41 (-2)	-0.965	4.68 (-2)
			17	-80.919	0.779	3975.490	4.94 (-2)	-0.433	4.69 (-2)
			18	-18.127	1.105	4039.274	4.08 (-2)	0.038	4.12 (-2)
0	0	3	0	-638.892		3438.954	1.46 (-1)		
			1	-635.309		3442.611	1.42 (-1)		
			2	-628.151		3449.919	1.40 (-1)		
			3	-617.437		3460.895	1.35 (-1)		
			4	-603.196		3475.668	1.20 (-1)		
			5	-585.466		3492.564	1.07 (-1)		
			6	-564.292		3514.313	1.17 (-1)		
			7	-539.716		3539.322	1.14 (-1)		
			8	-511.733		3567.645	1.09 (-1)		
			9	-479.940		3599.232	1.03 (-1)		
			10	-448.276		3634.010	9.60 (-2)		
			11	-410.795		3671.893	8.85 (-2)		
			12	-370.880		3712.825	8.12 (-2)		
			13	-328.396		3756.854	7.36 (-2)		
			14	-283.483		3804.542	6.62 (-2)		
			15	-236.344		3857.450	5.93 (-2)		
			16	-187.223		3913.640	4.41 (-2)		
			17	-136.414		3975.490	4.92 (-2)		
			18	-84.278		4039.274	4.08 (-2)		
			19	-31.263		4105.381	3.54 (-2)		
			20	22.034	1.1 (-14)	4173.532	2.98 (-2)		



TABLE BIV: continued

1	1	3	1	-563.320		0.109	3509.361	1.51 (-1)	0.112	1.51 (-1)
			2	-556.260		0.327	3516.511	1.49 (-1)	0.336	1.49 (-1)
			3	-545.696		0.650	3527.211	1.46 (-1)	0.670	1.46 (-1)
			4	-531.657		1.078	3541.436	1.42 (-1)	1.110	1.42 (-1)
			5	-514.186		1.604	3559.146	1.37 (-1)	1.653	1.37 (-1)
			6	-493.332		2.226	3580.294	1.32 (-1)	2.295	1.32 (-1)
			7	-469.159		2.936	3604.822	1.26 (-1)	3.029	1.26 (-1)
			8	-441.743		3.728	3632.663	1.19 (-1)	3.849	1.19 (-1)
			9	-411.169		4.593	3663.734	1.12 (-1)	4.747	1.12 (-1)
			10	-377.538		5.523	3697.947	1.04 (-1)	5.714	1.04 (-1)
			11	-340.966		6.506	3735.197	9.60 (-2)	6.740	9.61 (-2)
			12	-301.582		7.529	3775.364	8.78 (-2)	7.813	8.79 (-2)
			13	-259.533		8.578	3818.316	7.95 (-2)	8.921	7.95 (-2)
			14	-214.975		9.630	3863.903	7.13 (-2)	10.049	7.12 (-2)
			15	-168.045		10.633	3911.956	6.32 (-2)	11.178	6.34 (-2)
			16	-118.228		10.964	3962.288	5.52 (-2)	12.289	5.50 (-2)
			17	-69.354		17.528	4014.695	4.77 (-2)	13.348	4.73 (-2)
			18	-17.066		13.365	4069.019	4.05 (-2)	14.273	4.01 (-2)
			19	36.229		14.268	4122.338	2.33 (-2)	17.919	3.31 (-2)
			20	90.106		14.820	4179.096	2.61 (-2)	17.526	2.36 (-2)
1	0	0	0	-1080.273			2983.914	1.67 (-2)		
			1	-1075.617			2988.535	2.28 (-2)		
			2	-1066.314			2997.754	2.22 (-2)		
			3	-1052.379			3011.562	2.15 (-2)		
			4	-1033.839			3029.936	2.05 (-2)		
			5	-1010.726			3052.844	1.99 (-2)		
			6	-983.082			3080.246	1.76 (-2)		
			7	-950.958			3112.098	2.14 (-2)		
			8	-914.412			3148.334	1.52 (-2)		
			9	-873.514			3188.900	1.63 (-2)		
			10	-828.338			3233.718	1.81 (-2)		
			11	-778.971			3282.707	1.48 (-2)		
			12	-725.507			3335.782	1.63 (-2)		
			13	-668.049			3392.838	1.45 (-2)		
			14	-606.706			3453.768	1.31 (-2)		
			15	-541.592			3518.453	1.17 (-2)		
			16	-472.808			3586.766	1.04 (-2)		
			17	-400.389			3658.565	9.12 (-3)		
			18	-324.069			3733.702	7.90 (-3)		
			19	-249.689			3812.015	6.76 (-3)		
			20	-167.605			3893.331	5.70 (-3)		
			21	-83.423			3977.478	4.76 (-3)		
			22	2.932			4064.295	3.94 (-3)		
			23	91.234			4153.709	3.31 (-3)		
			24	180.973	4.5 (-12)		4245.960	3.01 (-3)		
			25	272.698	2.69 (-4)		4340.977	3.78 (-3)		
2	1	0	1	-982.522		0.266	3072.311	2.21 (-2)	0.262	2.31 (-2)
			2	-973.512		0.797	3081.277	2.32 (-2)	0.751	2.38 (-2)
			3	-960.014		1.589	3094.699	2.37 (-2)	1.483	2.38 (-2)
			4	-942.051		2.639	3112.551	2.33 (-2)	2.464	2.34 (-2)
			5	-919.653		3.940	3134.810	2.24 (-2)	3.683	2.29 (-2)
			6	-892.856		5.487	3161.443	2.14 (-2)	5.133	2.21 (-2)
			7	-861.705		7.273	3192.407	2.02 (-2)	6.808	2.12 (-2)
			8	-826.253		9.288	3227.652	1.88 (-2)	8.702	2.02 (-2)
			9	-786.563		11.526	3267.117	1.67 (-2)	10.808	1.92 (-2)
			10	-742.704		13.977	3310.753	1.95 (-2)	13.110	2.00 (-2)
			11	-694.758		16.635	3358.456	1.60 (-2)	15.464	1.76 (-2)
			12	-642.818		19.493	3410.162	1.42 (-2)	18.252	1.35 (-2)
			13	-586.999		22.558	3465.772	1.24 (-2)	21.108	1.26 (-2)
			14	-527.465		25.874	3525.177	9.90 (-3)	24.133	1.19 (-2)
			15	-464.670		29.763	3588.270	9.78 (-3)	27.310	1.03 (-2)

TABLE BIV: continued

			16	-395.450		30.915		3654.875	9.07 (-3)	30.683	9.10 (-3)
			17	-325.854		35.224		3724.661	8.10 (-3)	34.437	7.89 (-3)
			18	-252.428		39.060		3800.555	1.96 (-2)	35.487	6.97 (-3)
			19	-175.809		42.871		3876.013	8.47 (-3)	40.199	5.60 (-3)
			20	-96.258		46.707		3955.381	6.62 (-3)	44.041	5.18 (-3)
			21	-14.007		50.568		4037.662	4.39 (-3)	47.798	4.05 (-3)
			22	70.692	6.8 (-10)	54.444		4122.555	7.68 (-3)	51.544	3.86 (-3)
			23	157.469	1.86 (-2)	58.410		4209.802	4.16 (-3)	55.273	3.08 (-3)
			24	246.512	2.86 (-1)	61.936		4299.111	3.38 (-3)	58.993	2.34 (-3)
			25	336.889	2.50 (-1)	65.552	1.4 (-18)	4390.276	5.71 (-1)	62.577	1.78 (-3)
			26	428.389	2.19 (-1)	68.968	2.13 (-7)	4482.914	2.45 (-1)	66.018	2.00 (-3)
3	2	0	2	-727.971		0.007		3308.465	2.97 (-2)	0.002	2.97 (-2)
			3	-714.296		0.043		3322.059	2.95 (-2)	0.009	2.95 (-2)
			4	-696.172		0.166		3340.140	2.92 (-2)	0.026	2.92 (-2)
			5	-673.836 <sup>d</sup>		0.583 <sup>d</sup>		3362.672	2.89 (-2)	0.063	2.89 (-2)
			6	-644.629 <sup>d</sup>		-1.403 <sup>d</sup>		3389.602	2.85 (-2)	0.129	2.85 (-2)
			7	-613.409		-0.980		3420.871	2.81 (-2)	0.238	2.81 (-2)
			8	-577.577		-0.799		3456.403	2.77 (-2)	0.411	2.78 (-2)
			9	-537.395		-0.664		3496.104	2.73 (-2)	0.675	2.74 (-2)
			10	-493.005		-0.505		3539.858	2.68 (-2)	1.071	2.71 (-2)
			11	-444.525		-0.287		3587.512	2.62 (-2)	1.665	2.68 (-2)
			12	-392.077		0.015		3638.847	2.56 (-2)	2.572	2.66 (-2)
			13	-335.793		0.424		3693.535	2.48 (-2)	4.006	2.66 (-2)
			14	-275.819		0.954		3751.094	2.37 (-2)	6.317	2.66 (-2)
			15	-212.314		1.614		3824.431	3.19 (-2)	9.832	2.66 (-2)
			16	-145.457		2.398		3889.461	2.93 (-2)	-3.555	2.64 (-2)
			17	-75.480		3.307		3958.247	2.70 (-2)	-1.693	2.60 (-2)
			18	-2.383		4.199		4030.376	2.57 (-2)	0.702	2.52 (-2)
			19	73.340		4.992		4105.429	2.30 (-2)	1.647	2.40 (-2)
4	3	0	3	-337.791		0.000		3673.655	4.22 (-2)	0.002	4.25 (-2)
			4	-319.793		0.001		3691.567	4.11 (-2)	0.003	4.17 (-2)
			5	-297.358		0.003		3713.902	3.98 (-2)	0.003	4.05 (-2)
			6	-270.531		0.009		3740.618	3.87 (-2)	0.005	3.98 (-2)
			7	-239.372		0.029		3771.669	3.72 (-2)	0.009	3.80 (-2)
			8	-204.001		0.117		3806.996	3.54 (-2)	0.018	3.65 (-2)
			9	-163.358		-0.889		3846.515	3.43 (-2)	0.031	3.47 (-2)
			10	-120.078		-0.688		3890.327	3.40 (-2)	0.077	3.35 (-2)
			11	-72.245		0.992		3938.021	3.24 (-2)	0.121	3.12 (-2)
			12	-20.463		0.725		3989.662	2.91 (-2)	0.251	2.60 (-2)
			13	35.065	1.42 (-3)	0.995		4045.056	4.63 (-2)	0.504	2.69 (-2)
			14	93.876	3.55 (-3)	1.849		4103.031	3.08 (-2)	1.921	2.51 (-2)
			15	161.294	1.30 (-2)	-2.195		4168.656	2.63 (-2)	-0.812	3.03 (-2)
			16	226.035	5.16 (-3)	0.005		4234.194	1.35 (-1)	-1.099	2.55 (-2)
			17	295.320	2.00 (-3)	1.125		4304.245	2.47 (-2)	2.622	2.62 (-2)
			18	367.587	1.44 (-2)	2.464	5.3 (-14)	4376.894	2.19 (-2)	2.835	2.19 (-2)
5	4	0	4	174.714	3.27 (-7)	0.000	1.69 (-7)	4155.459	6.65 (-2)	0.000	6.64 (-2)
			5	196.769	2.85 (-6)	0.000	1.23 (-6)	4177.467	6.50 (-2)	-0.001	6.50 (-2)
			6	223.150	1.53 (-5)	0.000	5.74 (-6)	4203.781	6.30 (-2)	0.013	6.32 (-2)
			7	253.807	6.68 (-5)	0.001	2.38 (-5)	4234.380	6.35 (-2)	0.015	6.10 (-2)
			8	288.678	2.63 (-4)	0.002	1.19 (-4)	4269.220	5.80 (-2)	-0.006	5.93 (-2)
			9	327.776	5.17 (-3)	-0.050	6.37 (-4)	4308.203	5.50 (-2)	0.010	5.47 (-2)
			10	370.779	1.04 (-2)	0.265	8.10 (-3)	4351.277	5.18 (-2)	0.015	5.16 (-2)
			11	418.745	1.10 (-1)	-0.769	7.24 (-4)	4398.362	4.78 (-2)	0.040	4.76 (-2)
			12	469.332	5.03 (-3)	0.284	1.11 (-4)	4449.369	4.82 (-2)	-0.002	4.54 (-2)
			13	524.162	5.82 (-4)	0.120	2.78 (-5)	4504.191	4.37 (-2)	0.039	4.21 (-2)
			14	582.720	2.65 (-4)	0.170	1.24 (-4)	4562.677	5.88 (-2)	0.094	3.94 (-2)
			15	644.895	5.15 (-3)	0.383	1.11 (-2)	4624.400	2.44 (-1)	-0.379	1.04 (-1)
			16	710.283	4.32 (-2)	0.199	1.05 (-2)	4691.232	1.53 (-1)	-0.170	3.59 (-2)
			17	779.512	3.18 (-1)	0.567	1.91 (-1)	4759.775	3.74 (-2)	0.163	2.83 (-2)
			18	851.382	5.15 (-1)	1.163	4.37 (-1)	4830.668	5.50 (-2)	1.524	5.87 (-1)

TABLE BIV: continued

1	0	1	0	-734.044			3335.862	6.37 (-2)		
			1	-729.840			3340.052	6.32 (-2)		
			2	-721.436			3348.424	6.24 (-2)		
			3	-708.831			3360.964	6.11 (-2)		
			4	-691.999			3377.648	5.95 (-2)		
			5	-670.774 <sup>d</sup>			3398.449	5.74 (-2)		
			6	-647.906 <sup>d</sup>			3423.331	5.50 (-2)		
			7	-618.650			3452.260	5.24 (-2)		
			8	-585.733			3485.206	4.95 (-2)		
			9	-549.047			3522.183	4.66 (-2)		
			10	-508.626			3563.416	4.62 (-2)		
			11	-464.548			3605.841	5.21 (-2)		
			12	-416.917			3654.627	4.35 (-2)		
			13	-365.854			3707.068	3.86 (-2)		
			14	-311.497			3763.586	3.50 (-2)		
			15	-254.002			3811.044	2.23 (-2)		
			16	-193.548			3873.240	2.04 (-2)		
			17	-130.338			3937.779	1.82 (-2)		
			18	-64.606			4004.704	1.57 (-2)		
			19	3.367			4073.937	1.47 (-2)		
			20	73.220			4145.264	1.12 (-2)		
2	1	1	1	-621.269	0.333		3437.914	7.08 (-2)	0.340	8.78 (-2)
			2	-613.263	0.987		3445.937	6.90 (-2)	0.801	6.24 (-2)
			3	-601.255	1.944		3457.922	6.92 (-2)	1.806	6.32 (-2)
			4	-585.251	3.183		3473.689	7.83 (-2)	3.223	6.34 (-2)
			5	-565.268	4.681		3494.846	8.35 (-2)	3.468	6.18 (-2)
			6	-541.336	6.417		3518.584	7.15 (-2)	5.314	6.00 (-2)
			7	-513.492	8.373		3546.385	6.02 (-2)	7.219	5.72 (-2)
			8	-481.792	10.532		3578.085	5.48 (-2)	9.288	5.40 (-2)
			9	-446.298	12.878		3613.590	4.92 (-2)	11.538	5.06 (-2)
			10	-407.088	15.399		3652.844	6.34 (-2)	13.943	4.67 (-2)
			11	-364.248	18.077		3695.715	4.61 (-2)	16.539	4.32 (-2)
			12	-317.877	20.898		3742.147	4.06 (-2)	19.276	3.89 (-2)
			13	-268.077	23.834		3792.027	3.53 (-2)	22.141	3.29 (-2)
			14	-214.789	26.686		3845.218	7.07 (-2)	25.176	3.22 (-2)
			15	-158.962	30.247		3901.679	2.97 (-2)	28.239	3.02 (-2)
			16	-99.737	33.500		3961.180	2.67 (-2)	31.407	2.65 (-2)
			17	-37.765	37.239		4023.606	3.23 (-2)	34.623	2.19 (-2)
			18	26.605	2.5 (-10)	40.082	4088.802	2.16 (-2)	37.847	1.87 (-2)
			19	94.062	1.27 (-1)	43.008	4157.133	1.75 (-2)	40.489	1.77 (-2)
3	2	1	2	-354.991	0.002		3685.669	8.43 (-2)	0.002	8.43 (-2)
			3	-342.563	0.009		3697.998	8.51 (-2)	0.009	8.51 (-2)
			4	-326.043	0.028		3714.382	8.62 (-2)	0.028	8.61 (-2)
			5	-305.477	0.068		3734.769	8.77 (-2)	0.068	8.75 (-2)
			6	-280.933	0.146		3759.095	8.83 (-2)	0.142	8.78 (-2)
			7	-251.985	-0.350		3787.289	9.10 (-2)	0.270	9.08 (-2)
			8	-220.043	0.467		3819.260	9.23 (-2)	0.469	9.22 (-2)
			9	-184.020	0.740		3854.921	9.27 (-2)	0.768	9.26 (-2)
			10	-144.383	1.150		3894.172	9.19 (-2)	1.213	9.14 (-2)
			11	-101.285	1.726		3936.861	9.28 (-2)	1.915	8.79 (-2)
			12	-54.880	2.529		3983.502	8.40 (-2)	1.622	8.60 (-2)
			13	-5.329	3.687		4032.677	8.11 (-2)	5.084	6.49 (-2)
			14	47.191	19.571		4085.291	7.57 (-2)	7.606	5.24 (-2)
			15	102.669	24.097		4140.966	6.94 (-2)	10.747	4.27 (-2)
4	3	1	3	43.791	6.29 (-7)	0.000	4059.586	1.19 (-1)	-0.002	1.20 (-1)
			4	60.158	6.97 (-6)	0.000	4075.978	1.17 (-1)	-0.002	1.17 (-1)
			5	80.521	1.18 (-4)	0.002	4096.409	1.13 (-1)	-0.006	1.14 (-1)
			6	105.015	3.44 (-5)	0.006	4120.840	1.10 (-1)	-0.011	1.10 (-1)
			7	133.299	9.99 (-6)	0.015	4149.216	1.06 (-1)	-0.014	1.06 (-1)
			8	165.459	1.47 (-4)	0.039	4181.483	1.01 (-1)	-0.019	1.01 (-1)
			9	201.333	1.68 (-3)	0.129	4217.562	9.66 (-2)	-0.015	9.63 (-2)
			10	241.446	5.28 (-3)	-0.532	4257.366	9.18 (-2)	0.003	9.11 (-2)
			11	284.455	1.81 (-4)	0.491	4301.305	1.45 (-1)	0.127	9.42 (-2)

TABLE BIV: continued

			12	330.956	7.17 (-4)	0.750		4347.770	8.05 (-2)	0.146	8.01 (-2)
			13	382.340	1.65 (-1)	-0.562	2.57 (-2)	4398.016	7.62 (-2)	0.353	7.42 (-2)
			14	434.852	7.19 (-1)	0.837	4.08 (-1)	4453.481	1.21 (-1)	-1.471	6.79 (-2)
			15	491.325	1.26 (+0)	1.235	4.79 (-1)	4508.605	6.44 (-2)	1.722	6.23 (-2)
5	4	1	4	562.972	2.06 (-5)	0.000	1.84 (-5)	4548.040	3.49 (-1)	0.148	1.81 (-1)
			5	583.028	2.32 (-3)	0.027	1.01 (-4)	4568.340	1.77 (-1)	-0.039	1.71 (-1)
			6	607.074	1.35 (-5)	0.001	2.45 (-5)	4592.420	1.68 (-1)	0.099	1.98 (-1)
			7	634.945	4.71 (-5)	0.001	4.43 (-5)	4620.393	1.59 (-1)	0.031	1.65 (-1)
			8	666.649	2.67 (-4)	0.006	9.53 (-5)	4652.196	1.49 (-1)	0.020	1.51 (-1)
			9	702.176	3.71 (-3)	-0.034	2.08 (-6)	4687.900	2.64 (-1)	-0.092	1.32 (-1)
			10	741.221	1.42 (-1)	0.038	1.06 (-1)	4726.999	1.35 (-1)	0.044	1.37 (-1)
			11	783.881	2.01 (-1)	0.096	1.49 (-1)	4769.492	3.12 (-1)	0.685	1.25 (-1)
			12	830.062	2.87 (-1)	0.126	2.02 (-1)	4816.402	1.13 (-1)	0.002	1.12 (-1)
			13	879.534	4.44 (-1)	0.249	2.67 (-1)	4865.956	3.01 (-1)	0.413	3.23 (-1)
			14	932.186	6.78 (-1)	0.463	3.32 (-1)	4919.290	5.98 (-1)	0.196	4.52 (-1)
			15	987.868	9.80 (-1)	0.790	4.30 (-1)	4975.443	8.14 (-1)	0.412	5.62 (-1)
1	0	2	0	-445.659				3633.935	1.01 (-1)		
			1	-441.960				3637.728	9.90 (-2)		
			2	-434.573				3645.316	9.51 (-2)		
			3	-423.514				3656.713	8.80 (-2)		
			4	-408.813				3671.962	7.54 (-2)		
			5	-390.506				3691.154 <sup>e</sup>	5.79 (-2)		
			6	-368.645				3710.765 <sup>e</sup>	6.13 (-2)		
			7	-343.293				3736.614	6.65 (-2)		
			8	-314.528				3765.836	6.70 (-2)		
			9	-282.441				3798.382	6.49 (-2)		
			10	-247.141				3834.174	6.12 (-2)		
			11	-208.754				3873.113	5.67 (-2)		
			12	-167.427				3915.082	5.18 (-2)		
2	0	0	0	-606.428				3473.264	1.59 (-2)		
			1	-601.889				3477.690	2.39 (-2)		
			2	-592.831				3486.465	8.02 (-3)		
			3	-579.289				3499.672	9.93 (-3)		
			4	-561.307				3517.227	1.02 (-2)		
			5	-538.938				3539.105	9.94 (-3)		
			6	-512.240				3565.246	9.18 (-3)		
			7	-481.276				3595.588	7.92 (-2)		
			8	-446.116				3630.123	1.09 (-2)		
			9	-406.836				3668.719	9.84 (-3)		
			10	-363.522				3711.320	9.26 (-3)		
			11	-316.268				3757.832	9.28 (-3)		
			12	-265.180				3808.094	4.28 (-3)		
			13	-210.375				3862.185	5.16 (-3)		
			14	-151.985				3919.844	6.45 (-3)		
			15	-90.160				3980.857	4.23 (-3)		
			16	-25.019				4045.259	5.91 (-3)		
			17	43.188	1.16 (-6)			4113.123	1.17 (-2)		
			18	114.307	6.06 (-3)			4183.346	3.21 (-3)		
			19	188.100	4.94 (-3)			4256.639	1.93 (-2)		
			20	264.310	4.09 (-3)			4332.505	1.13 (-2)		
			21	342.652	3.53 (-3)			4410.676	8.54 (-3)		
			22	422.082	6.88 (-3)			4490.871	2.71 (-2)		
			23	503.851	1.29 (-2)			4572.738	7.62 (-3)		
3	1	0	1	-421.973		0.692		3634.579	2.07 (-2)	0.650	1.98 (-2)
			2	-414.064		2.070		3642.356	2.28 (-2)	1.954	1.97 (-2)
			3	-402.207		4.117		3653.974	2.74 (-2)	3.935	1.94 (-2)
			4	-386.412		6.812		3669.344	3.65 (-2)	6.645	1.92 (-2)
			5	-366.688		10.124		3688.322 <sup>e</sup>	4.99 (-2) <sup>e</sup>	10.190 <sup>e</sup>	1.89 (-2)
			6	-343.052		14.013		3714.358 <sup>e</sup>	4.18 (-2) <sup>e</sup>	11.057 <sup>e</sup>	1.87 (-2)
			7	-315.522		18.431		3741.550	3.12 (-2)	15.076	1.86 (-2)
			8	-284.121		23.313		3772.661	2.51 (-2)	19.387	1.89 (-2)
			9	-248.880		28.576		3807.617	2.10 (-2)	23.932	1.97 (-2)
			10	-209.834		33.980		3846.362	1.82 (-2)	28.586	2.16 (-2)

TABLE BIV: continued

	11	-167.038		40.080		3888.832	1.60 (-2)	33.138	2.53 (-2)		
	12	-120.619		45.808		3934.958	1.40 (-2)	37.233	3.22 (-2)		
	13	-69.975		50.574		3984.690	1.36 (-2)	53.070	5.89 (-2)		
	14	-16.370		54.873		4037.903	1.42 (-2)	54.994	5.40 (-2)		
	15	40.876		57.067		4093.562	2.86 (-2)	58.151	5.88 (-2)		
	16	101.532		56.961		4154.863	1.17 (-2)	58.779	3.61 (-2)		
4	2	0	2	-69.497	-0.581	3958.829	1.80 (-2)	-0.014	3.97 (-2)		
			3	-57.155	0.280	3971.330	2.03 (-2)	0.064	1.62 (-2)		
			4	-40.461	0.372	3987.958	2.01 (-2)	0.171	1.87 (-2)		
			5	-20.013	0.977	4008.634	2.34 (-2)	0.404	1.97 (-2)		
			6	4.280	3.77 (-3)	4033.294	2.04 (-2)	0.807	1.82 (-2)		
			7	31.948	1.66 (-2)	4061.841	3.10 (-2)	1.446	1.94 (-2)		
			8	62.327	3.28 (-2)	4094.164	2.28 (-2)	2.402	2.14 (-2)		
			9	107.213	2.94 (-2)	4130.119	2.13 (-2)	3.756	2.20 (-2)		
			10	145.625	1.38 (-2)	4169.696	2.57 (-2)	5.286	2.41 (-2)		
			11	187.879	5.63 (-3)	4212.431	2.81 (-2)	8.850	2.98 (-2)		
			12	233.747	2.07 (-2)	4258.352	2.99 (-2)	11.905	2.29 (-2)		
			13	282.491	2.02 (-3)	4307.146	3.43 (-2)	16.160	2.15 (-2)		
			14	334.301	2.48 (-3)	4358.435	4.28 (-2)	21.675	2.09 (-2)		
			15	389.011	1.20 (-2)	4411.576	6.27 (-2)	29.147	1.96 (-2)		
			16	445.333	2.65 (-1)	4465.612	5.50 (-2)	39.140	1.86 (-2)		
5	3	0	3	417.711	1.85 (-3)	0.084	2.56 (-3)	4413.468	3.75 (-2)	-0.008	3.62 (-2)
			4	434.162	4.91 (-4)	0.025	3.06 (-4)	4429.862	3.41 (-2)	0.042	3.58 (-2)
			5	454.703	2.43 (-4)	0.037	1.64 (-4)	4450.365	3.37 (-2)	0.037	3.53 (-2)
			6	479.245	1.03 (-4)	0.088	1.29 (-4)	4474.841	3.34 (-2)	0.074	3.47 (-2)
			7	507.709	1.63 (-4)	0.208	1.18 (-4)	4503.234	3.35 (-2)	0.164	3.44 (-2)
			8	539.997	8.28 (-4)	0.453	1.15 (-4)	4535.627	1.51 (-1)	0.424	4.70 (-2)
			9	575.979	3.22 (-3)	0.907	1.08 (-4)	4571.524	3.09 (-2)	0.772	4.63 (-2)
			10	615.503	1.18 (-2)	1.699	4.10 (-4)	4611.032	3.23 (-2)	1.082	2.93 (-2)
			11	658.319	3.13 (-2)	2.815	4.09 (-3)	4653.982	4.37 (-2)	2.018	2.95 (-2)
			12	705.115	1.11 (-2)	3.966	6.11 (-5)	4699.509	3.74 (-2)	3.540	3.50 (-2)
			13	753.377	1.72 (-1)	7.674	3.77 (-1)	4755.860	1.28 (-1)	0.989	9.38 (-2)
			14	806.232	2.33 (+0)	10.204	5.79 (-1)	4805.721	1.24 (-1)	5.164	2.54 (-2)
			15	860.972	2.79 (+0)	14.536	6.50 (-1)	4859.345	3.62 (-1)	9.868	4.25 (-2)
3	0	0	0	-203.844				3882.051	5.54 (-2)		
			1	-199.243				3885.966	4.92 (-2)		
			2	-190.026				3893.960	3.82 (-2)		
			3	-176.189				3906.287	2.65 (-2)		
			4	-157.769				3923.121	1.79 (-2)		
			5	-134.835				3944.444	1.38 (-2)		
			6	-107.439				3970.192	1.20 (-2)		
			7	-75.805				4000.094	1.11 (-2)		
			8	-39.999				4034.255	1.49 (-2)		
			9	-0.235				4071.937	1.14 (-2)		
			10	43.207				4113.304	1.20 (-2)		
			11	89.738				4157.943	1.30 (-2)		
			12	141.195	3.05 (-2)			4205.437	1.43 (-2)		
			13	192.989	9.45 (-1)			4255.462	1.55 (-2)		
			14	247.272	9.93 (-1)			4305.990	7.33 (-2)		

<sup>a</sup>The conversion of the label  $(v_r b k v_R J p)$  to the labels  $[v_r v_\theta v_R]$  and  $J_{K_a, K_c}$  of the vibrational state and the rotational level, respectively, is:  $v_\theta = b - k$ ,  $K_a = k$ , and  $K_c = J - k + \frac{1 - p k p}{2}$  with  $p_k = (-1)^k$ . The levels shown in the table represent 18 vibrational states:  $[v_r 0 0]$ ,  $[v_r 0 1]$ ,  $[v_r 0 2]$ ,  $[v_r 0 3]$ ,  $[v_r 1 0]$ ,  $[v_r 1 1]$ ,  $[v_r 1 2]$ ,  $[v_r 2 0]$ , and  $[v_r 3 0]$  with  $v_r = 0, 1$ .

<sup>b</sup> $\Gamma > 0$  in this column is due to decay of the corresponding state by rotational predissociation and/or tunneling.

<sup>c</sup> Bound state level of the highest  $J$ -value in the complex.

<sup>d</sup>A crossing between  $J^e = 5$  and  $J^e = 6$  levels from groups  $(v_r b k v_R) = (0 3 2 0)$  and  $(0 1 0 1)$ . It affects line intensities, in particular, in  $[0 0 0] \rightarrow [0 1 0]$  band, see Table BXI.C.

<sup>e</sup>There is a crossing between  $J^e = 5$  and  $J^e = 6$  levels from groups  $(v_r b k v_R) = (1 1 0 2)$  and  $(1 3 1 0)$ . Coriolis interactions between the close levels from these groups cause the disturbance in the  $K = 1$  doubling function for state  $[1 2 0]$  of  $\text{Li}^+ - \text{H}_2$  which is seen in Fig. 7 of the paper. Effects on the line intensities are seen in Table BX.C and in Fig. C4a of Part C (the panel for  $[0 0 0] \rightarrow [1 2 0]$  band).

TABLE BV: Positions ( $E$ ) and widths ( $\Gamma$ ) of lowest rotational levels in three groups ( $bk=bv_R=0$ ) below  $v=2j=0$  threshold<sup>a</sup>.  $v_r=2$ . All data are in  $\text{cm}^{-1}$ .

$J$	$k=0$		$k=1$				$k=2$			
	$E$	$\Gamma$	$E(e)$	$\Gamma(e)$	$\Delta E(f-e)^b$	$\Gamma(f)$	$E(e)$	$\Gamma(e)$	$\Delta E(f-e)$	$\Gamma(f)$
0	6197.85	1.1(-1)								
1	6202.75	1.2(-1)	6258.05	1.1(-1)	0.15	1.1(-1)				
2	6212.57	1.1(-1)	6267.68	1.1(-1)	0.46	1.1(-1)	6432.01	1.2(-1)	-0.01	1.2(-1)
3	6227.24	1.0(-1)	6282.07	1.2(-1)	0.94	1.1(-1)	6446.58	1.2(-1)	0.00	1.2(-1)
4	6246.77	9.8(-2)	6301.28	1.1(-1)	1.54	1.1(-1)	6465.98	1.3(-1)	0.00	1.2(-1)
5	6271.13	9.6(-2)	6325.23	1.0(-1)	2.29	1.0(-1)	6490.17	1.2(-1)	0.00	1.2(-1)
6	6300.29	9.4(-2)	6353.89	1.0(-1)	3.20	9.9(-2)	6519.12	1.2(-1)	-0.01	1.2(-1)
7	6334.20	1.2(-1)	6387.19	2.0(-1)	4.25	9.7(-2)	6552.79	1.1(-1)	-0.01	1.1(-1)
8	6372.79	8.5(-2)	6425.19	9.1(-2)	5.39	9.0(-2)	6591.14	1.1(-1)	-0.02	1.1(-1)
9	6416.02	8.0(-2)	6467.71	8.6(-2)	6.73	8.6(-2)	6634.09	1.0(-1)	-0.03	1.0(-1)
10	6463.82	8.3(-2)	6514.75	8.1(-2)	8.09	8.2(-2)	6681.60	9.7(-2)	-0.05	9.7(-2)
11	6516.12	9.0(-2)	6566.22	7.6(-2)	9.63	7.6(-2)	6733.58	9.1(-2)	-0.06	8.8(-2)
12	6572.82	7.2(-2)	6622.05	7.2(-2)	11.26	7.1(-2)	6789.96	8.5(-2)	-0.08	8.5(-2)
13	6633.84	6.7(-2)	6682.16	6.6(-2)	13.00	6.6(-2)	6850.65	7.8(-2)	-0.11	7.8(-2)
14	6699.08	6.0(-2)	6746.47	9.1(-2)	14.79	6.2(-2)	6915.54	7.2(-2)	-0.13	7.2(-2)
15	6768.44	5.6(-2)	6814.83	5.5(-2)	16.70	5.4(-2)	6984.54	6.5(-2)	-0.15	6.5(-2)
16	6841.79	5.1(-2)	6887.18	4.9(-2)	18.66	4.9(-2)	7057.53	5.9(-2)	-0.17	5.9(-2)
17	6919.01	4.6(-2)	6963.39	5.0(-2)	20.66	4.4(-2)	7134.40	7.1(-2)	-0.21	5.3(-2)
18	6999.96	4.1(-2)	7043.30	3.9(-2)	22.72	3.9(-2)	7214.96	4.7(-2)	-0.19	4.7(-2)
19	7084.51	3.6(-2)	7126.83	6.4(-2)	24.79	3.5(-2)	7299.11	4.2(-2)	-0.18	4.2(-2)
20	7172.50	3.0(-2)	7213.77	3.3(-2)	26.88	3.2(-2)	7386.68	3.6(-2)	-0.14	3.6(-2)

<sup>a</sup>As obtained from the asymptotic part of the PES for  $\text{LiHH}^+$  of Ref. 2, the threshold lies  $8072.85 \text{ cm}^{-1}$  above the  $v=0j=0$  threshold. This is too low by  $14.15 \text{ cm}^{-1}$  in comparison with the exact value of  $\varepsilon_{20}-\varepsilon_{00}$  for  $\text{H}_2^1$ .

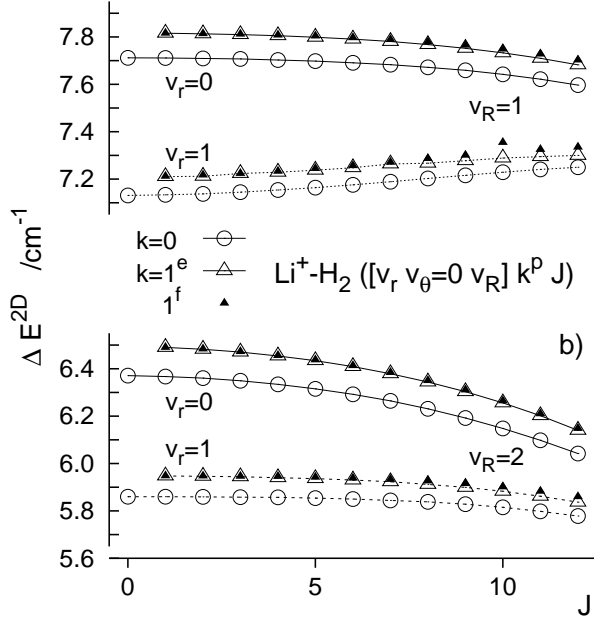
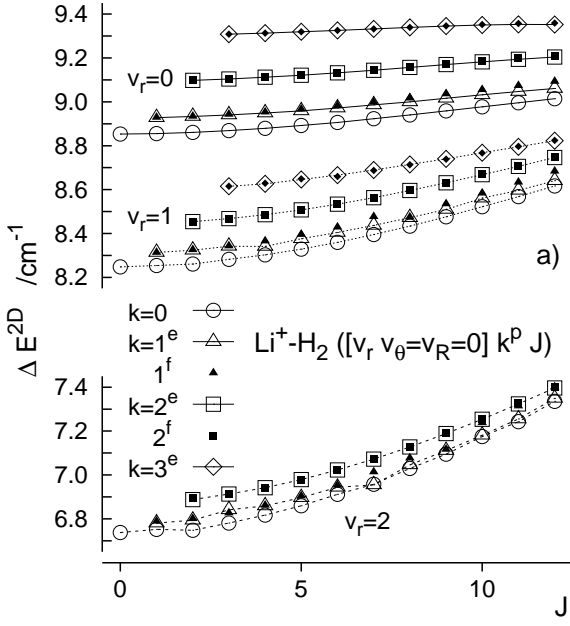
<sup>b</sup>Denotes  $E(f)-E(e)$ , i.e. the  $K$ -type doubling.

## COMMENTS

(i). The groups  $v_r b k v_R$  included into Tables BIV and BV are the ones whose lowest levels ( $J=k$ ) are marked with the yellow crosses in Fig. 2 of the paper. The rotational states shown in the two tables were used in the simulations of the infrared absorption spectrum of the complex, of the bands which are presented in Tables BVIII–BXI and in Figs. 13–15, B5a–e, and/or in the calculations of the integrated band intensities listed in Table XIII.

(ii). As it follows from Fig. B1 (and footnotes to Tables BI and BV), the thresholds  $\varepsilon_{vj=0}$  that result from the PES of the  $\text{LiHH}^+$  system depart from the true positions in  $\text{H}_2$  the more the higher they lie. This testifies on some inaccuracy of the asymptotic region of the PES. Actually, the higher energy parts of the PES may be less accurate not only at large  $R$ 's but also at close Li relative to  $\text{H}_2$  separations. Therefore the transitions energies predicted for the  $v_r=0\rightarrow 2$  band, and listed in Table BX.B, should be taken with some reservation. The relative positions of lines should be more reliable. For this reason the prediction is believed to be useful.

**Fig. B3.** Accuracy of 2D approximation in description of rotational energy levels



Deviations  $\Delta E^{2D}$  of rotational energy levels in states with excited intermolecular vibrations.

The curves in panel b) compared to those in panel a) indicate that the rotational constants for states  $[001]$  and  $[101]$  should be even less impaired by the 2D approximation than the constants for states  $[000]$  and  $[100]$ , respectively. In turn, a comparison of panels c)–d) with a) suggests that inaccuracy of 2D values of the constants for states with excited  $\theta$ -mode may be larger. These indications are partly confirmed in Table BVI.

Plotted are the deviations  $E^{2D} - E^{3D} := \Delta E^{2D}$  in the positions of the levels relative to the  $v=0, j=0$  threshold.

In the ground vibrational state  $[000]$ , the deviations  $\Delta E^{2D}$  clearly enlarge with increasing number  $k$  but are almost independent of  $J$ . In states with excited monomer vibrations, the deviations  $\Delta E^{2D}$  become visibly dependent on  $J$ ; the accuracy of 2D approximation in describing the rotational structure in  $[200]$  state is lower than in  $[000]$ . Obviously, the fact is reflected by the rotational constants in Table BVI. In  $[000]$  state, the percentage deviations of 2D and 3D values of the constants  $B$  and  $C$  are very small, about 10 times smaller than the deviations of the 3D values from the experimental data. In  $[200]$  state, the 2D relative to 3D deviations of the constants become about three times larger.

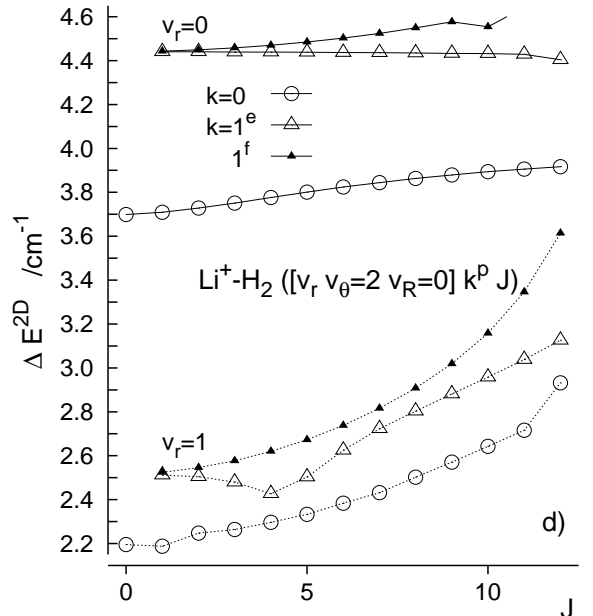
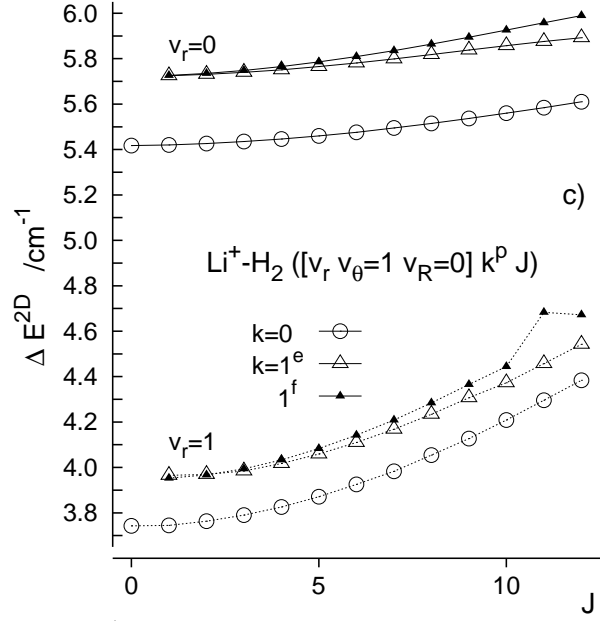


TABLE BVI: Li<sup>+</sup>-H<sub>2</sub>. Parameters of Watson A-reduced Hamiltonian from fitting to sets of lowest rotational energies in  $k=0, 1$  groups of eight vibrational states  $[v_r v_\theta v_R]$  calculated ‘exactly’ (3D) and in the 2D approximation. For each parameter, deviation 2D–3D is shown in lower line. Deviations 3D–Exp /and (3D/Exp–1)×100%/ from the experimental data of Ref. 10 for states [0 0 0] and [1 0 0] are shown in third lines. Except for the percentage deviations, all data are in cm<sup>-1</sup>

	[0 0 0]	[0 0 1]	[0 1 0]	[1 0 0]	[2 0 0]	[1 0 1]	[1 1 0]	[0 2 0]
$E_0^a$	-1674.606 8.853	-1269.455 7.712	-1080.273 5.417	2378.491 8.247	6197.852 6.739	2789.040 7.131	2983.914 3.743	-606.428 3.699
$N_{\text{fit}}^b$	45	45	39	45	45	45	39	24
$A$	65.537(4) <sup>c</sup> 0.074	67.896(7) 0.105	95.573(5) 0.309 *	61.487(3) 0.062	57.822(3) 0.042	63.536(6) 0.079	86.244(8) 0.199 *	182.682 0.735 *
$B$	2.5538(1) 0.0016	2.3330(2) -0.0001	2.4618(2) 0.0022	2.5410(1) 0.0031	2.5295(1) 0.0046	2.3306(2) 0.0016	2.4320(4) 0.0053	2.6072(31) 0.0050
$C$	-0.0162 /-0.6/ 2.4037(1) 0.0011	2.1945(2) -0.0005	2.1972(2) 0.0010	2.3891(1) 0.0024	2.3753(1) 0.0038	2.1902(2) 0.0009	2.1843(4) 0.0036	1.9130(34) 0.0019
$\Delta_J \times 10^4$	-0.0146 /-0.6/ 3.251(3) 0.022	3.593(6) 0.024	3.345(7) 0.022	3.118(3) 0.026	3.011(3) 0.025	3.401(5) 0.031	3.170(11) 0.020	3.73(26) 0.13
$\delta_J \times 10^5$	0.071 /2.2/ 1.59(3) 0.01	1.73(6) 0.01	2.32(7) 0.00	1.57(3) 0.01	1.56(3) 0.01	1.67(5) 0.04	2.20(1) -0.01	16.1(26) 0
$\Delta_{JK} \times 10^3$	-0.11 /-6.5/ 5.59(4) 0.07	4.66(7) 0.06	7.61(7) -0.14 *	5.04(4) 0.10	4.61(4) 0.07	4.63(6) 0.06	5.1610 -0.20 *	100.6(10) 1.7 *
$\sigma \times 10^{3d}$	0.09 /1.3/ 10 0	19 0	13 2	10 -2	10 0	17 0	20 -12	56 8

<sup>a</sup>Energy of  $J=0$  level relative to Li<sup>+</sup>+H<sub>2</sub>( $v=0, j=0$ ) threshold.

<sup>b</sup>Total number of rotational energies used in the fit: for  $k=0-1$ ,  $p=\pm 1$ , and  $J=1-J_{\text{max}}=N_{\text{fit}}/3$ .

<sup>c</sup>The numbers in parentheses are the calculated uncertainties of the constants in their last figures shown.

<sup>d</sup>Root mean square error of the fit; below — the difference between fitting errors of 2D and 3D results.

## COMMENTS

(i). The fits of the experimental transition energies and of the calculated energies of the initial and final states to energies of the A-reduced Hamiltonian truncated to three quartic terms show here practically the same consistency as the fits presented in Table II of the paper using only two quartic terms.

(ii). The deviations 2D–3D of the parameters  $A$  and  $\Delta_{JK}$  for states [0 1 0] and [1 1 0], marked with an asterisk in the table, change most significantly in comparison with the deviations for states [0 0 0] and [1 0 0], respectively. Generally, these increased deviations reflect a lower rigidity of the complex in the  $\theta$ -excited states. The changes in the deviations of  $\Delta_{JK}$  are connected with the significantly increased separations between the error curves  $k=0$  and  $k=1^{e,f}$  in panel c) of Fig. B3 as compared to the separations seen in panel a).

(iii). The set of parameters in the table allows for checking if the dependence on the quantum numbers  $v_r$  ( $:=v_1$ ),  $v_\theta$  ( $:=v_2$ ), and  $v_R$  ( $:=v_3$ ) is linear, as it is in semirigid asymmetric top molecules<sup>11</sup> or equivalently, if the parameters of states with  $\sum_i v_i > 1$  satisfy the relation:  $X([v_1 v_2 v_3]) \approx X([0 0 0])(1 - \sum_i v_i) + \sum_i X([\delta_{i,1} \delta_{i,2} \delta_{i,3}])v_i$ . The rotational constants  $X=A, B, C$

for states [2 0 0] and [1 0 1] and the constants  $B$  and  $C$  for state [1 1 0] satisfy this relation with deviations smaller than 1%. However, a dramatic departure from the linear behavior occurs in state [0 2 0]. The fitted values of  $A$ ,  $B$ , and  $B-C$  are larger than the values obtained from the above formula by 45, 10, and 83%, respectively. This fact is exhibited in Fig. 6 of the paper and interpreted as indicator of inapplicability of the semirigid rotor model to the Li<sup>+</sup>-H<sub>2</sub> complex excited in the bending mode above  $v_\theta=1$ .



TABLE BVII: Total internal partition sum<sup>a</sup> ( $Z$ ) of the  $\text{Li}^+\text{-H}_2$  ion at selected temperature values below 400 K. Contribution of resonances ( $Z_{\text{res}}$ ).

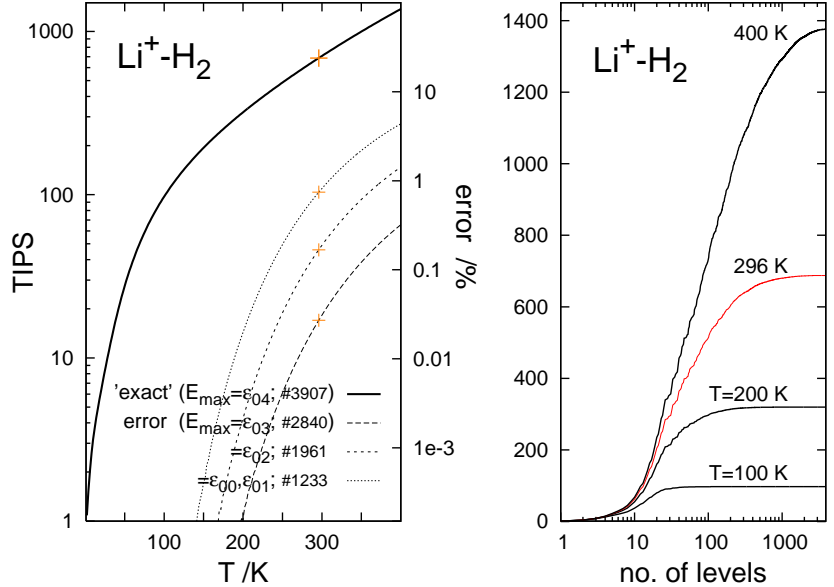
$T$	$Z$	$T$	$Z$	$T$	$Z$	$Z_{\text{res}}$	$T$	$Z$	$Z_{\text{res}}$
1	1.002	34	13.613	105	105.86	0.00	260	525.81	1.24
2	1.085	38	16.568	110	114.63	0.00	270	567.52	1.84
3	1.283	40	18.186	115	123.63	0.00	273.15	581.15	2.08
4	1.529	44	21.691	120	132.88	0.00	280	611.66	2.67
5	1.792	48	25.533	130	152.13	0.00	290	658.36	3.77
6	2.062	50	27.573	140	172.41	0.00	296	687.65	4.59
7	2.335	54	31.876	150	193.79	0.00	300	707.73	5.21
8	2.611	58	36.457	160	216.32	0.00	310	759.92	7.06
10	3.167	60	38.845	170	240.10	0.00	320	815.03	9.39
12	3.731	65	45.081	180	265.21	0.01	330	873.21	12.29
14	4.312	70	51.668	190	291.73	0.03	340	934.56	15.85
16	4.921	75	58.581	200	319.77	0.05	350	999.21	20.16
18	5.574	80	65.794	210	349.43	0.10	360	1067.3	25.3
20	6.283	85	73.289	220	380.81	0.18	370	1138.9	31.4
24	7.922	90	81.054	230	414.02	0.31	380	1214.1	38.6
28	9.909	95	89.075	240	449.18	0.51	390	1293.0	49.9
30	11.046	100	97.347	250	486.40	0.81	400	1375.8	56.4

<sup>a</sup>Evaluated according to Eq. (8) of the paper. Actually listed are the values of  $Z(T)/Z^{\text{ref}}(T)$  where  $Z^{\text{ref}} = \exp(-E_0/k_B T)$  and  $E_0 = -1674.606 \text{ cm}^{-1}$  is the energy of the lowest state of the complex relative to the  $\varepsilon_{00}$  threshold. States of energies up to  $E_{\text{max}} = \varepsilon_{04}$  (the  $\text{H}_2(v=0, j=4) + \text{Li}^+$  dissociation threshold) are included into the sum. About two-thirds of them are resonances of lifetimes no shorter than 1 ps ( $\Gamma < 5 \text{ cm}^{-1}$ ). See Fig. B4 below for some details on convergence of the TIPS with the number of included energy levels.

**Fig. B4.** Total internal partition sum

The error curves in the left panel show effects of shifting the upper bound  $E_{\text{max}}$  of the included levels to lower dissociation thresholds.  $E_{\text{max}} = \varepsilon_{00}, \varepsilon_{01}$  means that only bound state levels are included.

In full rigour, the TIPS function should account for all states of the system that exist in the energy range up to the assumed/necessary  $E_{\text{max}}$ , bound and continuum. All the continuum states, irrespective of the value of the collision-time delay characterizing them (large positive, small positive, or negative), should be included.



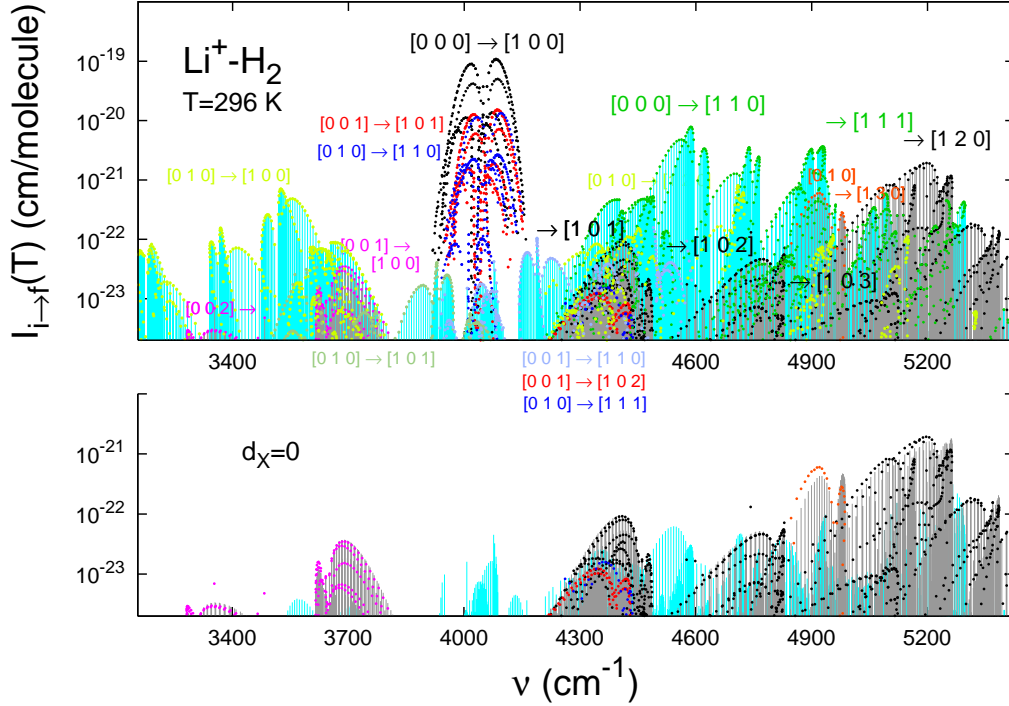
For this purpose, the following term, not shown in Eq. (8),

$$(2\pi\hbar)^{-1} \sum_{I=0,1} \int_{\varepsilon_0}^{E_{\text{max}}} \sum_{J,p} (2J+1) g_I \text{Tr} \mathbf{Q}^{IJP}(E) \exp(-E/kT) dE$$

needs to be evaluated. The present ‘exact’ TIPS includes the contribution of the overwhelming majority of the resonance peaks in the integrands  $\text{Tr} \mathbf{Q}^{IJP}(E)$  but omits their backgrounds stemming from ‘flat’ continuum states. Quite likely, however, this omission has negligible impact on the TIPS value at  $T=296 \text{ K}$ , i.e. at the temperature used in the calculation of the line intensities in this work. The highest lying red cross on the error curves shows that all the included resonances contribute merely 0.7% to the value. The continuum state contribution should be rather smaller (in absolute value, it may be negative), at this relatively low temperature.

# INFRARED ABSORPTION SPECTRUM

**Fig. B5.** Absolute intensities of lines at  $T=296$  K.  
The role of  $d_X$  dipole component



Upper: Extended version of the upper panel of Fig. 13 of the paper. Added are intensities of about 560 lines in four hot bands (listed below the bottom axis). The two  $b$ -type bands,  $[010] \rightarrow [101]$  and  $[001] \rightarrow [110]$ , surround and partly overlap with the  $[000] \rightarrow [100]$ , and the two bands with the net excitations in the  $\theta$ - and  $R$ -modes  $\Delta v_\theta=0$  and  $\Delta R=1$ , respectively, occur in the region of the combination band  $[000] \rightarrow [101]$ . Altogether, about 4680 lines are shown in the panel.

Bottom: Line intensities from calculations with the  $d_X$  dipole component set to zero. The intensities are represented by the heights of the gray and green sticks. The dots are at the same positions as in the upper panel. For clarity, the lines from the  $v_r=0 \rightarrow 1$  fundamental and the two hot  $a$ -type bands overlapping with it are omitted.

## COMMENTS

(i). The intensities in the bands added here are generally smaller than the intensities in the hot bands of the same type shown in Fig. 13 of the paper. This is an indication that no important information is missing there as to the most intense bands in the NIR range other than the  $v_r=0 \rightarrow 1$  fundamental.

(ii). The displacements of the dots from the tops of the corresponding lines in the bottom panel show the contributions of the  $d_X$  component to the intensities. In the majority of the  $a$ -type bands, these contributions are small, barely noticeable on the scale of the figure.

(iii). Since the  $d_X$  connects  $\lambda$ -components of the initial and final states differing by  $\pm 1$ , see Eqs. (20)–(24), it is the primary driver of  $\Delta K_a (: = k_f - k_i) = \pm 1$  transitions of which the bands with the labels  $[\cdot v_\theta \cdot] \rightarrow [\cdot v_\theta \pm 1 \cdot]$  are formed. Therefore, the omission of this dipole component lowers dramatically the line intensities in the  $b$ -type bands. The green sticks in the bottom panel are lower than their counterparts in the upper panel by more than one, even two, orders of magnitude. They represent actually intensities of  $\Delta \lambda = 0$  transitions between the small(er) components of the  $i$ - and/or  $f$ -states,  $\lambda \neq k_i$  and/or  $\lambda \neq k_f$ , which arise due to Coriolis interactions in these states.

(iv). The effect of the  $d_X$  component on the integrated intensities of the bands (cf. Table XII), described by the deviation  $\left( \frac{I_{[v] \rightarrow [v']}(d_X=0)}{I_{[v] \rightarrow [v']}} - 1 \right) \times 100\%$ , is  $< 1$ ,  $2$ , and  $6\%$  for  $[000] \rightarrow [100]$ ,  $[010] \rightarrow [110]$ , and  $[000] \rightarrow [120]$ , respectively, but  $-99\%$  for  $[000] \rightarrow [110]$ .

# Absorption cross-section $\sigma(\nu; T=296\text{ K})$

NEAR-INFRARED

**Fig. B6a.** Fundamental  $\nu_r=0\rightarrow 1$  band and two hot bands:  
 $\nu_r=0\rightarrow 1 + \nu_\theta=1\rightarrow 1$  and  $\nu_r=0\rightarrow 1 + \nu_R=1\rightarrow 1$   
 in R-branch region

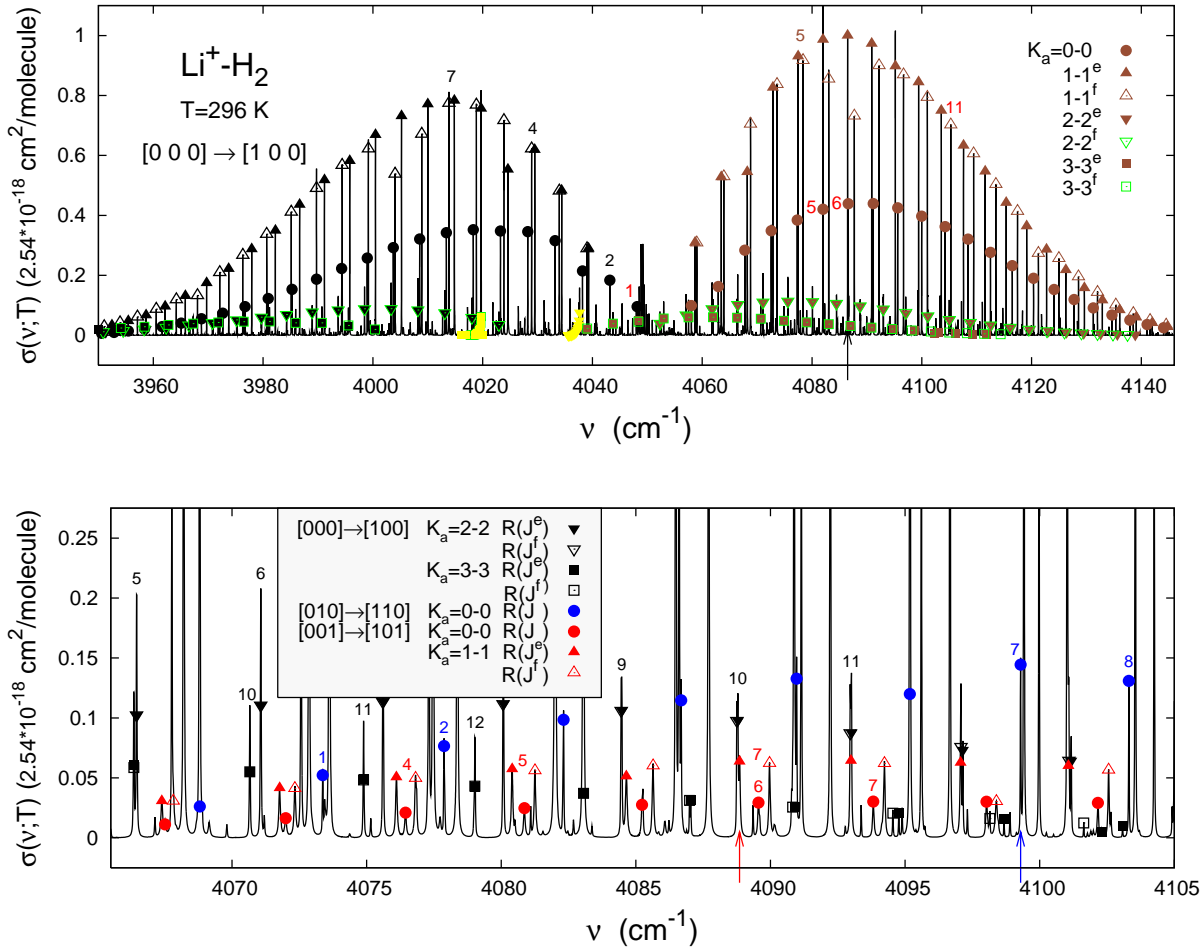


**Fig. B6b.** Overtone  $\nu_r=0\rightarrow 2$  band

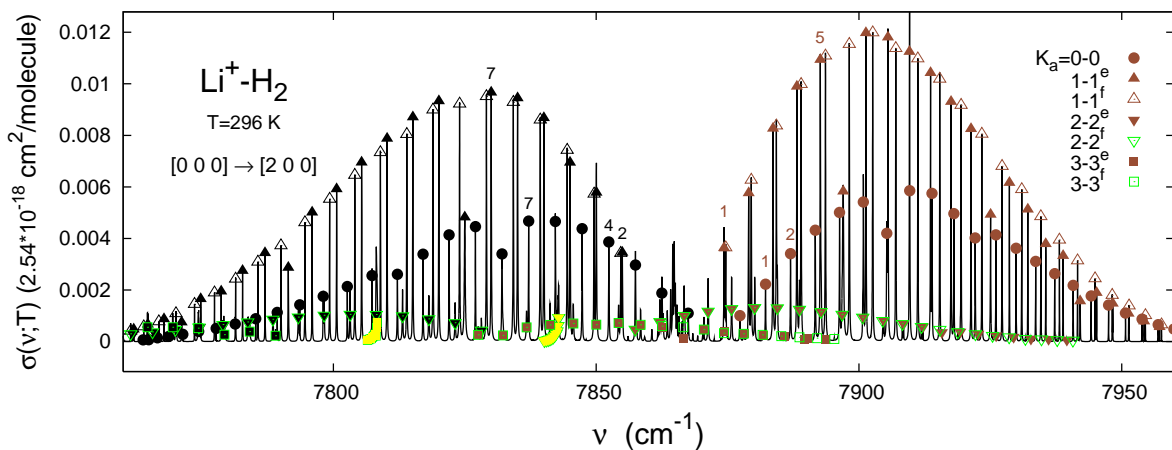
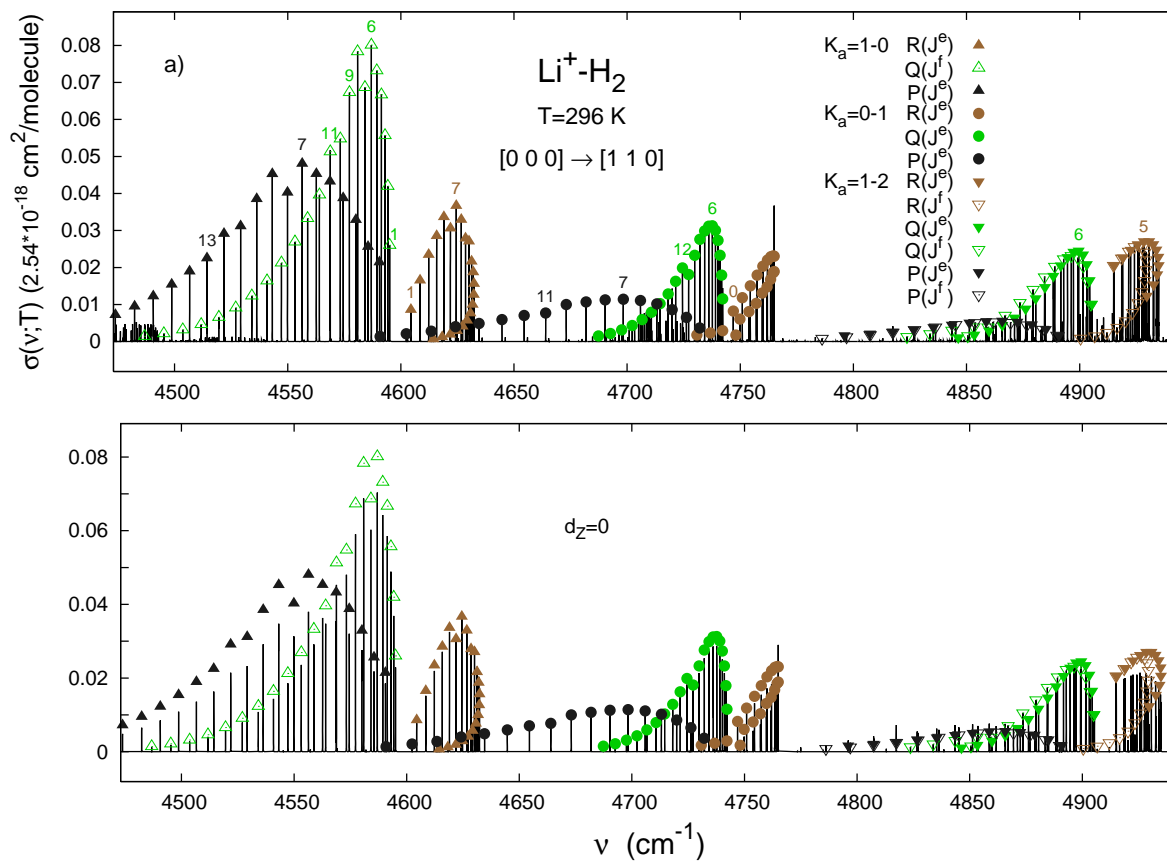
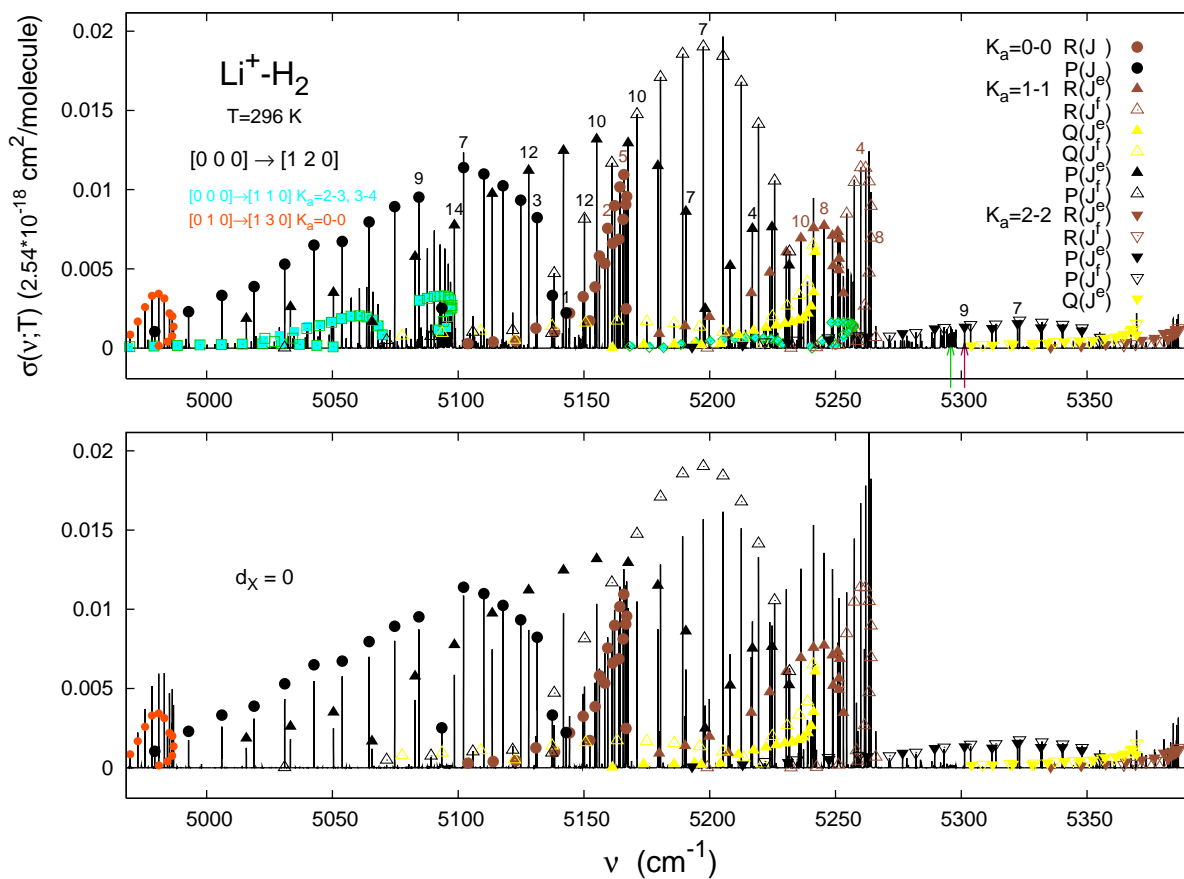


**Fig. B6c.** Two most intense combination bands,  
the role of  $d_X$  dipole component

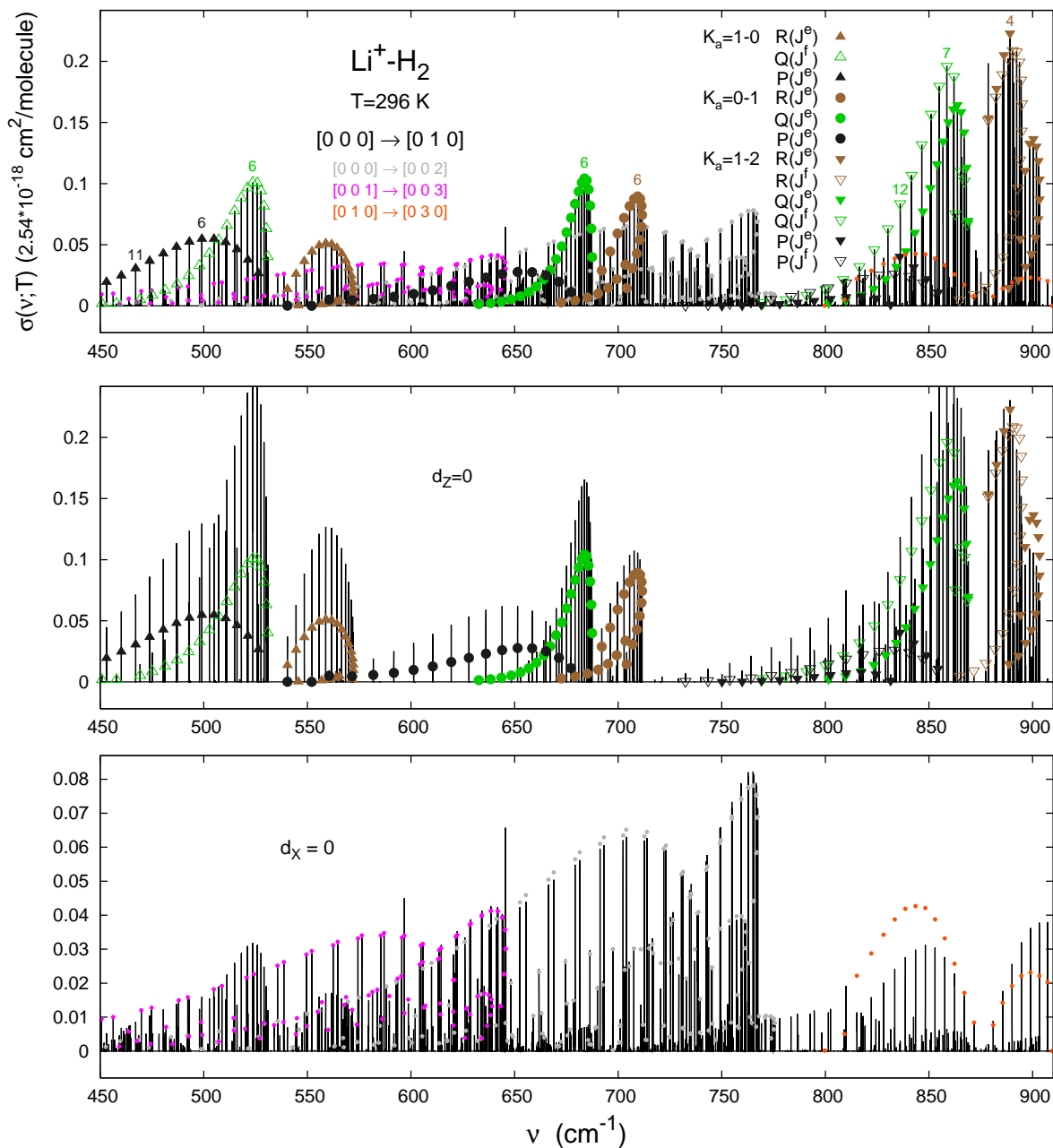
$$v_r=0 \rightarrow 1 + v_\theta=0 \rightarrow 1$$



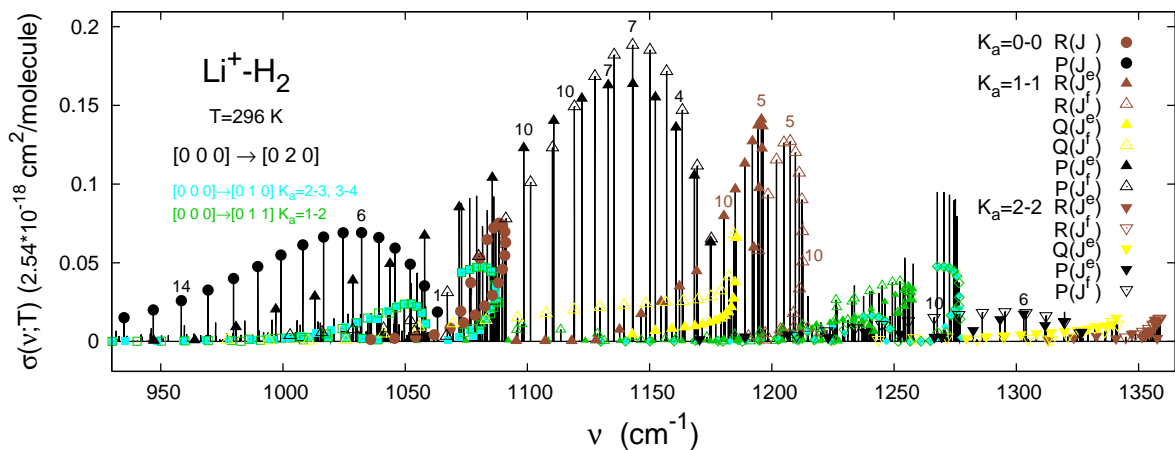
$$v_r=0 \rightarrow 1 + v_\theta=0 \rightarrow 2$$

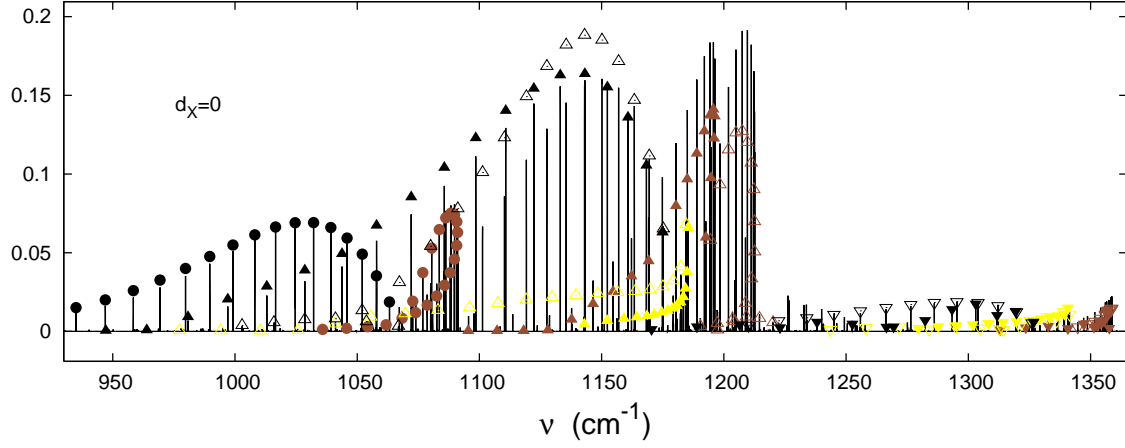


**Fig. B6d.** Fundamental  $\nu_\theta=0\rightarrow 1$  band  
The role of  $d_X$  dipole component



**Fig. B6e.** Overtone  $\nu_\theta=0\rightarrow 2$  band





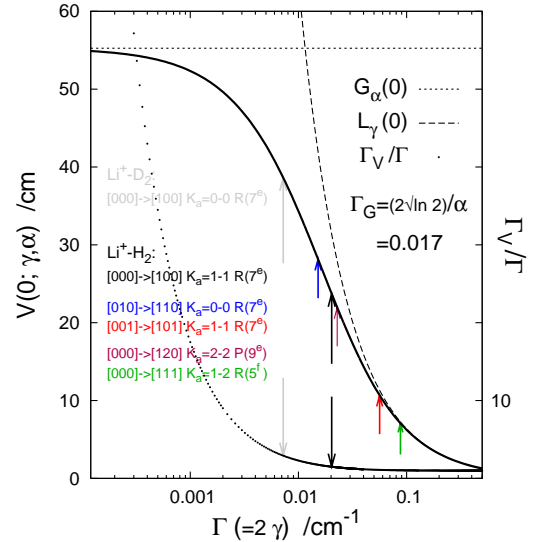
## COMMENTS

(i). As described in the paper, Secs. IIB and IV, the absorption cross-section  $\sigma(\nu; T)$  presented in the figures of this work is the sum of the individual absorption lines with the intensity distribution described by the Voigt profile,

$$\sigma_{i \rightarrow f}(\nu; T) = I_{i \rightarrow f}(T) \times V(\nu - \nu_{if}; \gamma, \alpha). \quad (\text{B1})$$

Some information on the parameters of the Voigt profiles involved in the construction of the function  $\sigma(\nu; T)$  in the region of several vibrational bands in the NIR is provided in Fig. B7.

**Fig. B7.** Voigt profile  $(L_\gamma * G_\alpha)(\nu) := V(\nu; \gamma, \alpha)$  used to describe the shape of individual absorption line, Eq. (B1). Plotted are: the maximum of the profile,  $V(0; \gamma, \alpha)$ , and its full-width-at half-maximum (FWHM),  $\Gamma_V$ , as functions of  $\Gamma$  — the FWHM of the Lorentzian component, i.e. the predissociation width of the f-state. The arrows indicate the heights and widths of the profiles which describe the lines  $\sigma_{i \rightarrow f}(\nu; T)$  due to transitions  $i \rightarrow f$  specified in the labels. The lines are selected from those which are included into the sums  $\sum_{i,f} \sigma_{i \rightarrow f}$  plotted in Figs. B6a,c and C4a (in Ref. 9). The centers  $\nu_{if}$  of the selected lines are marked by the arrows on  $\nu$ -axes of these figures. The black (grey) arrows indicate the parameters of the profile which describes the reference line in the plots of  $\sigma(\nu; T)$  for  $\text{Li}^+ - \text{H}_2$  ( $\text{Li}^+ - \text{D}_2$ ). The pairs of lines specified in the colored labels represent the subbands referred to in comment (v).



(ii). The highest peaks in the cross-section  $\sigma(\nu; T=296 \text{ K})$  plotted in Figs. B6a–e are given symbols to fully specify the underlying transition  $i(=[v_r v_\theta v_R] k J p) \rightarrow f(=[v'_r v'_\theta v'_R] k' J' p')$ , strictly, the rotational transition within the vibrational band specified in the (black) label or, equivalently, the subband  $K_a=k \rightarrow k'$ , the branch  $\Delta J$ , and the subbranch (i.e. the parity  $p$ ) if  $k > 0$  and  $k' > 0$ . The symbols are placed at the positions  $(\nu_{if}, \sigma_{i \rightarrow f}(\nu_{if}; T))$ . So, they may lie far below the tops of the peaks which result from accumulation of intensities (addition of the  $\sigma_{i \rightarrow f}$ s) from several transitions with very close frequencies  $\nu_{if}$ . In particular, such accumulation occurs as an effect of very small  $K$ -doubling of  $J$  and  $J'$  levels in the  $R$ - and  $P$ -branches of the subbands with  $k > 1$  and  $k' > 1$ . Examples: the  $K_a=2-2$  subbands of the bands  $[000] \rightarrow [1, 200]$  in Fig. B6a,b and  $K_a=2-3$  of  $[000] \rightarrow [1110]$  in Fig. B6c.

(iii). In Fig. B6c, devoted to the two important combination bands in the NIR, additional panels are enclosed which show the cross-section functions obtained for the same frequency intervals when one of the dipole-moment components is set to zero. In order to better see the role of the neglected component, the symbols labelling the peaks are left at the same positions as in the panels with the ‘complete’ cross-section.

The band  $[000] \rightarrow [110]$  is almost entirely determined by the component  $d_X$  (see also Fig. B5). The  $d_Z$  enhances the intensity (and the heights by the same) of lines in the most intense subband  $K_a=1-0$  by about 30%, at most. In turn, the band  $[000] \rightarrow [120]$ , as an  $a$ -type band, is determined by the component  $d_Z$ . The impact of the  $d_X$  is non-negligible, however. Easily noticeable is the alteration of the relative heights of  $R$ - and  $P$ -lines in the  $K_a=1-1$  subband caused by this component.

(iv). Figs. B6d and B6e demonstrate the cross-section  $\sigma(\nu; T=296\text{ K})$  in the frequency regions of the bands  $[000] \rightarrow [010]$  and  $[000] \rightarrow [020]$ . Viewed together with Fig. B6c, they inform on how the lack of excitation in the  $r$ -mode modifies the roles of the  $d_X$  and  $d_Z$  dipole components in producing line intensities in the  $b$ - and  $a$ -type bands. Substantial changes in this respect are expected upon looking at the matrix elements of the dipole strength functions  $\langle v | D_{L|\Lambda}|(r, R) | v' \rangle_r$  in Fig. 1b of the paper. While the elements  $\langle 0 | \dots | 1 \rangle$  for  $D_{L0}$  and  $D_{L1}$  are of comparable size, the  $\langle 0 | D_{00} | 0 \rangle$  clearly dominates among the (larger in overall) elements  $\langle 0 | \dots | 0 \rangle$ . The obvious consequences are: 1) the  $v_r=0 \rightarrow 0$  bands are generally more intense as their counterparts combined with the  $v_r=0 \rightarrow 1$  excitation and 2) the band  $[000] \rightarrow [010]$  dominates much less over the  $a$ -type bands in the same range than the  $[000] \rightarrow [110]$  does. A less obvious fact, revealed by the comparison of the upper and middle panels of Fig. B6d, is that the heights of lines in the  $[000] \rightarrow [010]$  band and their dominance over lines in the three bands specified in the colored labels is additionally reduced, even more than two times in the  $K_a=1-0$  subband, by a destructive interference of the  $d_X$  with the (much larger)  $d_Z$  dipole component. More extensively the interference is discussed in Part C of the material, in comments to Fig. C4 and C5.

The impact of the component  $d_X$  on the heights of lines in the band  $[020]$  (the lower panel of Fig. B6d) and in the other three  $a$ -type bands (the bottom panel of Fig. B6d) is qualitatively the same as that observed in the  $[000] \rightarrow [120]$ ; it is the intensity increase of  $P$ - and decrease of  $R$ -lines mentioned in comment (iii). Here, one may add that this impact is much smaller in the bands  $[000] \rightarrow [002]$  and  $[001] \rightarrow [003]$  than it is in the bands  $[000] \rightarrow [020]$  and  $[010] \rightarrow [030]$ . This should be attributed to the fact that excitations in the  $R$ -mode are primarily determined by the large isotropic ( $\sim D_{00}$ ) part of the  $d_Z(r, R)$  dipole component function while the anisotropic part of  $d_Z$ , of magnitude comparable to  $d_X$ , is more important in promoting excitations in the  $\theta$ -mode.

The  $Q$ -lines in the  $a$ -type bands are affected by the presence of the  $d_X$  even more than the  $R$ - and  $P$ -lines. Though not quite well-visible in the plots of the cross-section, this fact becomes evident in the analysis of the line strengths which is presented in Part C.

(v). The heights of lines  $\sigma_{i \rightarrow f}$  in the NIR region, where the  $f$ -states decay by vibrational predissociation and the predissociation widths vary from a few hundredths to a few dozens of  $\text{cm}^{-1}$  (see Table BIV), do not simply mirror the relations between the line intensities  $I_{i \rightarrow f}$  seen in Fig. B5. Indeed, numerous cases of changeover of the relation ‘greater’ between the  $I_{i \rightarrow f}$ s to the relation ‘smaller’ or ‘nearly equal’ between the  $\sigma_{i \rightarrow f}(\nu_{if})$ s are exhibited in the comparison of lines from the bands  $[001] \rightarrow [101]$  and  $[010] \rightarrow [110]$  in Fig. 16 of the paper. Further examples of the same effect emerge from comparison of lines belonging to the bands  $[000] \rightarrow [111]$  and  $[000] \rightarrow [120]$ , strictly, to their subbands  $K_a=1-2$  and  $K_a=2-2$ , respectively, in the frequency interval  $5250-5300\text{ cm}^{-1}$ . The intensities of lines from the former band are clearly seen in Fig. B5 as outgrowing the intensities of lines from the latter band. In the plot of the cross-section in turn, the third panel of Fig. B6c, the profiles of lines from the latter band appear higher.



TABLE BVIII: Infrared absorption spectrum of  $\text{Li}^+\text{-H}_2$ . Line positions ( $\nu$ , in  $\text{cm}^{-1}$ ), deviations from observed values ( $\Delta=\nu-\nu^{\text{obs}}$ ), vibrational factors of line strengths ( $S_{\text{vib}}$ , in  $10^{-3} \text{ D}^2$ ), and line intensities ( $I$ , in  $\text{cm}/\text{molecule}$ ) at  $T=296 \text{ K}$  in four subbands of  $\nu_r=0\rightarrow 1$  band, ( $b k=b \nu_R=0$ ) $\rightarrow(k k 0)$  for  $k=0-3$ <sup>a</sup>. (Extended version of Table XIII of the paper).

$J$	$R(J)$					$P(J)$					$Q(J)$			
	$\nu$	$\Delta$	$\Delta$ (Ref. 8)	$S_{\text{vib}}^b$	$I$	$\nu$	$\Delta$	$\Delta$ (Ref. 8)	$S_{\text{vib}}^b$	$I$	$\nu$	$\Delta$	$S_{\text{vib}}^b$	$I^c$
$k = 0 \quad p = 1$														
0	4058.02	-0.31	5.64	4.73	1.16 (-20)									
1	4062.92	-0.34	5.84	4.74	2.28 (-20)	4048.14			4.74	1.13 (-20)				
2	4067.77	-0.38	6.11	4.74	3.26 (-20)	4043.17	-0.20	5.50	4.73	2.15 (-20)				
3	4072.57	-0.42	6.46	4.76	4.07 (-20)	4038.18	-0.18	5.58	4.73	3.00 (-20)				
4	4077.31	-0.47	6.88	4.77	4.63 (-20)	4033.19	-0.15	5.75	4.72	3.63 (-20)				
5	4082.00			4.77	4.93 (-20)	4028.21	-0.14	5.96	4.74	4.03 (-20)				
6	4086.61			4.79	5.01 (-20)	4023.24	-0.12		4.74	4.19 (-20)				
7	4091.15	-0.61		4.79	4.85 (-20)	4018.30	-0.10		4.73	4.13 (-20)				
8	4095.60	-0.65		4.80	4.54 (-20)	4013.39	-0.08		4.75	3.91 (-20)				
9	4099.97	-0.72		4.81	4.09 (-20)	4008.53	-0.06		4.74	3.55 (-20)				
10	4104.25	-0.77		4.84	3.58 (-20)	4003.72	-0.05		4.75	3.12 (-20)				
11	4108.43			4.84	3.03 (-20)	3998.97	-0.03		4.76	2.66 (-20)				
12	4112.51			4.85	2.50 (-20)	3994.31			4.77	2.20 (-20)				
13	4116.49			4.87	2.00 (-20)	3989.74			4.78	1.77 (-20)				
14	4120.35			4.88	1.56 (-20)	3985.27			4.78	1.38 (-20)				
15	4124.10			4.89	1.19 (-20)	3980.92			4.79	1.05 (-20)				
16	4127.74			4.91	8.87 (-21)	3976.71			4.80	7.87 (-21)				
17	4131.25			4.92	6.46 (-21)	3972.66			4.80	5.73 (-21)				
18	4134.64			4.93	4.61 (-21)	3968.77			4.81	4.09 (-21)				
19	4137.91			4.93	3.22 (-21)	3965.08			4.82	2.86 (-21)				
20	4141.05			4.94	2.21 (-21)	3961.61			4.82	1.96 (-21)				
$k = 1 \quad p=1/p=-1^c$														
1	4058.70	-0.37	5.48	4.74	3.76 (-20)						4049.18	-0.31	4.68	3.71 (-20)
	4059.01	-0.37	5.44	4.72	3.75 (-20)						4048.88	-0.31	4.70	3.72 (-20)
2	4063.47	-0.41	5.76	4.73	6.39 (-20)	4039.30	-0.24	5.10	4.71	3.55 (-20)	4049.43	-0.33	4.62	1.94 (-20)
	4063.93	-0.41	5.71	4.72	6.35 (-20)	4039.00	-0.24	5.12	4.72	3.55 (-20)	4048.52	-0.30	4.66	1.95 (-20)
3	4068.21	-0.43	6.12	4.73	8.37 (-20)	4034.40	-0.22	5.18	4.71	5.88 (-20)	4049.80	-0.32	4.52	1.24 (-20)
	4068.80	-0.46	6.05	4.72	8.31 (-20)	4033.96	-0.20	5.22	4.72	5.87 (-20)	4048.00	-0.34	4.58	1.25 (-20)
4	4072.86	-0.50	6.56	4.77	9.84 (-20)	4029.49	-0.19	5.35	4.70	7.49 (-20)	4050.30	-0.32	4.39	8.46 (-21)
	4073.62	-0.50	6.48	4.73	9.70 (-20)	4028.91	-0.19	5.37	4.71	7.47 (-20)	4047.32	-0.28	4.48	8.56 (-21)
5	4077.47	-0.53		4.78	1.07 (-19)	4024.61	-0.16	5.57	4.68	8.49 (-20)	4050.91		4.25	5.93 (-21)
	4078.37	-0.55		4.73	1.04 (-19)	4023.88	-0.15	5.62	4.71	8.45 (-20)	4046.44		4.40	6.06 (-21)
6	4082.01	-0.58		4.79	1.09 (-19) <sup>d</sup>	4019.71	-0.14		4.71	9.00 (-20)	4051.64		4.06	4.15 (-21)
	4083.05	-0.61		4.71	1.06 (-19)	4018.86	-0.13		4.73	8.91 (-20)	4045.42		4.28	4.30 (-21)
7	4086.48	-0.66		4.81	1.07 (-19)	4014.84	-0.12		4.71	8.97 (-20)	4052.48		3.84	2.89 (-21)
	4087.70	-0.62		4.70	1.03 (-19)	4013.86	-0.10		4.72	8.82 (-20)	4044.24		4.13	3.04 (-21)
8	4090.88	-0.68		4.81	1.01 (-19)	4010.01	-0.11		4.71	8.54 (-20)	4053.48		3.61	1.99 (-21)
	4092.22	-0.69		4.76	9.70 (-20)	4008.90	-0.12		4.70	8.31 (-20)	4042.91		3.98	2.13 (-21)
9	4095.18	-0.74		4.83	9.13 (-20)	4005.21	-0.08		4.72	7.83 (-20)	4054.53		3.41	1.36 (-21)
	4096.67	-0.75		4.78	8.76 (-20)	4004.04	-0.05		4.69	7.55 (-20)	4041.44		3.79	1.46 (-21)
10	4099.42	-0.79		4.85	8.03 (-20)	4000.47	-0.06		4.71	6.91 (-20)	4055.69		3.16	9.07 (-22)
	4101.02	-0.82		4.77	7.61 (-20)	3999.18	-0.05		4.75	6.70 (-20)	4039.84		3.60	9.91 (-22)
11	4103.54	-0.86		4.86	6.84 (-20)	3995.78	-0.06		4.72	5.92 (-20)	4056.96		2.89	5.87 (-22)
	4105.28			4.80	6.45 (-20)	3994.41	-0.05		4.77	5.71 (-20)	4038.13		3.40	6.58 (-22)
12	4107.60	-0.90		4.88	5.67 (-20)	3991.18			4.73	4.92 (-20)	4058.33		2.62	3.73 (-22)
	4109.44			4.81	5.30 (-20)	3989.72			4.76	4.70 (-20)	4036.30		3.18	4.27 (-22)

TABLE BVIII: continued

13	4111.54		4.90	4.57 (-20)	3986.64		4.73	3.97 (-20)	4059.79		2.34	2.29 (-22)	
	4113.49		4.81	4.23 (-20)	3985.13		4.79	3.78 (-20)	4034.40		2.96	2.71 (-22)	
14	4115.37		4.91	3.59 (-20)	3982.23		4.75	3.13 (-20)	4061.32		2.05	1.37 (-22)	
	4117.43		4.83	3.29 (-20)	3980.65		4.79	2.95 (-20)	4032.41		2.72	1.68 (-22)	
15	4119.11		4.93	2.76 (-20)	3977.92		4.75	2.40 (-20)	4062.95		1.78	7.94 (-23)	
	4121.27		4.81	2.48 (-20)	3976.30		4.79	2.24 (-20)	4030.35		2.48	1.01 (-22)	
16	4122.73		4.95	2.07 (-20)	3973.74		4.76	1.80 (-20)	4064.64		1.49	4.40 (-23)	
	4124.97		4.85	1.85 (-20)	3972.10		4.81	1.67 (-20)	4028.26		2.23	5.97 (-23)	
17	4126.23		4.96	1.51 (-20)	3969.70		4.77	1.32 (-20)	4066.42		1.24	2.38 (-23)	
	4128.55		4.86	1.34 (-20)	3968.06		4.79	1.20 (-20)	4026.13		1.99	3.42 (-23)	
18	4129.63		4.98	1.09 (-20)	3965.83		4.78	9.48 (-21)	4068.25		1.00	1.22 (-23)	
	4132.01		4.87	9.54 (-21)	3964.19		4.82	8.59 (-21)	4024.01		1.74	1.90 (-23)	
19	4132.90		5.00	7.64 (-21)	3962.15		4.78	6.65 (-21)	4070.14		0.77	5.97 (-24)	
	4135.34		4.87	6.64 (-21)	3960.53		4.83	5.98 (-21)	4021.91		1.50	1.02 (-23)	
20	4136.05		5.01	5.27 (-21)	3958.67		4.79	4.60 (-21)	4072.10		0.56	2.72 (-24)	
	4138.53		4.88	4.53 (-21)	3957.11		4.83	4.08 (-21)	4019.86		1.26	5.28 (-24)	
21	4139.08		5.02	3.57 (-21)	3955.43		4.80	3.11 (-21)	4074.11		0.38	1.14 (-24)	
	4141.60		4.88	3.03 (-21)	3953.94		4.83	2.74 (-21)	4017.89		1.03	2.63 (-24)	
22	4141.98		5.02	2.38 (-21)	3952.46		4.80	2.07 (-21)	4076.17		0.24	4.25 (-25)	
	4144.53		4.88	2.00 (-21)	3951.06		4.83	1.80 (-21)	4016.03		0.81	1.25 (-24)	
$k = 2 \quad p=1/p=-1^d$													
2	4052.28	-0.51	5.16	4.69	5.32 (-21)				4037.65	-0.38	4.60	1.04 (-20)	
	4052.28	-0.51	5.15	4.69	5.32 (-21)				4037.65		4.60	1.04 (-20)	
3	4057.06	-0.54	5.60	4.71	8.96 (-21)	4022.95	-0.29	4.59	4.67	4.90 (-21)	4037.58	4.52	6.66 (-21)
	4057.06	-0.54	5.60	4.71	8.96 (-21)	4022.95	-0.29	4.59	4.67	4.90 (-21)	4037.58	4.52	6.66 (-21)
4	4061.79	-0.59	6.13	4.72	1.14 (-20)	4018.02	-0.23	4.84	4.67	8.00 (-21)	4037.50	4.42	4.57 (-21)
	4061.79	-0.60	6.12	4.72	1.14 (-20)	4018.02	-0.23	4.84	4.67	8.00 (-21)	4037.50	4.42	4.57 (-21)
5	4066.46	-0.64		4.72	1.29 (-20)	4013.10	-0.25	5.11	4.68	9.96 (-21)	4037.39	4.29	3.21 (-21)
	4066.46	-0.65		4.73	1.30 (-20)	4013.10	-0.25	5.11	4.68	9.96 (-21)	4037.39	4.29	3.21 (-21)
6	4071.07	-0.71		4.74	1.36 (-20)	4008.20			4.68	1.10 (-20)	4037.26	4.14	2.27 (-21)
	4071.07	-0.72		4.73	1.36 (-20)	4008.19			4.68	1.10 (-20)	4037.27	4.13	2.26 (-21)
7	4075.62			4.75	1.35 (-20)	4003.32			4.67	1.12 (-20)	4037.12	3.96	1.59 (-21)
	4075.61			4.75	1.35 (-20)	4003.32			4.69	1.12 (-20)	4037.13	3.96	1.59 (-21)
8	4080.09			4.76	1.28 (-20)	3998.48			4.69	1.08 (-20)	4036.96	3.77	1.11 (-21)
	4080.07			4.76	1.28 (-20)	3998.47			4.68	1.08 (-20)	4036.97	3.77	1.11 (-21)
9	4084.48			4.78	1.17 (-20)	3993.69			4.69	1.00 (-20)	4036.79	3.56	7.57 (-22)
	4084.45			4.78	1.17 (-20)	3993.68			4.69	1.00 (-20)	4036.80	3.55	7.56 (-22)
10	4088.79			4.80	1.03 (-20)	3988.96			4.70	8.91 (-21)	4036.61	3.33	5.07 (-22)
	4088.75			4.80	1.03 (-20)	3988.94			4.70	8.90 (-21)	4036.62	3.32	5.07 (-22)
11	4093.01			4.81	8.82 (-21)	3984.30			4.71	7.66 (-21)	4036.43	3.08	3.32 (-22)
	4092.96			4.81	8.81 (-21)	3984.26			4.71	7.65 (-21)	4036.44	3.08	3.32 (-22)
12	4097.15			4.83	7.30 (-21)	3979.72			4.72	6.38 (-21)	4036.25	2.82	2.12 (-22)
	4097.07			4.83	7.31 (-21)	3979.67			4.72	6.38 (-21)	4036.25	2.82	2.12 (-22)
13	4101.17			4.85	5.90 (-21)	3975.24			4.73	5.17 (-21)	4036.07	2.55	1.32 (-22)
	4101.08			4.85	5.90 (-21)	3975.17			4.73	5.16 (-21)	4036.06	2.54	1.32 (-22)
14	4105.10			4.87	4.64 (-21)	3970.88			4.74	4.07 (-21)	4035.91	2.28	8.00 (-23)
	4105.00			4.86	4.63 (-21)	3970.76			4.74	4.07 (-21)	4035.86	2.27	7.99 (-23)
15	4108.92			4.89	3.56 (-21)	3966.64			4.76	3.13 (-21)	4035.78	2.00	4.68 (-23)
	4108.80			4.86	3.54 (-21)	3966.48			4.75	3.12 (-21)	4035.67	1.99	4.66 (-23)
16	4112.64			4.91	2.67 (-21)	3962.54			4.78	2.35 (-21)	4035.66	1.71	2.64 (-23)
	4112.48			4.90	2.66 (-21)	3962.34			4.76	2.34 (-21)	4035.49	1.71	2.63 (-23)
17	4116.24			4.93	1.95 (-21)	3958.61			4.79	1.72 (-21)	4035.60	1.44	1.44 (-23)
	4116.05			4.92	1.95 (-21)	3958.34			4.76	1.71 (-21)	4035.31	1.43	1.43 (-23)
18	4119.73			4.95	1.40 (-21)	3954.86			4.80	1.24 (-21)	4035.60	1.17	7.49 (-24)
	4119.49			4.94	1.40 (-21)	3954.51			4.79	1.23 (-21)	4035.14	1.16	7.41 (-24)
19	4123.10			4.97	9.86 (-22)	3951.33			4.81	8.69 (-22)	4035.68	0.92	3.69 (-24)
	4122.82			4.95	9.80 (-22)	3950.86			4.80	8.64 (-22)	4034.99	0.91	3.65 (-24)
20	4126.36			4.99	6.80 (-22)	3948.05			4.83	6.00 (-22)	4035.88	0.68	1.69 (-24)
	4126.01			4.97	6.75 (-22)	3947.43			4.81	5.96 (-22)	4034.85	0.67	1.68 (-24)

TABLE BVIII: continued

$k = 3 \quad p=1/p=-1^c$											
3	4039.03	-0.69	4.69	3.56 (-21)				4019.75	-0.46	4.50	1.02 (-20)
	4039.03	-0.69	4.69	3.56 (-21)				4019.75		4.50	1.02 (-20)
4	4043.73	-0.71	4.70	5.95 (-21)	4000.39	4.65	3.18 (-21)	4019.68		4.40	7.01 (-21)
	4043.73	-0.72	4.70	5.95 (-21)	4000.39	4.65	3.18 (-21)	4019.68		4.40	7.01 (-21)
5	4048.38		4.71	7.46 (-21)	3995.55	4.65	5.17 (-21)	4019.59		4.28	4.94 (-21)
	4048.39		4.70	7.45 (-21)	3995.54	4.65	5.17 (-21)	4019.60		4.28	4.94 (-21)
6	4052.97	-0.83	4.73	8.29 (-21)	3990.72	4.66	6.32 (-21)	4019.51		4.12	3.48 (-21)
	4052.98	-0.83	4.73	8.29 (-21)	3990.72	4.66	6.32 (-21)	4019.50		4.12	3.49 (-21)
7	4057.50		4.74	8.50 (-21)	3985.93	4.65	6.81 (-21)	4019.40		3.96	2.47 (-21)
	4057.51		4.75	8.51 (-21)	3985.93	4.65	6.80 (-21)	4019.39		3.96	2.47 (-21)
8	4061.97		4.75	8.24 (-21)	3981.17	4.67	6.82 (-21)	4019.28		3.77	1.72 (-21)
	4061.97		4.76	8.25 (-21)	3981.17	4.67	6.82 (-21)	4019.28		3.77	1.72 (-21)
9	4066.35		4.78	7.66 (-21)	3976.47	4.68	6.44 (-21)	4019.16		3.56	1.18 (-21)
	4066.36		4.78	7.67 (-21)	3976.47	4.68	6.45 (-21)	4019.15		3.56	1.18 (-21)
10	4070.66		4.80	6.85 (-21)	3971.83	4.68	5.82 (-21)	4019.04		3.34	7.93 (-22)
	4070.66		4.80	6.85 (-21)	3971.82	4.69	5.83 (-21)	4019.02		3.34	7.93 (-22)
11	4074.89		4.83	5.92 (-21)	3967.27	4.69	5.08 (-21)	4018.92		3.10	5.23 (-22)
	4074.89		4.82	5.92 (-21)	3967.25	4.70	5.08 (-21)	4018.88		3.10	5.23 (-22)
12	4079.03		4.76	4.87 (-21)	3962.78	4.71	4.28 (-21)	4018.81		2.85	3.36 (-22)
	4079.02		4.85	4.96 (-21)	3962.77	4.71	4.28 (-21)	4018.74		2.85	3.37 (-22)
13	4083.08		4.87	4.04 (-21)	3958.43	4.72	3.50 (-21)	4018.71		2.58	2.10 (-22)
	4083.06		4.87	4.04 (-21)	3958.37	4.73	3.50 (-21)	4018.60		2.55	2.07 (-22)
14	4087.04		4.89	3.20 (-21)	3954.18	4.65	2.73 (-21)	4018.64		2.31	1.28 (-22)
	4086.99		4.90	3.20 (-21)	3954.09	4.75	2.78 (-21)	4018.46		2.32	1.29 (-22)
15	4090.93		4.91	2.47 (-21)	3950.09	4.73	2.14 (-21)	4018.63		2.02	7.53 (-23)
	4090.82		4.92	2.47 (-21)	3949.93	4.76	2.15 (-21)	4018.32		2.05	7.63 (-23)
16	4094.77		4.90	1.85 (-21)	3946.21	4.70	1.60 (-21)	4018.72		1.72	4.24 (-23)
	4094.54		4.95	1.86 (-21)	3945.90	4.78	1.63 (-21)	4018.19		1.78	4.37 (-23)
17	4098.68		4.78	1.33 (-21)	3942.68	4.53	1.14 (-21)	4019.03		1.38	2.21 (-23)
	4098.15		4.97	1.38 (-21)	3942.02	4.80	1.20 (-21)	4018.07		1.51	2.42 (-23)
18	4103.08		4.08	8.19 (-22)	3939.95	3.76	6.84 (-22)	4020.03		0.89	9.16 (-24)
	4101.64		5.00	9.94 (-22)	3938.31	4.82	8.69 (-22)	4017.96		1.25	1.28 (-23)
19	4102.31		2.68	3.70 (-22)	3932.39	2.84	3.57 (-22)	4016.07		0.69	4.43 (-24)
	4105.00		5.02	7.03 (-22)	3934.80	4.84	6.16 (-22)	4017.84		1.00	6.49 (-24)
20	4106.18		3.66	3.52 (-22)	3929.87	3.83	3.35 (-22)	4017.03		0.68	2.74 (-24)
	4108.24		5.05	4.88 (-22)	3931.49	4.86	4.28 (-22)	4017.73		0.77	3.10 (-24)

<sup>a</sup>The labeling of vibration-rotation states by the set of quantum numbers ( $v_r b k v_R J p$ ) exposes similarity of  $\text{Li}^+-\text{H}_2$  to van der Waals complexes of intermediate anisotropy strength of atom-diatom interaction. In the labeling referring to asymmetric top model, the symbols  $J_{K_a K_c}$  and  $[v_r v_\theta v_R]$  are used to denote rotation and vibration state, respectively. The relation between the two labels is:  $v_\theta=b-k$ ,  $K_a=k$ , and  $K_c=J-k + \frac{1-(-1)^k p}{2}$ .

<sup>b</sup> $S_{\text{vib}}=S/S_{\text{rot}}$  where  $S_{\text{rot}}$  is the Hönl-London factor for  $\Delta k=0$  symmetric top transitions<sup>12</sup>,  
 $S_{\text{rot}}(J \rightarrow J'; k) = J+1 - \frac{k^2}{J+1}$ ,  $J - \frac{k^2}{J}$ , and  $k^2 \frac{2J+1}{J^2+J}$  for  $J'=J+1$ ,  $J-1$ , and  $J$ , respectively.

<sup>c</sup>The entries in the lower lines concern  $(J p) \rightarrow (J \pm 1 p)$ ,  $(J - p)$  transitions from the initial  $p=-1$  parity state.

<sup>d</sup>Underlined, here as well in Tables BIX-BXI and CXIII-CXVI (in Part C of the Material), is the largest line intensity in the band shown.

TABLE BIX: Near-infrared absorption spectrum of  $\text{Li}^+\text{-H}_2$ . Line positions ( $\nu$ , in  $\text{cm}^{-1}$ ), vibrational factors of line strengths ( $S_{\text{vib}}^a$ , in  $10^{-3} \text{ D}^2$ ), and line intensities ( $I$ , in  $10^{-21} \text{ cm/molecule}$ ) at  $T=296 \text{ K}$  in two hot bands overlapping with fundamental  $v_r=0 \rightarrow 1$  band.

$K_a=0-0$ of $[v_r v_\theta v_R]=[010] \rightarrow [110]$										$K_a=0-0$ of $[001] \rightarrow [101]$								
$(bk)=(10) \rightarrow (10)$										$(bk)=(00) \rightarrow (00)$								
$R(J)$			$P(J)$			$Q(J)$			$R(J)$			$P(J)$			$Q(J)$			
$J$	$\nu$	$S_{\text{vib}}$	$I$	$\nu$	$S_{\text{vib}}$	$I$	$\nu$	$S_{\text{vib}}$	$I$	$\nu$	$S_{\text{vib}}$	$I$	$\nu$	$S_{\text{vib}}$	$I$	$\nu$	$S_{\text{vib}}$	$I$
0	4068.81	7.36	3.03							4063.01	4.66	1.60						
1	4073.37	7.36	5.93	4059.53	7.37	2.95				4067.51	4.66	3.13	4053.97	4.65	1.56			
2	4077.88	7.36	8.51	4054.85	7.37	5.64				4071.99	4.66	4.51	4049.45	4.65	2.98			
3	4082.31	7.36	10.61	4050.13	7.38	7.91				4076.45	4.67	5.64	4044.94	4.65	4.18			
4	4086.68	7.36	12.13	4045.40	7.38	9.64				4080.86	4.67	6.47	4040.45	4.65	5.10			
5	4090.97	7.36	13.03	4040.66	7.39	10.76				4085.23	4.67	6.97	4035.99	4.64	5.70			
6	4095.18	7.37	<u>13.31</u>	4035.93	7.39	11.28				4089.55	4.68	7.15	4031.57	4.64	6.00			
7	4099.29	7.37	13.03	4031.20	7.40	11.25				4093.82	4.68	7.03	4027.20	4.64	6.00			
8	4103.31	7.38	12.30	4026.51	7.41	10.77				4098.03	4.68	6.67	4022.90	4.64	5.76			
9	4107.23	7.40	11.24	4021.85	7.41	9.93				4102.16	4.68	6.12	4018.66	4.63	5.34			
10	4111.04	7.39	9.93	4017.24	7.42	8.86				4106.23	4.68	5.44	4014.52	4.63	4.78			
11	4114.75	7.41	8.54	4012.69	7.45	7.68				4110.22	4.68	4.71	4010.48	4.62	4.16			
12	4118.34	7.41	7.15	4008.21	7.44	6.45				4114.13	4.68	3.97	4006.55	4.62	3.52			
13	4121.82	7.41	5.83	4003.83	7.45	5.29				4117.95	4.68	3.26	4002.76	4.61	2.90			
14	4125.16	7.40	4.63	3999.54	7.44	4.22				4121.69	4.67	2.62	3999.12	4.60	2.33			
15	4128.36	7.38	3.59	3995.36	7.41	3.27				4125.33	4.66	2.05	3995.65	4.59	1.83			
16	4131.37	7.29	2.70	3991.26	7.32	2.46				4128.89	4.65	1.58	3992.37	4.57	1.41			
17	4134.09	7.00	1.93	3987.15	6.98	1.76				4132.34	4.63	1.19	3989.31	4.55	1.06			
18	4136.08	5.78	1.16	3982.63	5.65	1.04				4135.71	4.61	0.88	3986.49	4.53	0.79			
19	4143.02	4.24	0.63	3983.39	4.60	0.62				4138.96	4.59	0.64	3983.94	4.49	0.57			
20	4145.08	5.64	0.59	3979.62	6.07	0.58				4142.12	4.55	0.45	3981.71	4.45	0.41			
$K_a=1-1$										$K_a=1-1$								
$(bk)=(21) \rightarrow (21)$										$(bk)=(11) \rightarrow (11)$								
$R(J^e) / R(J^f)$			$P$			$Q$			$R$			$P$			$Q$			
$J$	$\nu$	$S_{\text{vib}}$	$I$	$\nu$	$S_{\text{vib}}$	$I$	$\nu$	$S_{\text{vib}}$	$I$	$\nu$	$S_{\text{vib}}$	$I$	$\nu$	$S_{\text{vib}}$	$I$	$\nu$	$S_{\text{vib}}$	$I$
1	4063.80	7.04	0.90				4055.09	7.02	0.89	4063.00	4.60	5.06				4054.26	4.56	5.00
	4064.28	7.04	0.90				4054.57	7.03	0.89	4063.28	4.60	5.05				4053.99	4.58	5.01
2	4068.21	7.05	1.53	4045.82	7.03	0.86	4055.54	6.99	0.47	4067.39	4.61	8.64	4045.24	4.59	4.81	4054.53	4.50	2.62
	4068.90	7.04	1.53	4045.29	7.04	0.85	4053.99	7.00	0.47	4067.82	4.60	8.60	4044.97	4.59	4.80	4053.70	4.52	2.63
3	4072.56	7.06	2.02	4041.29	7.02	1.42	4056.20	6.94	0.31	4071.77	4.62	11.42	4040.81	4.58	7.99	4054.93	4.41	1.68
	4073.44	7.04	2.00	4040.45	7.04	1.41	4053.12	6.98	0.31	4072.34	4.60	11.33	4040.40	4.60	7.98	4053.26	4.46	1.70
4	4076.86	7.06	2.38	4036.75	7.03	1.83	4057.07	6.87	0.22	4076.11	4.63	13.45	4036.39	4.58	10.29	4055.46	4.28	1.16
	4077.91	7.04	2.34	4035.59	7.04	1.81	4051.96	6.93	0.21	4076.82	4.60	13.28	4035.86	4.59	10.26	4052.70	4.37	1.17
5	4081.10	7.08	2.60	4032.20	7.03	2.10	4058.15	6.79	0.16	4080.41	4.63	14.72	4032.00	4.57	11.81	4056.12	4.13	0.81
	4082.29	7.04	2.54	4030.73	7.04	2.06	4050.52	6.87	0.15	4081.25	4.60	14.47	4031.35	4.59	11.74	4051.99	4.26	0.83
6	4085.26	7.09	2.69	4027.67	7.02	2.24	4059.43	6.70	0.11	4084.65	4.64	<u>15.26</u>	4027.65	4.57	12.60	4056.91	3.95	0.58
	4086.58	7.05	2.60	4025.86	7.05	2.18	4048.81	6.81	0.11	4085.64	4.60	14.92	4026.88	4.59	12.49	4051.16	4.12	0.59
7	4089.36	7.10	2.66	4023.15	7.04	2.26	4060.92	6.58	0.08	4088.85	4.65	15.13	4023.34	4.57	12.74	4057.82	3.74	0.41
	4090.79	7.05	2.55	4021.01	7.05	2.19	4046.84	6.73	0.08	4089.97	4.60	14.71	4022.46	4.59	12.57	4050.21	3.97	0.42
8	4093.37	7.12	2.54	4018.66	7.05	2.19	4062.61	6.45	0.06	4092.99	4.65	14.45	4019.09	4.57	12.33	4058.85	3.52	0.28
	4094.89	7.05	2.40	4016.18	7.06	2.09	4044.62	6.63	0.06	4094.23	4.60	13.96	4018.12	4.59	12.11	4049.15	3.80	0.30
9	4097.32	7.13	2.34	4014.21	7.05	2.03	4064.49	6.30	0.04	4097.06	4.66	13.34	4014.92	4.56	11.49	4060.00	3.28	0.19
	4098.90	7.03	2.18	4011.39	7.06	1.92	4042.15	6.51	0.04	4098.39	4.31	11.98	4013.85	4.59	11.22	4047.99	3.61	0.21
10	4101.16	7.14	2.09	4009.82	7.06	1.83	4066.57	6.12	0.03	4101.07	4.67	11.95	4010.82	4.56	10.35	4061.22	2.83	0.12
	4102.65	6.05	1.65	4006.65	7.06	1.71	4039.48	6.38	0.03	4102.56	4.59	11.36	4009.67	4.58	10.05	4046.74	3.41	0.14
11	4104.92	7.15	1.81	4005.51	7.06	1.60	4068.68	5.09	0.02	4105.00	4.67	10.40	4006.82	4.55	9.05	4062.64	2.75	0.08
	4106.54	7.05	1.64	4001.98	7.06	1.47	4036.58	6.24	0.02	4106.61	4.59	9.82	4005.56	4.29	8.18	4045.41	3.19	0.09
12	4108.59	7.16	1.53	4001.27	7.07	1.35	4071.23	5.73	0.01	4108.86	4.67	8.82	4002.93	4.55	7.71	4064.13	2.47	0.05
	4110.20	7.06	1.37	3997.24	6.07	1.06	4033.49	6.09	0.01	4110.57	4.59	8.25	4001.66	4.57	7.37	4044.02	2.96	0.06

TABLE BIX: continued

13	4112.18	7.15	1.25	3997.16	7.06	1.12	4073.88	5.47	0.01	4112.64	4.68	7.29	3999.17	4.54	6.39	4065.73	2.19	0.03
	4113.75	7.06	1.11	3992.85	7.08	1.00	4030.21	5.91	0.01	4114.45	4.59	6.76	3997.85	4.56	6.07	4042.58	2.72	0.04
14	4115.76	7.12	1.00	3993.24	6.98	0.89	4076.77	5.05	0.01	4116.33	4.68	5.89	3995.55	4.54	5.17	4067.41	1.91	0.02
	4117.17	7.06	0.88	3988.47	7.09	0.80	4026.77	5.71	0.01	4118.23	4.58	5.41	3994.20	4.56	4.87	4041.12	2.48	0.02
15	4119.54	6.66	0.74	3989.85	6.33	0.64	4080.25	3.86	0.00	4119.94	4.67	4.65	3992.09	4.53	4.09	4069.216	1.64	0.01
	4120.47	7.06	0.68	3984.22	7.09	0.62	4023.18	5.50	0.00	4121.93	4.57	4.23	3990.74	4.54	3.82	4039.655	2.23	0.01
16	4120.11	4.05	0.34	3983.72	5.20	0.40	4081.01	5.09	0.00	4123.46	4.67	3.59	3988.82	4.52	3.16	4071.10	1.37	0.00
	4123.63	7.05	0.51	3980.11	7.09	0.47	4019.41	5.20	0.00	4125.52	4.55	3.24	3987.47	4.53	2.93	4038.21	1.97	0.00
17	4126.41	5.65	0.36	3980.73	6.46	0.37	4084.95	5.28	0.00	4126.89	4.66	2.72	3985.77	4.50	2.40	4073.08	1.12	0.00
	4126.67	7.05	0.38	3976.19	7.09	0.35	4015.29	4.49	0.00	4129.03	4.47	2.39	3984.44	4.51	2.20	4036.81	1.72	0.00
18	4128.44	7.04	0.33	3977.09	6.16	0.26	4088.47	5.05	0.00	4130.24	4.65	2.02	3982.94	4.48	1.78	4075.16	0.87	0.00
	4129.58	7.03	0.27	3972.47	7.08	0.25	4013.92	4.26	0.00	4132.43	4.51	1.79	3981.67	4.48	1.62	4035.48	1.47	0.00
19	4131.19	7.15	0.24	3976.36	5.14	0.16	4092.02	4.81	0.00	4133.49	4.63	1.48	3980.40	4.46	1.30	4077.34	0.66	0.00
	4132.36	7.02	0.19	3968.98	7.07	0.18	4008.95	5.13	0.00	4135.73	4.48	1.29	3979.19	4.39	1.15	4034.27	1.23	0.00
20	4133.92	7.18	0.18	3972.27	6.92	0.15	4095.68	4.59	0.00	4136.65	4.61	1.06	3978.16	4.43	0.93	4079.62	0.47	0.00
	4135.01	6.99	0.14	3965.76	7.05	0.13	4004.93	4.98	0.00	4138.93	4.45	0.92	3977.06	4.42	0.83	4033.21	1.00	0.00

$K_a=2-2$   
( $bk$ )=(32)  $\rightarrow$  (32)

$K_a=2-2$   
( $bk$ )=(22)  $\rightarrow$  (22)

2	4050.03	6.74	0.83				4036.44	6.61	1.62	4055.97	4.55	0.70				4042.57	4.44	1.37
	4050.03	6.74	0.83				4036.43	6.62	1.62	4055.97	4.55	0.70				4042.57	4.44	1.37
3	4054.44	6.72	1.39	4022.76	6.69	0.77	4036.36	6.45	1.04	4060.40	4.67	1.22	4029.16	4.53	0.65	4042.56	4.35	0.88
	4054.42	6.74	1.40	4022.72	6.73	0.77	4036.31	6.50	1.04	4060.40	4.56	1.19	4029.16	4.53	0.65	4042.56	4.35	0.88
4	4058.84	6.59	1.75	4018.23	6.52	1.23	4036.34	6.10	0.69	4064.79	4.57	1.53	4024.72	4.53	1.07	4042.56	4.22	0.60
	4058.74	6.74	1.79	4018.07	6.73	1.27	4036.15	6.34	0.72	4064.80	4.57	1.53	4024.72	4.53	1.07	4042.55	4.32	0.62
5	4063.44	5.84	1.77	4013.98	5.65	1.33	4036.57	5.02	0.42	4069.15	4.58	1.75	4020.32	4.64	1.38	4042.57	4.07	0.42
	4062.98	6.73	2.04	4013.42	6.73	1.58	4035.92	6.13	0.51	4069.15	4.57	1.75	4020.31	4.53	1.34	4042.54	4.07	0.42
6	4065.50	3.14	1.00	4007.30	3.44	0.89	4034.36	3.30	0.20	4073.47	4.59	1.86	4015.97	4.53	1.50	4042.58	3.89	0.30
	4067.14	6.73	2.15	4008.77	6.72	1.76	4035.63	5.90	0.36	4073.47	4.58	1.86	4015.94	4.53	1.50	4042.53	3.90	0.30
7	4069.81	4.64	1.48	4003.01	4.98	1.34	4034.52	4.49	0.20	4077.73	4.59	1.87	4011.67	4.53	1.55	4042.61	3.69	0.21
	4071.20	6.72	2.15	4004.12	6.72	1.81	4035.26	5.61	0.25	4077.73	4.59	1.87	4011.63	4.53	1.55	4042.51	3.70	0.21
8	4073.68	5.12	1.57	3998.45	5.51	1.45	4034.39	4.71	0.16	4081.94	4.61	1.80	4007.44	4.53	1.53	4042.65	3.46	0.15
	4075.16	6.70	2.06	3999.49	6.71	1.77	4034.78	5.29	0.18	4081.93	4.59	1.80	4007.37	4.53	1.53	4042.49	3.48	0.15
9	4077.25	5.18	1.46	3993.80	5.67	1.40	4034.17	4.60	0.11	4086.09	4.62	1.68	4003.29	4.53	1.44	4042.72	3.22	0.10
	4078.99	6.67	1.89	3994.87	6.70	1.66	4034.16	4.91	0.12	4086.07	4.60	1.67	4003.19	4.53	1.44	4042.47	3.24	0.10
10	4080.52	5.02	1.27	3989.11	5.68	1.26	4033.93	4.35	0.08	4090.20	4.63	1.51	3999.23	4.54	1.31	4042.82	2.96	0.07
	4082.69	6.62	1.68	3990.29	6.68	1.49	4033.37	4.47	0.08	4090.14	4.60	1.50	3999.09	4.53	1.30	4042.45	2.98	0.07
11	4083.37	4.60	1.01	3984.38	5.57	1.08	4033.70	4.01	0.05	4094.19	4.64	1.32	3995.28	4.54	1.15	4042.97	2.69	0.05
	4086.23	6.56	1.44	3985.74	6.65	1.30	4032.32	3.97	0.05	4094.13	4.60	1.31	3995.09	4.53	1.14	4042.46	2.72	0.05
12	4085.61	3.86	0.71	3979.59	5.33	0.88	4033.50	3.63	0.03	4098.13	4.65	1.12	3991.49	4.55	0.98	4043.15	2.40	0.03
	4089.60	6.47	1.20	3981.24	6.61	1.09	4030.91	3.38	0.03	4098.06	4.62	1.11	3991.20	4.53	0.98	4042.42	2.44	0.03
13	4086.89	2.74	0.42	3974.64	4.89	0.67	4033.33	3.21	0.02	4101.99	4.65	0.93	3987.79	4.54	0.82	4043.43	2.13	0.02
	4092.78	6.35	0.96	3976.79	6.55	0.89	4028.90	2.65	0.02	4101.90	4.61	0.92	3987.44	4.52	0.81	4042.41	2.16	0.02
14	4100.25	4.32	0.53	3969.35	4.14	0.46	4033.23	2.76	0.01	4105.79	4.67	0.75	3984.29	4.54	0.66	4043.77	1.83	0.01
	4095.74	6.20	0.75	3972.41	6.47	0.71	4025.96	1.79	0.01	4105.65	4.61	0.74	3983.84	4.53	0.66	4042.41	1.88	0.01
15	4101.77	5.00	0.48	3963.41	3.01	0.26	4033.19	2.30	0.01	4109.52	4.67	0.60	3981.01	4.53	0.52	4044.25	1.54	0.01
	4098.47	6.02	0.57	3968.11	6.37	0.55	4035.13	1.32	0.00	4109.31	4.61	0.58	3980.39	4.51	0.52	4042.41	1.60	0.01
16	4103.70	5.31	0.39	3969.89	4.18	0.28	4033.22	1.84	0.00	4113.22	4.67	0.46	3978.00	4.51	0.41	4044.91	1.26	0.00
	4100.96	5.83	0.43	3963.93	6.24	0.41	4032.52	1.42	0.00	4112.88	4.60	0.45	3977.13	4.50	0.40	4042.41	1.33	0.00
17	4105.86	5.44	0.30	3964.94	4.88	0.25	4033.38	1.41	0.00	4116.97	4.63	0.35	3975.43	4.43	0.30	4045.90	0.97	0.00
	4103.25	5.64	0.31	3959.94	6.08	0.30	4030.42	1.32	0.00	4116.36	4.60	0.34	3974.09	4.49	0.30	4042.40	1.06	0.00
18	4107.81	5.25	0.22	3960.63	5.21	0.20	4033.46	1.03	0.00	4121.11	4.47	0.25	3973.68	4.15	0.21	4047.64	0.65	0.00
	4105.26	5.24	0.21	3956.08	5.75	0.21	4028.56	1.03	0.00	4119.73	4.58	0.25	3971.28	4.47	0.23	4042.35	0.82	0.00

TABLE BX: Near-infrared absorption spectrum of  $\text{Li}^+\text{-H}_2$ . Line positions ( $\nu$ , in  $\text{cm}^{-1}$ ), vibrational factors of line strengths ( $S_{\text{vib}}$ ), and line intensities ( $I$ ) at  $T=296$  K in four vibrational bands non-overlapping with fundamental  $v_r=0\rightarrow 1$  band.

A. Combination  $v_r=0\rightarrow 1$   $v_\theta=0\rightarrow 1$  band ( $S_{\text{vib}}^a$  in  $10^{-4} \text{ D}^2$ ,  $I$  in  $10^{-22} \text{ cm/molecule}$ ).

$[v_r v_\theta v_R]=[000] \rightarrow [110]$																		
$K_a=1-0$									$K_a=0-1$									
$(bk)=(11) \rightarrow (10)$									$(bk)=(00) \rightarrow (21)$									
$R(J^e)$			$P(J^e)$			$Q(J^f)$			$R(J^e)$			$P(J^e)$			$Q(J^e)$			
$J$	$\nu$	$S_{\text{vib}}$	$I$	$\nu$	$S_{\text{vib}}$	$I$	$\nu$	$S_{\text{vib}}$	$I$	$\nu$	$S_{\text{vib}}$	$I$	$\nu$	$S_{\text{vib}}$	$I$	$\nu$	$S_{\text{vib}}$	$I$
0										4746.92	3.25	9.33						
1	4604.42	3.24	9.75	4590.58	3.40	20.37	4595.05	3.34	30.06	4750.93	3.29	13.84				4742.22	3.20	13.46
2	4608.50	3.19	18.33	4585.47	3.45	29.58	4594.24	3.34	47.63	4754.45	3.33	17.85	4732.06	3.12	4.15	4741.78	3.19	21.33
3	4612.30	3.14	25.24	4580.11	3.51	37.29	4593.03	3.33	61.82	4757.47	3.38	21.04	4726.19	3.07	7.61	4741.10	3.19	27.70
4	4615.80	3.09	30.16	4574.52	3.57	43.06	4591.41	3.32	71.84	4759.98	3.41	23.20	4719.87	3.03	10.22	4740.19	3.17	32.21
5	4619.01	3.05	33.02	4568.70	3.62	46.61	4589.38	3.30	77.35	4762.00	3.46	24.38	4713.11	2.99	11.90	4739.05	3.16	34.76
6	4621.91	3.00	33.92	4562.65	3.68	47.90	4586.96	3.28	78.62	4763.51	3.51	24.46	4705.91	2.94	12.66	4737.68	3.14	35.38
7	4624.47	2.95	33.09	4556.39	3.74	47.16	4584.13	3.26	76.16	4764.51	3.55	23.59	4698.30	2.90	12.68	4736.08	3.12	34.32
8	4626.71	2.91	30.92	4549.90	3.80	44.67	4580.90	3.24	70.69	4765.00	3.59	21.94	4690.29	2.86	12.03	4734.24	3.09	31.91
9	4628.59	2.87	27.84	4543.21	3.86	40.84	4577.27	3.22	63.23	4764.99	3.63	19.75	4681.89	2.81	10.92	4732.16	3.06	28.58
10	4630.11	2.82	24.13	4536.30	3.92	36.18	4573.24	3.20	54.72	4764.45	3.68	17.24	4673.11	2.76	9.53	4729.86	3.03	24.68
11	4631.25	2.77	20.28	4529.19	3.98	31.13	4568.82	3.17	45.73	4763.40	3.72	14.62	4663.99	2.71	8.03	4727.16	2.57	17.75
12	4632.00	2.72	16.52	4521.87	4.04	25.96	4564.01	3.14	37.15	4761.83	3.76	12.05	4654.51	2.66	6.55	4724.47	2.97	16.84
13	4632.34	2.66	13.06	4514.35	4.10	21.10	4558.80	3.11	29.32	4759.72	3.79	9.65	4644.70	2.60	5.18	4721.42	2.93	13.33
14	4632.25	2.60	10.03	4506.63	4.15	16.69	4553.20	3.08	22.52	4757.08	3.83	7.56	4634.58	2.54	3.97	4718.12	2.89	10.26
15	4631.72	2.54	7.50	4498.72	4.20	12.88	4547.22	3.04	16.86	4753.85	3.87	5.76	4624.15	2.47	2.95	4714.56	2.85	7.70
16	4630.72	2.46	5.45	4490.61	4.25	9.70	4540.86	3.01	12.34	4749.83	3.76	4.14	4613.44	2.22	1.98	4710.73	2.81	5.63
17	4629.25	2.38	3.85	4482.31	4.30	7.14	4534.13	2.97	8.81	4748.09	2.29	1.82	4602.41	2.29	1.49	4706.63	2.77	4.02
18	4627.28	2.27	2.64	4473.83	4.33	5.13	4527.03	2.93	6.16	4742.22	3.60	2.03	4590.87	2.02	0.94	4702.25	2.72	2.81
19	4624.79	2.15	1.75	4465.16	4.36	3.61	4519.56	2.90	4.22	4736.75	3.80	1.49	4581.92	1.76	0.57	4697.58	2.67	1.92
20	4621.79	1.99	1.11	4456.32	4.36	2.48	4511.75	2.86	2.83	4730.85	3.87	1.03	4569.20	2.19	0.49	4692.61	2.61	1.29

$K_a=2-1$									$K_a=1-2$									
$(bk)=(22) \rightarrow (21)$									$(bk)=(11) \rightarrow (32)$									
$R(J^e) / R(J^f)$			$P(J^e) / P(J^f)$			$Q(J^e) / Q(J^f)$			$R(J^e) / R(J^f)$			$P(J^e) / P(J^f)$			$Q(J^e) / Q(J^f)$			
$J$	$\nu$	$S_{\text{vib}}$	$I$	$\nu$	$S_{\text{vib}}$	$I$	$\nu$	$S_{\text{vib}}$	$I$	$\nu$	$S_{\text{vib}}$	$I$	$\nu$	$S_{\text{vib}}$	$I$	$\nu$	$S_{\text{vib}}$	$I$
1										4915.13	2.99	28.76						
										4914.98	2.98	28.70						
2	4505.55	3.05	0.38	4483.16	3.67	4.14	4492.88	3.43	2.16	4919.00	3.09	31.52				4905.40	2.78	14.15
	4507.03	3.07	0.39	4483.42	3.67	4.15	4492.12	3.42	2.15	4918.56	3.07	31.29				4904.95	2.77	14.05
3	4508.70	2.91	0.77	4477.43	3.78	4.41	4492.33	3.44	3.52	4922.50	3.19	34.13	4890.83	2.50	2.37	4904.43	2.77	22.95
	4511.16	2.95	0.78	4478.18	3.80	4.43	4490.85	3.42	3.50	4921.63	3.16	33.63	4889.93	2.48	2.34	4903.52	2.74	22.63
4	4511.39	2.77	1.07	4471.28	3.90	4.65	4491.60	3.44	4.45	4925.63	3.29	35.90	4885.02	2.40	4.65	4903.13	2.75	28.79
	4515.08	2.83	1.09	4472.77	3.92	4.67	4489.14	3.41	4.41	4924.21	3.23	35.03	4883.54	2.37	4.55	4901.61	2.70	28.10
5	4513.63	2.64	1.25	4464.74	4.01	4.75	4490.68	3.45	5.02	4928.37	3.40	36.68	4878.90	2.31	6.34	4901.50	2.72	32.14
	4518.76	2.71	1.29	4467.20	4.04	4.79	4487.00	3.39	4.94	4926.27	3.30	35.23	4876.71	2.26	6.14	4899.21	2.65	30.89
6	4515.40	2.50	1.32	4457.80	4.11	4.69	4489.57	3.46	5.26	4930.68	3.51	36.29	4872.48	2.21	7.30	4899.54	2.69	33.28
	4522.21	2.60	1.38	4461.48	4.17	4.75	4484.43	3.39	5.16	4927.82	3.36	34.19	4869.45	2.15	6.99	4896.31	2.58	31.41
7	4516.70	2.35	1.30	4450.49	4.23	4.50	4488.26	3.46	5.22	4932.54	3.63	34.86	4865.74	2.11	7.62	4897.25	2.65	32.52
	4525.40	2.48	1.37	4455.62	4.29	4.57	4481.45	3.37	5.08	4928.85	3.41	32.03	4861.77	2.03	7.17	4892.91	2.49	29.92
8	4517.52	2.21	1.19	4442.81	4.34	4.17	4486.75	3.47	4.96	4933.91	3.76	32.54	4858.68	2.02	7.39	4894.62	2.61	30.28
	4528.32	2.37	1.28	4449.61	4.42	4.26	4478.05	3.36	4.78	4929.35	3.43	28.97	4853.68	1.91	6.81	4888.97	2.38	26.90
9	4517.87	2.06	1.04	4434.77	4.44	3.76	4485.05	3.48	4.53	4934.73	3.90	29.60	4851.27	1.92	6.77	4891.65	2.55	27.00
	4530.98	2.25	1.14	4443.47	4.55	3.85	4474.23	3.34	4.33	4929.30	3.44	25.30	4845.19	1.79	6.08	4884.48	2.23	22.83
10	4517.73	1.91	0.87	4426.39	4.55	3.29	4483.14	3.48	3.98	4934.91	4.05	26.27	4843.50	1.84	5.94	4888.33	2.48	23.11
	4533.19	1.84	0.84	4437.19	4.67	3.38	4470.02	3.32	3.78	4928.70	3.42	21.32	4836.31	1.66	5.15	4879.39	2.03	18.20



TABLE BX: B. Overtone  $v_r=0\rightarrow 2$  band ( $S_{\text{vib}}$  in  $10^{-4}$  D<sup>2</sup>,  $I$  in  $10^{-22}$  cm/molecule).

$[v_r v_\theta v_R]=[000] \rightarrow [200]$															
$K_a=0-0$							$K_a=1-1$								
$(bk)=(00) \rightarrow (00)$							$(bk)=(11) \rightarrow (11)$								
$J$	$R(J^e)$			$P(J^e)$			$R(J^e)/R(J^f)$			$P(J^e)/P(J^f)$			$Q(J^e)/Q(J^f)$		
	$\nu$	$S_{\text{vib}}$	$I$	$\nu$	$S_{\text{vib}}$	$I$	$\nu$	$S_{\text{vib}}$	$I$	$\nu$	$S_{\text{vib}}$	$I$	$\nu$	$S_{\text{vib}}$	$I$
0	7877.36	1.05	5.00												
1	7882.22	1.05	9.75	7867.50	1.05	4.89	7874.34	1.05	16.17				7864.86	1.05	16.21
							7874.65	1.05	16.21				7864.57	1.05	16.16
2	7886.99	1.05	13.94	7862.50	1.05	9.33	7879.01	1.04	27.28	7854.99	1.06	15.52	7865.07	1.05	8.60
							7879.50	1.05	27.45	7854.68	1.05	15.42	7864.16	1.04	8.49
3	7891.69	1.04	17.29	7857.48	1.05	13.01	7883.65	1.04	35.81	7850.04	1.06	25.74	7865.38	1.05	5.61
							7884.29	1.05	35.88	7849.60	1.05	25.51	7863.54	1.03	5.46
4	7896.31	1.04	19.61	7852.41	1.06	15.79	7888.19	1.04	41.64	7845.04	1.06	32.88	7865.78	1.05	3.94
							7888.99	1.05	41.67	7844.49	1.06	32.54	7862.76	1.02	3.78
5	7900.85	1.04	20.86	7847.33	1.06	17.53	7892.65	1.04	45.00	7840.05	1.06	37.59	7866.29	1.05	2.85
							7893.63	1.05	44.72	7839.36	1.06	36.88	7861.77	1.00	2.69
6	7905.30	1.05	21.19	7842.24	1.06	18.24	7897.00	1.05	<u>46.19</u>	7835.04	1.07	39.74	7866.89	1.05	2.09
							7898.15	1.05	45.56	7834.23	1.06	38.76	7860.60	0.99	1.93
7	7909.65	1.04	20.35	7837.15	1.06	18.02	7901.33	1.03	44.46	7830.03	1.07	39.78	7867.58	1.05	1.54
							7902.62	1.05	44.14	7829.12	1.05	38.36	7859.23	0.97	1.39
8	7913.91	1.03	18.90	7832.08	1.07	17.14	7905.52	1.03	41.62	7825.00	1.08	38.22	7868.39	1.05	1.12
							7907.01	1.02	39.99	7824.01	1.06	36.43	7857.76	0.94	0.97
9	7918.06	1.03	16.98	7827.03	1.06	15.50	7909.62	1.03	37.55	7820.06	1.07	34.66	7869.32	1.02	0.79
							7911.21	1.04	36.90	7818.96	1.05	33.11	7856.09	0.91	0.68
10	7922.12	1.03	14.72	7822.02	1.06	13.61	7913.62	1.03	32.77	7815.11	1.07	30.70	7870.24	1.05	0.58
							7915.37	1.04	32.07	7813.97	1.03	28.26	7854.27	0.88	0.47
11	7926.06	1.03	12.41	7817.06	1.06	11.60	7917.52	1.02	27.78	7810.22	1.07	26.29	7871.32	1.05	0.41
							7919.43	1.04	27.00	7808.95	1.05	24.67	7852.33	0.85	0.32
12	7929.89	1.03	10.16	7812.18	1.06	9.56	7921.32	1.02	22.81	7805.38	1.07	21.84	7872.48	1.05	0.29
							7923.38	1.04	22.06	7804.07	1.05	20.33	7850.28	0.82	0.21
13	7933.62	0.99	7.86	7807.36	1.06	7.68	7925.04	1.01	18.23	7800.62	1.08	17.66	7873.73	1.04	0.20
							7927.23	1.04	17.53	7799.28	1.05	16.26	7848.12	0.78	0.14
14	7937.25	1.02	6.28	7802.65	1.06	6.00	7928.63	1.01	14.24	7795.95	1.07	13.86	7875.06	1.04	0.13
							7930.97	1.03	13.57	7794.59	1.05	12.65	7845.91	0.74	0.09
15	7940.76	1.01	4.75	7798.06	1.03	4.44	7932.13	1.01	10.83	7791.42	1.07	10.60	7876.49	1.03	0.09
							7934.61	1.03	10.24	7790.04	1.05	9.59	7843.60	0.71	0.06
16	7944.18	1.01	3.51	7793.61	1.06	3.39	7935.54	1.00	8.03	7786.99	1.07	7.94	7878.00	1.02	0.06
							7938.15	1.03	7.55	7785.64	1.05	7.10	7841.28	0.67	0.03
17	7947.50	1.00	2.54	7789.32	1.05	2.46	7938.85	0.99	5.78	7782.72	1.07	5.80	7879.60	1.02	0.04
							7941.59	1.02	5.43	7781.40	1.04	5.13	7838.95	0.63	0.02
18	7950.72	1.00	1.79	7785.22	1.05	1.75	7942.09	0.99	4.16	7778.65	1.06	4.14	7881.29	1.01	0.02
							7944.94	1.02	3.83	7777.37	1.04	3.63	7836.63	0.58	0.01
19	7953.87	0.99	1.24	7781.33	1.05	1.22	7945.23	0.98	2.89	7774.76	1.05	2.87	7883.07	0.99	0.01
							7948.20	1.01	2.64	7773.57	1.03	2.51	7834.38	0.55	0.01
20	7956.93	0.98	0.84	7777.70	1.04	0.83	7948.29	0.97	1.97	7771.14	1.06	1.99	7884.96	0.98	0.01
							7951.39	1.00	1.78	7770.04	1.02	1.70	7832.19	0.51	0.00
$K_a=2-2$															
$(bk)=(22) \rightarrow (22)$															
2							7857.43	1.05	2.32				7842.85	1.05	4.62
							7857.43	1.05	2.32				7842.86	1.05	4.63
3							7862.13	1.05	3.89	7828.16	1.06	2.17	7842.73	1.05	3.00
							7862.12	1.05	3.89	7828.15	1.06	2.16	7842.73	1.05	3.00
4							7866.75	1.05	4.95	7823.17	1.06	3.55	7842.56	1.04	2.09
							7866.75	1.05	4.95	7823.17	1.06	3.55	7842.56	1.04	2.09
5							7871.31	1.05	5.58	7818.16	1.07	4.43	7842.35	1.03	1.50
							7871.30	1.05	5.57	7818.16	1.07	4.43	7842.35	1.03	1.50



TABLE BX: B. continued

6	7875.79	1.05	5.83	7813.16	1.07	4.88	7842.10	1.02	1.09
	7875.77	1.05	5.83	7813.15	1.07	4.88	7842.11	1.02	1.09
7	7880.18	1.05	5.76	7808.17	1.07	4.99	7841.82	1.01	0.79
	7880.16	1.05	5.76	7808.16	1.07	4.99	7841.84	1.01	0.79
8	7884.49	1.05	5.44	7803.19	1.07	4.82	7841.51	1.00	0.57
	7884.46	1.05	5.44	7803.18	1.07	4.82	7841.53	1.00	0.57
9	7888.72	1.04	4.94	7798.26	1.07	4.46	7841.18	0.98	0.41
	7888.67	1.05	4.95	7798.23	1.07	4.46	7841.21	0.98	0.41
10	7892.85	1.04	4.33	7793.37	1.07	3.96	7840.82	0.97	0.29
	7892.78	1.01	4.18	7793.32	1.07	3.97	7840.86	0.97	0.29
11	7896.90	1.04	3.68	7788.54	1.07	3.40	7840.46	0.91	0.19
	7896.80	1.04	3.68	7788.47	1.07	3.41	7840.50	0.95	0.20
12	7900.86	1.04	3.03	7783.79	1.07	2.83	7840.08	0.92	0.14
	7900.72	1.04	3.03	7783.70	1.04	2.74	7840.14	0.93	0.14
13	7904.72	1.04	2.43	7779.13	1.07	2.29	7839.72	0.90	0.09
	7904.54	1.04	2.43	7779.00	1.07	2.29	7839.77	0.90	0.09
14	7908.49	1.03	1.90	7774.60	1.07	1.80	7839.36	0.88	0.06
	7908.26	1.03	1.89	7774.41	1.07	1.80	7839.41	0.88	0.06
15	7912.17	1.03	1.44	7770.18	1.07	1.38	7839.03	0.85	0.04
	7911.88	1.03	1.44	7769.93	1.07	1.38	7839.06	0.85	0.04
16	7915.79	1.02	1.06	7765.93	1.07	1.03	7838.75	0.82	0.02
	7915.40	1.03	1.07	7765.60	1.07	1.03	7838.74	0.83	0.02
17	7919.29	1.02	0.78	7761.86	1.06	0.75	7838.52	0.79	0.02
	7918.83	1.02	0.78	7761.42	1.07	0.75	7838.47	0.79	0.02
18	7922.73	1.01	0.55	7758.02	1.05	0.53	7838.38	0.76	0.01
	7922.17	1.02	0.55	7757.43	1.06	0.54	7838.19	0.77	0.01
19	7926.10	1.01	0.38	7754.38	1.05	0.37	7838.35	0.72	0.01
	7925.42	1.01	0.38	7753.65	1.06	0.37	7837.99	0.73	0.01
20	7929.43	1.00	0.26	7751.05	1.05	0.25	7838.48	0.68	0.00
	7928.59	1.00	0.26	7750.11	1.05	0.26	7837.85	0.70	0.00

TABLE BX: C. Combination  $v_r=0 \rightarrow 1$   $v_\theta=0 \rightarrow 2$  band ( $S_{\text{vib}}$  in  $10^{-5}$  D<sup>2</sup>,  $I$  in  $10^{-22}$  cm/molecule).

$J$	$[v_r v_\theta v_R]=[000] \rightarrow [120]$														
	$K_a=0-0$						$K_a=1-1$								
	$(bk)=(00) \rightarrow (20)$						$(bk)=(11) \rightarrow (31)$								
	$R(J^e)$			$P(J^e)$			$R(J^e)/R(J^f)$			$P(J^e)/P(J^f)$			$Q(J^e)/Q(J^f)$		
$E_{\text{trn}}$	$S_{\text{vib}}$	$I$	$\nu$	$S_{\text{vib}}$	$I$	$\nu$	$S_{\text{vib}}$	$I$	$\nu$	$S_{\text{vib}}$	$I$	$\nu$	$S_{\text{vib}}$	$I$	
0	5152.30	6.57	2.05												
1	5156.11	6.50	3.96	5142.91	6.78	2.07	5249.02	5.81	5.98			5241.89	6.25	6.41	
							5250.83	5.38	5.53			5241.09	6.89	7.06	
2	5159.42	6.39	5.58	5137.44	6.85	3.97	5250.91	5.53	9.64	5231.52	5.80	5.67	5241.25	6.82	3.71
							5254.40	5.07	8.82	5231.72	6.57	6.41	5238.84	8.90	4.83
3	5162.14	6.19	6.70	5131.38	6.95	5.61	5251.70	4.94	11.28	5224.72	5.46	8.82	5240.27	7.72	2.74
							5257.45	4.75	10.81	5225.77	6.89	11.08	5235.44	12.43	4.39
4	5164.27	6.11	7.51	5124.85	7.06	6.90	5251.28	3.95	10.51	5216.93	4.79	9.89	5238.95	9.05	2.25
							5259.98	4.41	11.66	5219.38	7.18	14.73	5230.82	17.74	4.38
5	5165.80	5.98	7.83	5117.78	7.06	7.64	5253.12	2.21	6.36	5208.11	3.63	8.52	5237.28	10.92	1.97
							5261.95	4.05	11.56	5212.53	7.46	17.34	5224.86	23.89 <sup>a</sup>	4.25 <sup>a</sup>

TABLE BX: C. continued

6	5166.69	6.12	8.10	5110.20	7.23	8.11	5251.36	2.78	8.17	5198.13	2.14	5.30	5235.22	13.53	1.79
							5263.34	3.68	10.66	5205.22	7.73	18.86	5221.07	3.54 <sup>a</sup>	0.46 <sup>a</sup>
7	5166.98	5.73	7.34	5102.10	7.36	8.16	5248.80	3.06	8.75	5190.50	6.41	15.80	5232.77	17.14	1.66
							5264.08	3.26	9.17	5197.45	7.99	<u>19.33</u>	5213.58	9.56	0.91
8	5166.60	5.59	6.67	5093.47	7.86	8.23	5245.42	3.15	8.44	5179.36	7.11	16.66	5229.85	22.17	1.57
							5264.12	2.79	7.31	5189.19	8.23	18.83	5205.23	18.14	1.25
9	5165.55	5.44	5.83	5084.36	7.70	7.31	5241.23	3.13	7.58	5167.53	7.44	15.95	5226.42	29.21	1.50
							5263.32	2.25	5.29	5180.42	8.41	17.50	5195.99	29.44	1.46
10	5163.83	5.29	4.93	5074.71	7.88	6.58	5236.23	3.05	6.44	5155.02	7.62	14.40	5222.35	39.02	1.44
							5261.50	1.62	3.31	5171.08	8.49	15.50	5185.89	44.02	1.55
11	5161.33	4.82	3.79	5064.55	8.08	5.72	5230.42	2.92	5.23	5141.83	7.72	12.46	5217.44	52.22	1.36
							5258.30	0.94	1.61	5161.06	8.40	13.00	5174.94	62.64	1.55
12	5158.24	4.96	3.20	5053.89	8.29	4.84	5223.85	2.75	4.07	5127.99	7.78	10.41	5211.35	67.61	1.23
							5265.98	1.30	1.85	5150.19	7.95	10.13	5163.18	86.22	1.48
13	5154.39	4.77	2.45	5042.64	7.98	3.73	5216.47	2.55	3.02	5113.52	7.82	8.42	5204.20	52.25	0.66
							5258.86	0.85	0.95	5138.15	6.89	7.01	5150.65	116.00	1.36
14	5149.67	4.65	1.86	5030.99	8.70	3.18	5207.36	1.36	1.26	5098.48	7.82	6.61	5194.01	77.59	0.66
							5251.15	0.38	0.33	5137.20	3.21	2.55	5137.34	152.90	1.20
15	5144.24	4.51	1.37	5018.82	8.88	2.47	5199.81	2.21	1.56	5082.85	7.77	5.02	5196.66	64.39	0.37
							5242.41	0.10	0.06	5121.67	4.15	2.50	5122.33	132.90	0.69
16	55138.29	3.55	0.80	5006.03	9.21	1.91	5190.18	1.98	1.04	5065.72	4.68	2.26	5185.80	100.20	0.38
							5232.29	0.00	0.00	5105.81	4.24	1.89	5108.96	253.30	0.86
17	55130.88	4.19	0.68	4992.79	9.51	1.44	5179.87	1.73	0.66	5050.41	7.85	2.77	5173.74	130.40	0.32
							5198.98	0.05	0.02	5089.20	3.75	1.21	5093.59	324.70	0.71
$K_a=2-2$															
$(bk)=(22) \rightarrow (42)$															
2							5382.18	4.15	0.63				5369.66	5.16	1.55
							5382.24	4.14	0.62				5369.68	5.17	1.55
3							5384.11	3.62	0.91	5354.98	5.07	0.71	5367.54	5.77	1.13
							5384.28	3.97	1.00	5354.96	5.06	0.71	5367.48	5.79	1.13
4							5385.22	3.41	1.10	5347.91	5.23	1.19	5364.71	6.61	0.90
							5385.62	3.79	1.22	5347.98	5.23	1.19	5364.54	6.03	0.82
5							5385.48	3.45	1.25	5340.14	4.88	1.38	5361.22	7.74	0.76
							5386.29	3.56	1.29	5340.31	5.38	1.52	5360.82	7.00	0.69
6							5384.83	3.62	1.37	5331.62	4.92	1.53	5357.09	9.09	0.66
							5386.28	3.07	1.16	5332.03	5.50	1.71	5356.28	8.91	0.64
7							5383.21	3.15	1.18	5322.34	5.32	1.69	5352.33	9.99	0.53
							5385.61	3.23	1.21	5323.14	5.55	1.76	5350.88	11.97	0.63
8							5380.52	2.96	1.05	5312.24	5.96	1.83	5346.97	13.57	0.52
							5384.27	3.05	1.08	5313.68	5.14	1.58	5344.56	13.55	0.52
9							5376.82	2.52	0.81	5301.28	5.53	1.57	5340.99	16.71	0.47
							5382.10	2.80	0.90	5303.68	5.81	1.65	5337.23	16.80	0.47
10							5371.71	2.49	0.70	5289.39	5.49	1.38	5334.26	20.59	0.41
							5380.55	2.20	0.62	5293.14	5.85	1.47	5328.96	18.31	0.36
11							5365.29	2.27	0.54	5276.64	5.50	1.18	5328.22	19.69	0.28
							5377.18	2.29	0.55	5281.91	5.45	1.17	5319.36	24.81	0.35
12							5357.36	2.00	0.40	5262.64	5.48	0.98	5320.47	27.94	0.27
							5373.49	2.13	0.42	5271.46	5.90	1.06	5308.53	30.60	0.30
13							5347.61	1.69	0.27	5247.53	5.30	0.76	5312.48	34.81	0.23
							5369.24	1.91	0.30	5259.38	6.25	0.90	5296.27	36.83	0.25
14							5335.53	1.30	0.16	5231.10	4.99	0.56	5304.06	42.34	0.19
							5364.59	1.75	0.22	5247.17	6.32	0.72	5282.30	42.82	0.19

<sup>a</sup>Affected by the crossing between levels of the groups  $(v_r b k v_R)=(1310)$  and  $(1102)$  noted in Table BIV.

TABLE BX: D. Difference  $v_r=0 \rightarrow 1$   $v_\theta=1 \rightarrow 0$  band ( $S_{\text{vib}}$  in  $10^{-4}$  D<sup>2</sup>,  $I$  in  $10^{-22}$  cm/molecule).

$[v_r v_\theta v_R]=[010] \rightarrow [100]$																		
$J$	$K_a=1-0$ $(bk)=(21) \rightarrow (00)$									$K_a=0-1$ $(bk)=(10) \rightarrow (11)$								
	$R(J^e)$			$P(J^e)$			$Q(J^f)$			$R(J^e)$			$P(J^e)$			$Q(J^e)$		
	$\nu$	$S_{\text{vib}}$	$I$	$\nu$	$S_{\text{vib}}$	$I$	$\nu$	$S_{\text{vib}}$	$I$	$\nu$	$S_{\text{vib}}$	$I$	$\nu$	$S_{\text{vib}}$	$I$	$\nu$	$S_{\text{vib}}$	$I$
0										3522.64	5.10	1.81						
1	3375.79	5.46	0.19	3361.01	5.59	0.39	3365.67	5.53	0.58	3527.66	5.15	2.69				3518.13	5.03	2.63
2	3381.53	5.41	0.37	3356.93	5.61	0.57	3365.98	5.51	0.93	3532.85	5.20	3.47	3508.68	4.93	0.82	3518.81	5.03	4.17
3	3387.67	5.37	0.51	3353.28	5.64	0.71	3366.44	5.48	1.20	3538.23	5.20	4.06	3504.42	4.88	1.51	3519.82	5.00	5.43
4	3394.19	5.31	0.62	3350.07	5.66	0.82	3367.07	5.47	1.41	3543.74	5.30	4.54	3500.37	4.81	2.04	3521.17	4.97	6.35
5	3401.09	5.24	0.69	3347.31	5.70	0.88	3367.85	5.43	1.52	3549.43	5.34	4.78	3496.57	4.74	2.39	3522.87	4.95	6.91
6	3408.36	5.19	0.72	3344.99	5.71	0.91	3368.81	5.37	1.55	3555.28	5.39	4.83	3492.98	4.70	2.59	3524.91	4.90	7.08
7	3415.99	5.11	0.71	3343.14	5.73	0.89	3369.94	5.33	1.51	3561.30	5.44	4.70	3489.66	4.63	2.61	3527.29	4.84	6.90
8	3423.97	5.04	0.68	3341.76	5.75	0.85	3371.25	5.26	1.41	3567.48	5.47	4.40	3486.61	4.56	2.51	3530.08	4.75	6.44
9	3432.30	4.95	0.62	3340.85	5.75	0.78	3372.76	5.20	1.27	3573.82	5.50	4.00	3483.86	4.49	2.31	3533.17	4.77	5.92
10	3440.96	4.87	0.55	3340.42	5.76	0.69	3374.46	5.13	1.11	3580.35	5.54	3.53	3481.41	4.39	2.04	3536.63	4.73	5.21
11	3449.95	4.77	0.47	3340.49	5.77	0.60	3376.38	5.06	0.94	3587.06	5.56	3.03	3479.28	4.33	1.76	3540.47	4.65	4.43
12	3459.28	4.65	0.39	3341.07	5.79	0.51	3378.52	4.97	0.77	3593.95	5.57	2.52	3477.52	4.22	1.45	3544.68	4.61	3.68
13	3468.95	4.49	0.31	3342.20	5.79	0.42	3380.90	4.88	0.61	3601.02	5.56	2.05	3476.13	4.09	1.16	3549.27	4.55	2.97
14	3479.01	4.24	0.24	3343.93	5.78	0.33	3383.54	4.79	0.48	3608.29	5.53	1.61	3475.14	3.95	0.90	3554.24	4.49	2.34
15	3489.80	3.43	0.15	3346.62	5.44	0.25	3386.45	4.69	0.36	3615.75	5.45	1.23	3474.56	3.76	0.67	3559.59	4.44	1.81
16	3498.01	3.91	0.13	3346.99	3.78	0.13	3389.66	4.59	0.27	3623.38	5.26	0.90	3474.39	3.47	0.48	3565.29	4.36	1.35
17	3509.57	4.27	0.11	3350.98	5.05	0.13	3393.20	4.48	0.19	3631.08	4.77	0.61	3474.55	2.94	0.30	3571.26	4.28	0.99
18	3520.86	4.16	0.08	3354.99	5.25	0.10	3397.09	4.36	0.14	3638.43	3.35	0.31	3474.64	1.78	0.13	3577.06	3.76	0.64
19	3532.35	4.01	0.06	3359.53	5.30	0.07	3401.37	4.24	0.09	3651.13	4.72	0.32	3480.38	3.53	0.20	3588.37	1.82	0.23
20	3544.12	3.85	0.04	3364.69	5.30	0.05	3406.09	4.11	0.06	3659.34	5.59	0.27	3481.97	3.80	0.15	3595.39	2.69	0.24

TABLE BXI: Far- and mid-infrared absorption spectrum of  $\text{Li}^+\text{-H}_2$ . Line positions ( $\nu$ , in  $\text{cm}^{-1}$ ), vibrational factors of line strengths ( $S_{\text{vib}}$ ), and line intensities ( $I$ ) at  $T=296$  K in one rotational and in four vibrational bands.

A. Rotational band ( $S_{\text{vib}}$  in  $\text{D}^2$ ,  $I$  in  $10^{-20}$  cm/molecule).

$[v_r v_\theta v_R]=[000] \rightarrow [000]$												
$K_a=0-0$ ( $bk)=(00) \rightarrow (00)$				$K_a=1-1$ ( $bk)=(11) \rightarrow (11)$			$K_a=2-2$ ( $bk)=(22) \rightarrow (22)$			$K_a=3-3$ ( $bk)=(33) \rightarrow (33)$		
$R(J^e)$				$R(J^e)/R(J^f)$			$R(J^e)/R(J^f)$			$R(J^e)/R(J^f)$		
$J$	$\nu$	$S_{\text{vib}}$	$I$	$\nu$	$S_{\text{vib}}$	$I$	$\nu$	$S_{\text{vib}}$	$I$	$\nu$	$S_{\text{vib}}$	$I$
0	4.955	2.326	0.02									
1	9.902	2.329	0.13	9.729	2.323	0.20						
				10.028	2.323	0.22						
2	14.834	2.334	0.41	14.576	2.328	0.77	14.699	2.314	0.07			
				15.023	2.328	0.82	14.699	2.314	0.07			
3	19.741	2.342	0.89	19.400	2.335	1.77	24.399	2.331	0.38	19.351	2.301	0.08
				19.994	2.336	1.87	24.399	2.331	0.38	19.351	2.301	0.08
4	24.617	2.352	1.55	24.197	2.345	3.19	29.195	2.342	0.61	24.133	2.310	0.19
				24.931	2.346	3.36	29.195	2.342	0.61	24.133	2.310	0.19
5	29.453	2.364	2.35	28.955	2.356	4.90	33.946	2.356	0.86	28.878	2.322	0.34
				29.828	2.358	5.14	33.948	2.356	0.86	28.878	2.322	0.34
6	34.243	2.378	3.20	33.669	2.370	6.74	38.645	2.373	1.09	33.577	2.335	0.51
				34.677	2.373	7.03	38.645	2.373	1.09	33.578	2.335	0.51
7	38.976	2.395	3.99	38.333	2.387	8.48	43.279	2.392	1.29	38.224	2.351	0.67
				39.468	2.390	8.80	43.283	2.392	1.29	38.226	2.351	0.67
8	43.646	2.414	4.65	42.936	2.405	9.94	47.846	2.413	1.44	42.808	2.370	0.81
				44.195	2.410	10.25	47.850	2.413	1.44	42.812	2.369	0.81
9	48.242	2.437	5.10	47.471	2.427	10.96	52.332	2.438	1.51	47.324	2.390	0.92
				48.845	2.433	11.23	52.340	2.437	1.51	47.330	2.390	0.92
10	52.758	2.462	5.30	51.932	2.451	11.47	56.732	2.465	1.51	51.760	2.414	0.97
				53.414	2.458	<u>11.67</u>	56.745	2.464	1.51	51.771	2.414	0.97
11	57.185	2.490	5.26	56.309	2.478	11.45	61.033	2.495	1.44	56.107	2.440	0.98
				57.889	2.487	11.57	61.052	2.495	1.44	56.126	2.440	0.98
12	61.512	2.521	5.01	60.591	2.508	10.96	65.229	2.529	1.33	60.356	2.470	0.95
				62.263	2.519	10.98	65.257	2.528	1.33	60.387	2.470	0.95
13	65.732	2.556	4.59	64.774	2.542	10.09	69.305	2.567	1.18	64.490	2.502	0.88
				66.526	2.554	10.02	69.348	2.565	1.18	64.544	2.502	0.88
14	69.833	2.594	4.05	68.844	2.579	8.97	73.254	2.608	1.01	68.494	2.538	0.79
				70.665	2.594	8.83	73.313	2.607	1.01	68.588	2.539	0.79
15	73.806	2.637	3.46	72.793	2.620	7.71	77.061	2.654	0.84	72.331	2.576	0.68
				74.672	2.637	7.52	77.145	2.652	0.84	72.509	2.578	0.68
16	77.640	2.684	2.87	76.611	2.665	6.43	80.714	2.705	0.68	75.912	2.605	0.56
				78.535	2.685	6.20	80.829	2.702	0.68	76.295	2.622	0.57
17	81.322	2.736	2.31	80.284	2.715	5.20	84.193	2.762	0.54	78.904	2.552	0.43
				82.240	2.738	4.98	84.355	2.758	0.54	79.936	2.671	0.46
18	84.842	2.793	1.81	83.803	2.770	4.10	87.483	2.826	0.41	87.383	0.357	0.05
				85.776	2.797	3.88	87.707	2.819	0.41	83.418	2.725	0.37
19	88.182	2.857	1.38	87.150	2.831	3.15	90.552	2.897	0.31	85.827	2.734	0.27
				89.125	2.862	2.95	90.873	2.887	0.31	86.727	2.784	0.28
20	91.329	2.927	1.03	90.315	2.899	2.37	93.357	2.978	0.23	89.428	2.873	0.21
				92.273	2.934	2.20	93.833	2.962	0.23	89.844	2.850	0.21
21	94.263	3.006	0.75	93.275	2.974	1.74	95.804	3.071	0.16	92.385	2.951	0.16
				95.199	3.015	1.60	96.569	3.046	0.16	92.734	2.925	0.16
22	96.964	3.094	0.54	96.014	3.059	1.25	97.615	3.175	0.11	92.682	2.096	0.07
				97.883	3.105	1.14	99.055	3.140	0.11	95.259	3.004	0.11
23	99.406	3.192	0.38	98.506	3.153	0.88	97.713	3.234	0.08	101.105	1.166	0.03
				100.297	3.207	0.80	101.268	3.246	0.08	100.087	2.029	0.05
24	101.558	3.304	0.26	100.724	3.259	0.61	93.777	3.477	0.05			
				102.409	3.321	0.55	103.169	3.366	0.05			

TABLE BXI: B. Fundamental  $v_R=0 \rightarrow 1$  band ( $S_{\text{vib}}$  in  $10^{-2}$  D<sup>2</sup>,  $I$  in  $10^{-21}$  cm/molecule).

$J$	$[v_r v_\theta v_R]=[000] \rightarrow [001]$														
	$K_a=0-0$						$K_a=1-1$								
	$(bk)=(00) \rightarrow (00)$						$(bk)=(11) \rightarrow (11)$								
	$R(J^e)$			$P(J^e)$			$R(J^e)/R(J^f)$			$P(J^e)/P(J^f)$			$Q(J^e)/Q(J^f)$		
$\nu$	$S_{\text{vib}}$	$I$	$\nu$	$S_{\text{vib}}$	$I$	$\nu$	$S_{\text{vib}}$	$I$	$\nu$	$S_{\text{vib}}$	$I$	$\nu$	$S_{\text{vib}}$	$I$	
0	409.67	3.83	8.20												
1	413.76	3.73	15.78	400.20	5.85	8.23	416.18	3.74	26.45				407.44	3.96	27.20
							416.45	3.74	26.43				407.15	3.96	27.18
2	417.39	3.63	22.22	394.82	6.12	15.89	419.76	3.64	44.19	397.57	4.19	26.61	406.87	3.96	14.42
							420.14	3.64	44.10	397.26	4.19	26.55	406.00	3.98	14.39
3	420.57	3.54	27.14	389.02	6.41	22.45	422.89	3.55	57.01	391.88	4.32	44.59	406.01	3.98	9.41
							423.36	3.55	56.77	391.40	4.33	44.40	404.29	4.00	9.37
4	423.27	3.45	30.31	382.82	6.73	27.50	425.55	3.47	65.35	385.78	4.46	57.71	404.86	4.00	6.61
							426.11	3.46	64.89	385.12	4.47	57.30	402.00	4.04	6.57
5	425.50	3.37	31.72	376.21	7.08	30.83	427.75	3.39	69.43	379.29	4.61	66.37	403.40	4.02	4.80
							428.38	3.38	68.70	378.44	4.63	65.67	399.13	4.08	4.75
6	427.23	3.29	31.49	369.20	7.47	32.39	429.47	3.31	69.67	372.40	4.78	70.77	401.64	4.05	3.52
							430.14	3.31	68.64	371.35	4.80	69.73	395.70	4.13	3.47
7	428.46	3.21	29.90	361.80	7.90	32.29	430.69	3.24	66.69	365.13	4.95	<u>71.28</u>	399.57	4.08	2.59
							431.39	3.23	65.38	363.87	4.98	69.91	391.69	4.20	2.55
8	429.17	3.14	27.28	354.01	8.37	30.80	431.40	3.17	61.28	357.47	5.14	68.52	397.16	4.12	1.90
							432.12	3.16	59.73	356.00	5.17	66.84	387.12	4.28	1.86
9	429.34	3.08	24.01	345.84	8.90	28.24	431.59	3.10	54.27	349.42	5.34	63.25	394.42	4.15	1.38
							432.29	3.10	52.57	347.73	5.38	61.33	381.97	4.37	1.34
10	428.97	3.01	20.43	337.28	9.50	24.98	431.24	3.04	46.46	340.99	5.57	56.30	391.32	4.20	0.99
							431.90	3.03	44.69	339.08	5.61	54.23	376.24	4.47	0.96
11	428.02	2.95	16.84	328.34	10.16	21.38	430.32	2.98	38.53	332.19	5.80	48.46	387.84	4.24	0.70
							430.93	2.97	36.78	330.03	5.86	46.36	369.95	4.59	0.68
12	426.48	2.89	13.47	319.02	10.90	17.74	428.83	2.92	31.01	322.99	6.06	40.44	383.98	4.28	0.49
							429.35	2.91	29.35	320.60	6.14	38.39	363.08	4.73	0.47
13	424.33	2.83	10.46	309.32	10.36	14.29	426.73	2.86	24.24	313.42	6.35	32.77	379.70	4.33	0.33
							427.14	2.85	22.75	310.78	6.43	30.86	355.63	4.89	0.33
14	421.54	2.77	7.90	299.24	10.73	11.19	424.00	2.80	18.43	303.46	6.66	25.82	374.98	4.37	0.23
							424.27	2.79	17.13	300.56	6.76	24.11	347.60	5.06	0.22
15	418.09	2.71	5.81	288.77	11.12	8.53	420.62	2.75	13.64	293.11	7.00	19.80	369.79	4.42	0.15
							420.71	2.73	12.55	289.95	7.12	18.33	338.98	5.26	0.15
16	413.94	2.65	4.16	277.91	11.53	6.34	416.54	2.69	9.84	282.37	7.38	14.81	364.10	4.46	0.10
							416.42	2.67	8.95	278.94	7.52	13.58	329.77	5.49	0.10
17	409.04	2.58	2.90	266.64	11.98	4.59	411.73	2.63	6.91	271.21	7.79	10.80	357.87	4.49	0.06
							411.36	2.61	6.22	267.51	7.96	9.81	319.95	5.74	0.06
18	403.37	2.51	1.97	254.97	12.45	3.25	406.14	2.56	4.73	259.65	8.26	7.69	351.06	4.52	0.04
							405.48	2.54	4.21	255.65	8.46	6.92	309.51	6.03	0.04
19	396.87	2.43	1.30	242.88	12.96	2.24	399.72	2.49	3.16	247.64	8.78	5.35	343.61	4.53	0.02
							398.71	2.47	2.77	243.35	9.02	4.76	298.43	6.35	0.02
20	389.49	2.34	0.83	230.35	13.50	1.51	392.40	2.42	2.06	235.19	9.37	3.64	335.47	4.53	0.01
							390.99	2.39	1.78	230.58	9.66	3.21	286.69	6.72	0.02
21	381.20	2.22	0.52	217.36	12.96	1.00	384.10	2.33	1.30	222.26	10.05	2.42	326.56	4.52	0.01
							382.22	2.29	1.11	217.31	10.39	2.11	274.24	7.14	0.01
22	371.99	2.07	0.31	203.90	13.50	0.64	374.71	2.24	0.80	208.81	10.82	1.57	316.79	4.48	0.00
							372.28	2.18	0.67	203.52	11.23	1.36	261.06	7.61	0.01

TABLE BXI: B. continued

$[v_r v_\theta v_R]=[000] \rightarrow [001]$																		
$K_a=2-2$ $(bk)=(22) \rightarrow (22)$									$K_a=3-3$ $(bk)=(33) \rightarrow (33)$									
$J$	$R(J^e) / R(J^f)$			$P$			$Q$			$R$			$P$			$Q$		
	$\nu$	$S_{\text{vib}}$	$I$	$\nu$	$S_{\text{vib}}$	$I$	$\nu$	$S_{\text{vib}}$	$I$	$\nu$	$S_{\text{vib}}$	$I$	$\nu$	$S_{\text{vib}}$	$I$	$\nu$	$S_{\text{vib}}$	$I$
2	424.06	3.65	3.78				410.65	3.97	7.89									
	424.06	3.65	3.78				410.65	3.97	7.89									
3	427.20	3.56	6.24	395.95	4.29	3.78	409.36	4.00	5.16	431.64	3.53	2.51				413.91	3.93	7.96
	427.21	3.56	6.24	395.95	4.29	3.78	409.36	4.00	5.16	431.64	3.53	2.51				413.91	3.93	7.96
4	429.87	3.48	7.82	389.80	4.42	6.24	407.64	4.03	3.63	434.40	3.43	4.10	394.56	4.45	2.57	412.29	3.93	5.56
	429.89	3.48	7.83	389.80	4.42	6.24	407.63	4.04	3.63	434.40	3.43	4.11	394.56	4.45	2.57	412.29	3.93	5.56
5	432.06	3.40	8.68	383.23	4.56	7.82	405.49	4.08	2.64	436.70	3.35	5.04	388.16	4.60	4.22	410.26	3.93	4.00
	432.10	3.40	8.68	383.24	4.56	7.83	405.47	4.08	2.64	436.70	3.35	5.04	388.16	4.60	4.22	410.26	3.93	4.00
6	433.76	3.32	8.92	376.28	4.71	8.69	402.90	4.13	1.94	438.55	3.26	5.44	381.38	4.76	5.21	407.82	3.92	2.90
	433.82	3.32	8.93	376.29	4.71	8.70	402.87	4.14	1.94	438.55	3.26	5.44	381.38	4.76	5.21	407.82	3.92	2.90
7	434.95	3.25	8.65	368.92	4.87	8.94	399.88	4.19	1.43	439.94	3.17	5.44	374.25	4.92	5.66	404.97	3.91	2.11
	435.05	3.25	8.67	368.95	4.88	8.97	399.81	4.21	1.43	439.93	3.18	5.44	374.24	4.92	5.66	404.97	3.91	2.11
8	435.61	3.17	8.02	361.17	5.04	8.69	396.41	4.25	1.05	440.85	3.09	5.13	366.75	5.10	5.70	401.71	3.89	1.52
	435.77	3.18	8.05	361.23	5.06	8.74	396.30	4.28	1.05	440.84	3.09	5.14	366.75	5.10	5.70	401.71	3.89	1.52
9	435.74	3.10	7.13	353.03	5.22	8.08	392.49	4.32	0.76	441.28	3.00	4.61	358.91	5.28	5.42	398.04	3.87	1.09
	435.96	3.12	7.17	353.12	5.26	8.13	392.33	4.36	0.77	441.27	3.01	4.62	358.90	5.28	5.42	398.04	3.87	1.09
10	435.30	3.04	6.11	344.49	5.43	7.21	388.12	4.40	0.55	441.22	2.91	3.98	350.72	5.46	4.91	393.95	3.85	0.76
	435.62	3.06	6.16	344.64	5.47	7.28	387.88	4.44	0.55	441.20	2.92	3.99	350.70	5.47	4.92	393.94	3.84	0.76
11	434.27	2.97	5.07	335.56	5.65	6.22	383.29	4.48	0.39	440.66	2.82	3.30	342.20	5.66	4.27	389.46	3.81	0.53
	434.71	3.00	5.12	335.77	5.71	6.29	382.95	4.53	0.39	440.64	2.83	3.31	342.17	5.67	4.28	389.44	3.81	0.53
12	432.63	2.90	4.07	326.23	5.89	5.18	378.00	4.56	0.27	439.59	2.71	2.64	333.36	5.85	3.58	384.55	3.75	0.36
	433.22	2.94	4.13	326.53	5.96	5.26	377.51	4.61	0.27	439.57	2.72	2.65	333.30	5.87	3.60	384.51	3.76	0.36
13	430.34	2.83	3.17	316.51	6.15	4.20	372.22	4.64	0.19	437.99	2.59	2.03	324.20	6.02	2.90	379.25	3.68	0.24
	431.13	2.88	3.23	316.91	6.24	4.27	371.55	4.70	0.19	437.99	2.60	2.04	324.12	6.07	2.92	379.16	3.69	0.24
14	427.36	2.76	2.39	306.37	6.44	3.30	365.96	4.73	0.13	435.80	2.43	1.49	314.75	6.17	2.26	373.57	3.57	0.15
	428.42	2.82	2.46	306.91	6.55	3.37	365.04	4.78	0.13	435.89	2.45	1.50	314.63	6.25	2.28	373.37	3.60	0.16
15	423.59	2.67	1.75	295.81	6.75	2.53	359.19	4.83	0.08	432.28	1.88	0.88	305.01	6.26	1.69	367.52	3.39	0.10
	425.04	2.76	1.82	296.53	6.89	2.58	357.93	4.84	0.08	433.15	2.22	1.04	304.85	6.40	1.73	367.08	3.48	0.10
16	418.89	2.55	1.23	284.80	7.10	1.88	351.91	4.92	0.05	431.05	2.02	0.70	294.98	6.18	1.20	361.05	3.09	0.06
	420.98	2.70	1.31	285.76	7.27	1.93	350.16	4.86	0.05	432.91	1.40	0.49	294.79	6.47	1.25	359.54	2.80	0.05

TABLE BXI: C. Fundamental  $v_\theta=0 \rightarrow 1$  band ( $S_{\text{vib}}$  in  $10^{-3}$  D<sup>2</sup>),  $I$  in  $10^{-22}$  cm/molecule

$[v_r v_\theta v_R]=[000] \rightarrow [010]$																		
$K_a=1-0$ $(bk)=(11) \rightarrow (10)$									$K_a=0-1$ $(bk)=(00) \rightarrow (21)$									
$J$	$R(J^e)$			$P(J^e)$			$Q(J^f)$			$R(J^e)$			$P(J^e)$			$Q(J^e)$		
	$\nu$	$S_{\text{vib}}$	$I$	$\nu$	$S_{\text{vib}}$	$I$	$\nu$	$S_{\text{vib}}$	$I$	$\nu$	$S_{\text{vib}}$	$I$	$\nu$	$S_{\text{vib}}$	$I$	$\nu$	$S_{\text{vib}}$	$I$
0										692.08	3.28	13.26						
1	540.35	1.90	6.23	526.39	1.92	12.18	530.90	1.91	18.37	696.14	3.43	20.42				687.40	3.12	18.36
2	544.56	1.90	11.94	521.32	1.92	17.26	530.17	1.91	28.99	699.74	3.57	27.20	677.23	2.82	5.18	687.03	3.12	29.07
3	548.52	1.88	16.74	516.05	1.93	21.21	529.09	1.89	37.42	702.86	3.71	33.04	671.40	2.67	9.03	686.49	3.10	37.71
4	552.24	1.87	20.33	510.58	1.93	23.84	527.63	1.88	43.18	705.52	3.84	37.48	665.16	2.52	11.50	685.76	3.09	43.79
5	555.68	1.86	22.58	504.92	1.93	25.11	525.81	1.86	46.11	707.70	3.97	40.22	658.51	2.37	12.66	684.84	3.07	47.16
6	558.85	1.84	23.47	499.08	1.93	25.11	523.63	1.84	46.36	709.40	4.09	41.13	651.45	2.23	12.72	683.74	3.05	47.90
7	561.73	1.82	23.11	493.06	1.93	24.01	521.08	1.82	44.32	710.61	4.20	40.28	644.01	2.09	11.95	682.43	3.03	46.34
8	564.29	1.79	21.73	486.85	1.94	22.07	518.15	1.79	40.54	711.32	4.26	37.63	636.18	1.95	10.63	680.92	3.01	42.98
9	566.53	1.76	19.59	480.46	1.94	19.58	514.86	1.76	35.64	711.54	4.35	34.21	627.99	1.82	9.03	679.20	2.98	38.37
10	568.43	1.72	16.97	473.89	1.94	16.81	511.19	1.72	30.21	711.24	4.39	29.75	619.43	1.72	7.47	677.27	2.94	33.09

TABLE BXI: C. continued

11	569.96	1.68	14.16	467.13	1.94	13.99	507.14	1.69	24.74	710.42	4.37	24.82	610.54	1.59	5.84	675.12	2.91	27.61
12	571.11	1.62	11.37	460.19	1.94	11.31	502.72	1.65	19.62	709.06	4.25	19.64	601.30	1.49	4.50	672.73	2.87	22.35
13	571.86	1.54	8.76	453.06	1.94	8.90	497.91	1.61	15.09	707.08	3.86	14.13	591.72	1.43	3.41	670.10	2.83	17.57
14	572.20	1.44	6.44	445.75	1.94	6.82	492.73	1.57	11.27	704.14	2.36	6.67	581.81	1.41	2.60	667.22	2.79	13.44
15	572.14	1.29	4.42	438.24	1.94	5.09	487.18	1.52	8.19	703.53	7.24	15.46	571.51	1.53	2.12	664.07	2.74	10.01
16	571.77	1.03	2.63	430.57	1.94	3.71	481.29	1.47	5.78	699.32	6.39	10.02	560.50	2.27	2.30	660.64	2.69	7.26
17	571.48	0.52	0.97	422.74	1.92	2.63	475.17	1.40	3.92	695.10	6.02	6.78	552.08	0.01	0.01	656.90	2.64	5.15
18	565.57	1.60	2.12	414.87	1.87	1.78	469.25	1.19	2.32	690.40	5.83	4.62	540.36	0.15	0.08	652.84	2.59	3.56
<hr/>																		
$K_a=1-2$									$K_a=2-3$									
$(bk)=(11) \rightarrow (32)$									$(bk)=(22) \rightarrow (43)$									
$R(J^e)/R(J^f)$			$P(J^e)/P(J^f)$			$Q(J^e)/Q(J^f)$			$R(J^e)/R(J^f)$			$P(J^e)/P(J^f)$			$Q(J^e)/Q(J^f)$			
$J$	$\nu$	$S_{\text{vib}}$	$I$	$\nu$	$S_{\text{vib}}$	$I$	$\nu$	$S_{\text{vib}}$	$I$	$\nu$	$S_{\text{vib}}$	$I$	$\nu$	$S_{\text{vib}}$	$I$	$\nu$	$S_{\text{vib}}$	$I$
1	878.69	4.16	70.64															
	878.55	4.12	69.79															
2	882.64	4.52	81.67				868.97	3.61	32.07	1073.06	4.49	20.15						
	882.24	4.36	78.55				868.52	3.47	30.78	1073.06	4.49	20.15						
3	886.19	4.96	94.37	854.39	3.11	5.05	868.11	3.59	52.02	1076.36	4.78	21.03				1058.36	3.56	5.13
	885.46	4.60	86.95	853.50	2.89	4.67	867.17	3.26	46.93	1076.36	4.78	21.03				1058.36	3.56	5.13
4	889.13	5.27	<u>102.56</u>	848.66	3.05	10.08	866.96	3.58	65.28	1079.23	5.07	21.68	1038.79	2.52	0.46	1056.79	3.54	8.33
	888.22	4.83	93.10	847.22	2.65	8.67	865.30	2.80	50.64	1079.23	5.07	21.67	1038.79	2.52	0.46	1056.79	3.54	8.33
5	894.13	1.31	25.29 <sup>a</sup>	842.59	3.12	14.56	865.51	3.55	72.92	1081.66	5.36	21.85	1032.39	2.29	0.89	1054.83	3.50	10.21
	890.51	5.05	96.09	840.53	2.41	11.11	862.70	1.71	34.62 <sup>a</sup>	1081.66	5.35	21.83	1032.39	2.29	0.89	1054.83	3.50	10.20
6	896.40	2.74	50.85 <sup>a</sup>	835.97	3.33	18.57	863.78	3.52	75.57	1083.62	5.65	21.45	1025.63	2.06	1.15	1052.47	3.45	11.03
	892.32	5.26	95.59	833.46	2.19	11.98	862.08	4.09	86.22	1083.65	5.64	21.42	1025.64	2.06	1.15	1052.46	3.44	11.00
7	898.56	3.53	61.04	831.51	0.09	0.55 <sup>a</sup>	861.75	3.48	73.98	1085.04	5.90	20.36	1018.51	1.85	1.24	1049.70	3.39	10.99
	893.66	5.45	91.72	826.00	1.97	11.59	858.63	4.35	90.16	1085.16	5.92	20.42	1018.52	1.84	1.23	1049.67	3.36	10.89
8	900.41	4.02	62.80	824.40	0.47	2.88	859.43	3.44	69.08	1087.04	4.14	12.65	1011.03	1.64	1.19	1046.52	3.29	10.28
	894.51	5.62	84.97	818.18	1.75	10.35	854.99	4.24	82.65	1086.15	6.18	18.87	1011.05	1.63	1.18	1046.40	3.15	9.83
9	901.87	4.38	60.01	817.29	0.63	3.65	856.81	3.39	61.87	1087.04	6.16	16.21	1003.12	1.48	1.07	1042.87	3.14	9.00
	894.86	5.77	76.04	810.00	1.55	8.65	850.98	4.11	72.14	1086.35	6.07	15.97	1003.23	1.43	1.03	1043.76	2.88	8.26
10	902.88	4.66	54.56	810.01	0.64	3.37	853.89	3.33	53.34	1087.03	6.54	14.47	995.92	0.58	0.39	1038.51	2.59	6.56
	894.72	5.89	65.76	801.47	1.36	6.83	846.52	3.96	60.64	1088.01	5.12	11.34	995.02	1.25	0.85	1039.19	3.27	8.28
11	903.39	4.89	47.63	802.46	0.58	2.68	850.66	3.25	44.35	1086.48	6.82	12.37	986.87	0.88	0.54	1035.69	3.00	6.49
	894.05	5.97	54.94	792.60	1.17	5.11	841.59	3.82	49.18	1087.19	6.46	11.73	986.16	1.09	0.67	1034.68	3.15	6.81
12	903.37	5.09	40.10	794.63	0.49	1.93	847.10	3.16	35.59	1085.28	7.01	10.16	977.97	0.75	0.40	1030.47	3.13	5.60
	892.85	6.00	44.32	783.41	1.00	3.64	836.15	3.66	38.49	1086.24	6.87	9.98	978.93	0.49	0.26	1029.72	3.01	5.38
13	902.75	5.24	32.62	786.49	0.40	1.26	843.20	3.06	27.58	1083.05	6.73	7.63	968.72	0.60	0.26	1025.24	3.02	4.35
	891.10	5.96	34.44	773.90	0.84	2.46	830.17	3.48	29.06	1084.85	7.15	8.11	969.39	0.55	0.24	1024.19	2.81	4.03
14	901.48	5.35	25.66	778.00	0.30	0.76	838.93	2.92	20.59	1077.76	3.59	3.09	959.01	0.45	0.16	1019.67	2.90	3.26
	888.74	5.83	25.69	764.07	0.69	1.58	823.62	3.28	21.15	1082.97	7.38	6.39	959.93	0.45	0.16	1017.75	2.38	2.66
15	899.49	5.41	19.56	769.13	0.21	0.41	834.25	2.75	14.76	1080.68	6.77	4.37	948.52	0.30	0.08	1013.74	2.78	2.38
	885.71	5.56	18.28	753.91	0.55	0.96	816.46	3.06	14.80	1080.56	7.56	4.88	950.25	0.34	0.09	1008.34	0.95	0.81
16	896.68	5.54	14.72	759.84	0.13	0.19	829.10	2.53	10.09	1076.71	7.58	3.58	935.20	0.97	0.02	1007.43	2.65	1.68
	881.92	5.15	12.33	743.40	0.42	0.55	808.64	2.80	9.93	1077.66	7.79	3.67	940.31	0.25	0.05	1007.25	2.38	1.51
17	893.16	5.12	9.82	750.09	0.07	0.07	823.37	2.23	6.46	1071.92	7.73	2.60	930.36	0.13	0.02	1000.78	2.49	1.15
	877.38	4.15	7.07	732.50	0.31	0.29	800.08	2.45	6.22	1074.12	7.89	2.66	930.11	0.16	0.03	999.39	2.30	1.06

<sup>a</sup>The dips in the intensities as functions of  $J$  are effects of the crossing between the levels from groups  $(v_r bk v_R)=(0310)$  and  $(0101)$  noted in Table BIV.

TABLE BXI: D. Overtone  $v_R=0 \rightarrow 2$  band ( $S_{\text{vib}}$  in  $10^{-3}$  D<sup>2</sup>,  $I$  in  $10^{-22}$  cm/molecule).

$J$	$[v_r v_\theta v_R]=[000] \rightarrow [002]$														
	$K_a=0-0$						$K_a=1-1$								
	$(bk)=(00) \rightarrow (00)$						$(bk)=(11) \rightarrow (11)$								
	$R(J^e)$			$P(J^e)$			$R(J^e)/R(J^f)$			$P(J^e)/P(J^f)$			$Q(J^e)/Q(J^f)$		
$\nu$	$S_{\text{vib}}$	$I$	$\nu$	$S_{\text{vib}}$	$I$	$\nu$	$S_{\text{vib}}$	$I$	$\nu$	$S_{\text{vib}}$	$I$	$\nu$	$S_{\text{vib}}$	$I$	
0	754.43	0.87	3.86												
1	757.60	0.87	7.61	745.40	0.87	3.71	763.02	0.82	11.89			755.15	0.83	11.98	
							763.25	0.82	11.92			754.88	0.83	11.94	
2	759.87	0.88	11.03	739.57	0.87	7.05	765.27	0.82	20.28	745.30	0.83	11.31	753.67	0.86	6.52
							765.56	0.82	20.36	744.98	0.83	11.25	752.85	0.85	6.44
3	761.22	0.89	13.92	732.87	0.88	9.83	766.61	0.82	26.80	738.72	0.85	18.82	751.43	0.89	4.42
							766.95	0.83	26.90	738.20	0.84	18.66	749.79	0.88	4.31
4	761.65	0.91	16.12	725.30	0.89	11.92	767.04	0.83	31.57	731.29	0.86	24.24	748.44	0.94	3.26
							767.39	0.84	31.67	730.54	0.86	23.94	745.72	0.92	3.13
5	761.12	0.93	17.57	716.87	0.90	13.27	766.55	0.84	34.58	723.01	0.88	27.81	744.68	1.00	2.50
							766.88	0.85	34.65	722.02	0.88	27.36	740.62	0.96	2.36
6	759.63	0.96	18.26	707.58	0.92	13.87	765.11	0.86	35.91	713.89	0.90	29.65	740.15	1.08	1.96
							765.39	0.87	<u>35.92</u>	712.63	0.90	29.04	734.50	1.02	1.81
7	757.16	1.00	18.24	697.43	0.94	13.79	762.71	0.88	35.70	703.93	0.93	29.94	734.82	1.16	1.54
							762.90	0.90	35.62	702.37	0.92	29.18	727.34	1.09	1.40
8	753.69	1.04	17.62	686.42	0.97	13.15	759.32	0.90	34.20	693.11	0.96	28.92	728.67	1.26	1.21
							759.39	0.92	34.02	691.25	0.95	28.04	719.13	1.16	1.07
9	749.19	1.09	16.56	674.54	1.00	12.09	754.91	0.93	31.70	681.44	0.99	26.90	721.69	1.38	0.95
							754.82	0.95	31.42	679.24	0.99	25.94	709.88	1.25	0.82
10	743.63	1.17	15.22	661.80	1.03	10.73	749.46	0.97	28.53	668.91	1.03	24.19	713.85	1.50	0.73
							749.17	0.99	28.15	666.35	1.03	23.20	699.57	1.35	0.62
11	737.01	1.26	13.79	648.19	1.06	9.22	742.93	1.01	24.97	655.51	1.07	21.10	705.11	1.64	0.56
							742.40	1.04	24.51	652.56	1.07	20.12	688.17	1.45	0.46
12	729.29	1.41	12.52	633.69	1.10	7.68	735.29	1.05	21.30	641.22	1.12	17.89	695.44	1.78	0.42
							734.46	1.09	20.80	637.87	1.13	16.97	675.69	1.57	0.34
13	720.50	1.70	11.89	618.31	1.14	6.19	726.49	1.11	17.73	626.03	1.18	14.78	684.81	1.94	0.31
							725.32	1.15	17.21	622.25	1.19	13.93	662.09	1.71	0.25
14	710.94	2.58	13.78	602.04	1.16	4.78	716.48	1.17	14.43	609.93	1.24	11.92	673.15	2.10	0.22
							714.91	1.21	13.91	605.67	1.26	11.17	647.36	1.85	0.18
15	697.31	0.04	0.15	584.93	1.12	3.42	705.19	1.24	11.49	592.87	1.32	9.39	660.42	2.27	0.16
							703.16	1.29	10.99	588.13	1.34	8.74	631.45	2.01	0.12
16	685.57	0.51	1.48	567.30	0.81	1.77	692.56	1.32	8.96	574.84	1.41	7.24	646.55	2.44	0.11
							690.00	1.38	8.50	569.57	1.44	6.70	614.34	2.19	0.08
17	672.39	0.62	1.28	545.87	1.91	2.91	678.49	1.42	6.85	555.78	1.51	5.47	631.45	2.61	0.07
							675.33	1.48	6.44	549.95	1.55	5.03	595.96	2.39	0.06
18	646.55	0.97	1.36	526.60	1.86	1.94	662.89	1.53	5.14	535.66	1.63	4.05	615.03	2.77	0.05
							659.04	1.59	4.78	529.23	1.69	3.71	576.27	2.60	0.04
19	632.17	1.46	1.39	506.23	1.71	1.19	645.62	1.66	3.80	514.40	1.77	2.95	597.17	2.91	0.03
							640.97	1.72	3.48	507.32	1.85	2.68	555.17	2.83	0.02
20	613.63	1.71	1.07	473.52	1.08	0.47	626.52	1.82	2.76	491.93	1.95	2.11	577.73	3.00	0.02
							620.93	1.88	2.49	484.14	2.04	1.91	532.58	3.04	0.02



TABLE BXI: E. Overtone  $v_{\theta}=0 \rightarrow 2$  band ( $S_{\text{vib}}$  in  $10^{-3}$  D<sup>2</sup>,  $I$  in  $10^{-22}$  cm/molecule).

$[v_r v_{\theta} v_R]=[000] \rightarrow [020]$															
$J$	$K_a=0-0$ ( $bk)=(00) \rightarrow (20)$						$K_a=1-1$ ( $bk)=(11) \rightarrow (31)$								
	$R(J^e)$			$P(J^e)$			$R(J^e)/R(J^f)$			$P(J^e)/P(J^f)$			$Q(J^e)/Q(J^f)$		
	$\nu$	$S_{\text{vib}}$	$I$	$\nu$	$S_{\text{vib}}$	$I$	$\nu$	$S_{\text{vib}}$	$I$	$\nu$	$S_{\text{vib}}$	$I$	$\nu$	$S_{\text{vib}}$	$I$
0	1072.72	1.37	8.83												
1	1076.82	1.36	17.18	1063.22	1.37	8.58	1192.60	1.18	27.41				1185.39	1.31	30.24
							1194.52	1.14	26.60				1184.54	1.35	31.20
2	1080.46	1.34	24.32	1057.86	1.37	16.24	1194.73	1.13	44.80	1174.96	1.32	28.90	1184.94	1.41	17.24
							1198.40	1.08	42.84	1175.21	1.37	29.95	1182.42	1.55	18.87
3	1083.61	1.32	29.75	1052.08	1.37	22.55	1195.95	1.09	56.35	1168.30	1.35	48.45	1184.27	1.56	12.50
							1201.87	1.02	53.03	1169.47	1.43	51.25	1179.26	1.87	14.80
4	1086.24	1.29	33.16	1045.89	1.38	27.27	1196.27	1.04	62.84	1160.75	1.36	62.45	1183.36	1.79	10.03
							1204.91	0.96	58.02	1163.38	1.48	67.52	1175.06	2.36	13.02
5	1088.32	1.26	34.54	1039.25	1.39	30.33	1195.71	0.99	64.83	1152.35	1.38	71.29	1182.20	2.10	8.52
							1207.50	0.90	58.48	1156.94	1.53	78.84	1169.85	3.06	12.16
6	1089.83	1.23	34.05	1032.17	1.41	31.78	1194.29	0.95	63.08	1143.12	1.39	75.23	1180.77	2.52	7.47
							1209.62	0.83	55.21	1150.15	1.59	85.10	1163.66	4.06	11.69
7	1090.75	1.19	32.03	1024.62	1.44	31.76	1192.02	0.90	58.48	1133.09	1.40	74.83	1179.05	3.07	6.68
							1211.23	0.76	49.18	1143.00	1.63	<u>86.53</u>	1156.51	5.43	11.37
8	1091.05	1.15	28.91	1016.61	1.47	30.48	1188.93	0.86	51.96	1122.29	1.40	70.92	1177.00	3.79	6.04
							1212.26	0.69	41.40	1135.48	1.68	83.68	1148.45	7.28	11.02
9	1090.72	1.12	25.13	1008.12	1.51	28.20	1185.04	0.81	44.41	1110.75	1.41	64.46	1174.57	4.76	5.49
							1212.52	0.59	32.07	1127.56	1.72	77.39	1139.49	9.76	10.57
10	1089.73	1.08	21.09	999.16	1.55	25.23	1180.36	0.77	36.61	1098.52	1.41	56.46	1171.55	5.93	4.90
							1212.57	0.49	23.23	1119.22	1.75	68.61	1129.69	13.01	9.96
11	1088.06	1.04	17.13	989.72	1.59	21.87	1174.85	0.72	29.05	1085.63	1.41	47.79	1168.51	7.65	4.46
							1211.30	0.39	15.37	1110.26	1.71	56.60	1119.08	17.21	9.18
12	1085.68	1.00	13.49	979.79	1.64	18.38	1169.18	0.62	20.51	1072.12	1.41	39.18	1164.35	10.15	4.13
							1208.82	0.25	8.21	1101.27	1.71	46.45	1107.61	22.32	8.18
13	1082.56	0.96	10.31	969.36	1.69	15.01	1162.20	0.61	16.09	1057.95	1.40	30.90	1159.17	13.27	3.70
							1204.46	0.11	2.89	1091.15	1.67	35.85	1095.99	27.78	6.89
14	1078.65	0.92	7.69	958.43	1.73	11.91	1154.67	0.57	11.56	1043.82	1.32	22.64	1152.30	16.17	3.05
							1197.38	0.02	0.41	1080.03	1.50	24.85	1083.07	37.30	6.16
15	1073.96	0.86	5.45	946.99	1.77	9.21	1146.48	0.51	7.98	1028.58	1.37	17.83	1142.89	16.28	2.04
							1220.09	0.70	10.71	1067.27	1.15	14.29	1069.65	47.72	5.16
16	1068.36	0.83	3.85	935.01	1.82	6.94	1137.70	0.45	5.21	1013.03	1.37	13.09			
							1214.55	0.72	8.14	1052.04	0.67	6.07			
$K_a=2-2$ ( $bk)=(22) \rightarrow (42)$															
2							1353.69	0.83	3.14				1340.77	0.93	6.94
							1353.97	0.75	2.83				1341.35	0.67	5.01
3							1355.69	0.51	3.24	1326.65	0.81	2.81	1339.27	1.05	5.12
							1356.06	0.79	5.01	1326.07	0.71	2.46	1338.99	1.19	5.79
4							1356.57	0.78	6.28	1319.43	1.06	5.96	1336.50	1.37	4.67
							1357.55	0.77	6.23	1319.71	1.01	5.69	1336.12	0.89	3.06
5							1356.47	0.72	6.56	1311.72	0.68	4.75	1333.15	1.68	4.15
							1358.42	0.74	6.75	1312.10	1.08	7.52	1332.17	1.74	4.28
6							1354.94	0.63	5.97	1302.98	1.06	8.09	1329.22	2.07	3.73
							1358.68	0.70	6.71	1303.95	1.11	8.42	1327.27	2.10	3.78
7							1351.37	0.47	4.39	1293.32	1.03	7.91	1324.73	2.56	3.38
							1358.35	0.66	6.26	1295.27	1.12	8.68	1320.99	2.44	3.21
8							1357.61	0.33	2.97	1282.35	0.92	6.79	1319.71	3.18	3.05
							1357.47	0.62	5.55	1286.09	1.14	8.44	1312.73	2.50	2.38
9							1352.75	0.40	3.27	1269.45	0.69	4.67	1314.19	3.95	2.73
							1356.04	0.58	4.70	1276.43	1.15	7.83	1314.33	2.09	1.45
10							1347.15	0.42	2.96	1266.49	0.66	3.98	1308.20	4.89	2.41
							1354.08	0.54	3.81	1266.34	1.16	6.97	1304.89	3.54	1.74
11							1340.69	0.37	2.20	1252.57	0.82	4.19	1301.76	6.02	2.09
							1351.68	0.49	2.96	1255.85	1.17	5.98	1294.80	5.08	1.76

TABLE BXI: F. Hot  $v_R=1 \rightarrow 3$  band ( $S_{\text{vib}}$  in  $10^{-3} \text{ D}^2$ ,  $I$  in  $10^{-22} \text{ cm/molecule}$ ).

$[v_r v_\theta v_R]=[001] \rightarrow [003]$															
$K_a=0-0$							$K_a=1-1$								
$(bk)=(00) \rightarrow (00)$							$(bk)=(11) \rightarrow (11)$								
$J$	$R(J^e)$			$P(J^e)$			$R(J^e)/R(J^f)$			$P(J^e)/P(J^f)$			$Q(J^e)/Q(J^f)$		
	$\nu$	$S_{\text{vib}}$	$I$	$\nu$	$S_{\text{vib}}$	$I$	$\nu$	$S_{\text{vib}}$	$I$	$\nu$	$S_{\text{vib}}$	$I$	$\nu$	$S_{\text{vib}}$	$I$
0	634.15	3.44	1.76												
1	636.78	3.39	3.40	626.04	3.61	1.78	643.11	3.65	6.07				642.87	3.69	1.72
							643.30	3.66	6.09				642.87	3.69	1.72
2	638.46	3.36	4.86	620.59	3.71	3.47	644.79	3.66	10.40	627.16	3.74	5.78	640.12	3.74	1.14
							645.02	3.68	10.43	626.86	3.73	5.76	640.12	3.74	1.14
3	639.16	3.36	6.07	614.21	3.82	4.95	645.52	3.68	13.81	620.92	3.79	9.66	636.46	3.82	0.82
							645.77	3.71	13.85	620.42	3.78	9.60	636.44	3.83	0.82
4	638.88	3.38	7.00	606.91	3.94	6.14	645.29	3.72	16.37	613.78	3.86	12.53	631.86	3.94	0.61
							645.52	3.75	16.41	613.06	3.85	12.40	631.83	3.96	0.62
5	637.61	3.41	7.59	598.71	4.05	6.98	644.07	3.77	18.07	605.75	3.94	14.49	626.33	4.08	0.47
							644.25	3.81	18.09	604.78	3.94	14.30	626.27	4.12	0.47
6	635.34	3.44	7.79	589.59	4.18	7.45	641.85	3.83	18.93	596.83	4.04	15.61	619.85	4.25	0.36
							641.94	3.88	18.91	595.58	4.04	15.34	619.75	4.32	0.36
7	632.14	3.34	7.40	579.58	4.31	7.55	638.60	3.91	<u>19.01</u>	587.01	4.16	15.96	612.41	4.44	0.27
							638.56	3.97	18.94	585.46	4.16	15.62	612.24	4.55	0.28
8	628.46	2.39	4.98	568.69	4.43	7.30	634.28	4.01	18.40	576.29	4.30	15.64	603.98	4.66	0.21
							634.07	4.08	18.28	574.42	4.30	15.24	603.72	4.83	0.22
9	620.43	2.84	5.34	556.98	4.43	6.61	628.87	4.12	17.26	564.66	4.46	14.78	594.56	4.90	0.16
							628.44	4.20	17.08	562.44	4.47	14.33	594.16	5.14	0.16
10	614.10	3.90	6.44	544.96	3.42	4.46	622.32	4.25	15.72	552.11	4.64	13.53	584.10	5.17	0.12
							621.62	4.34	15.48	549.51	4.67	13.06	583.52	5.48	0.12
11	606.15	4.18	5.87	528.74	3.46	3.79	614.58	4.40	13.93	538.63	4.86	12.04	572.59	5.46	0.09
							613.57	4.50	13.65	535.61	4.89	11.55	571.77	5.86	0.09
12	596.82	4.41	5.13	514.42	4.98	4.47	605.61	4.57	12.04	524.18	5.10	10.43	559.98	5.77	0.06
							604.23	4.69	11.73	520.72	5.15	9.96	558.80	6.22	0.07
13	586.09	4.64	4.34	498.69	5.47	3.91	595.36	4.76	10.14	508.75	5.38	8.81	546.25	6.09	0.05
							593.53	4.89	9.82	504.82	5.45	8.37	543.89	5.25	0.04
14	573.87	4.89	3.58	481.81	5.91	3.26	583.79	4.94	8.30	492.30	5.70	7.28	531.35	6.42	0.03
							581.40	5.10	8.00	487.86	5.80	6.87	529.66	7.20	0.04
15	560.04	5.16	2.88	463.78	6.37	2.65	571.56	4.32	5.59	474.82	6.07	5.87			
							567.90	5.23	6.26	469.82	6.20	5.51			
16	544.47	5.44	2.26	444.54	6.89	2.10	554.98	5.50	5.31	456.29	6.44	4.60			
							549.81	3.84	3.39	450.64	6.65	4.32			
17	526.96	5.74	1.73	424.01	7.50	1.63	538.55	5.55	3.92	437.39	5.73	2.95			
							533.98	5.46	3.50	430.41	7.02	3.24			
18	507.23	6.02	1.29	402.08	8.21	1.23	520.04	5.94	3.00	414.46	7.24	2.60			
							514.70	6.09	2.76	405.95	5.57	1.77			

- 
- <sup>1</sup> L. Wolniewicz, J. Chem. Phys. Phys. **103**, 1792 (1995); J. Komasa, K. Piszczatowski, G. Łach, M. Przybytek, B. Jeziorski and K. Pachucki, J. Chem. Theory Comput. **7**, 3105 (2011).
  - <sup>2</sup> W. P. Kraemer and V. Špirko, Chem. Phys. **330**, 190 (2006).
  - <sup>3</sup> L. Wolniewicz, J. Chem. Phys. **99**, 1851 (1993).
  - <sup>4</sup> K. K. Irikura, J. Phys. Ref. Data, **36**, 389 (2007).
  - <sup>5</sup> V. P. Bulychev, K. M. Bulanin, and M. O. Bulanin, Opt. Spectrosc. **96**, 205 (2004).
  - <sup>6</sup> C. Sanz, E. Bodo, and F. A. Gianturco, Chem. Phys. **314**, 135 (2005). **125**, 044310 (2006).
  - <sup>7</sup> A. J. Page and E. I. von Nagy-Felsobuki, J. Phys. Chem. **A 111**, 4478 (2007).
  - <sup>8</sup> A. J. Page and E. I. von Nagy-Felsobuki, Theor. Chem. Acc. **122**, 87 (2009).
  - <sup>9</sup> Part C of this material.
  - <sup>10</sup> C. Emmeluth, B. L. J. Poad, C. D. Thompson, G. H. Weddle, and E. J. Bieske, J. Chem. Phys. **126**, 204309 (2007).
  - <sup>11</sup> D. Papoušek and M. R. Aliev, *Molecular Vibrational-Rotational Spectra* (Elsevier, Amsterdam, 1982).
  - <sup>12</sup> R. N. Zare, *Angular Momentum* (John Wiley, 1988).
  - <sup>13</sup> L. S. Rothman, C. P. Rinsland, A. Goldman, S. T. Massie, D. P. Edwards, J.-M. Flaud, A. Perrin, C. Camy-Peyret, V. Dana, J.-Y. Mandin, J. Schroeder, A. McMann, R. R. Gamache, R. B. Wattson, K. Yoshino, K. V. Chance, K. W. Jucks, L. R. Brown, V. Nemtchinov, and P. Varasi, JQSRT **60**, 665 (1996).